

Aus dem Institut für Klinische Pharmakologie und Toxikologie  
der Medizinischen Fakultät Charité – Universitätsmedizin Berlin

DISSERTATION

**Alterations at the cell membrane of breast cancer  
cells by estrogens and antiestrogens**

zur Erlangung des akademischen Grades  
Doctor medicinae (Dr. med.)

vorgelegt der Medizinischen Fakultät  
Charité – Universitätsmedizin Berlin

von

Philip Bischoff

aus Leipzig

Datum der Promotion: 01.03.2019

# Index

|   |    |
|---|----|
| List of figures .....   | 4  |
| List of tables .....  | 5  |
| List of abbreviations .....   | 6  |
| 1. Zusammenfassung .....  | 8  |
| 2. Abstract.....  | 9  |
| 3. Introduction .....   | 10 |
| 3.1. Breast cancer at a glance .....  | 10 |
| 3.1.1. Epidemiology and etiology .....  | 10 |
| 3.1.2. From symptoms to diagnosis.....  | 11 |
| 3.1.3. Therapy and prognosis .....  | 12 |
| 3.2. Estrogen in breast cancer and the effects of antiestrogen therapy .....  | 13 |
| 3.2.1. Mechanisms of ER $\alpha$ signaling and antiestrogen therapy .....     | 13 |
| 3.2.2. The role of ER $\alpha$ signaling in breast cancer carcinogenesis..... | 14 |
| 3.2.3. The role of ER $\alpha$ signaling in breast cancer metastasis.....     | 15 |
| 3.3. The adherens junction protein complex .....                              | 17 |
| 3.3.1. Structure and function of the E-cadherin protein .....                 | 17 |
| 3.3.2. Dynamics of the cortical actomyosin cytoskeleton.....                  | 17 |
| 3.3.3. Interactions between E-cadherin and the actomyosin cytoskeleton.....   | 18 |
| 3.4. Aims of the study .....  | 19 |
| 4. Material and methods .....   | 21 |
| 4.1. Material .....   | 21 |
| 4.1.1. Equipment and commodities .....  | 21 |
| 4.1.2. Cells and tissue samples .....   | 23 |
| 4.1.3. Chemicals, reagents, and cell culture supplements .....                | 23 |
| 4.1.4. Kits .....   | 27 |
| 4.1.5. Buffers, solutions, and media .....                                    | 27 |
| 4.1.6. Antibodies .....   | 29 |
| 4.1.7. Oligonucleotides.....  | 30 |
| 4.1.8. Software .....   | 30 |
| 4.2. Methods.....   | 31 |
| 4.2.1. Cell culture and treatment .....                                       | 31 |
| 4.2.2. Immunofluorescence microscopy .....                                    | 31 |

|   |    |
|---|----|
| 4.2.3. Transmission electron microscopy.....  | 32 |
| 4.2.4. Atomic force microscopy.....   | 33 |
| 4.2.5. Quantitative real-time polymerase chain reaction.....  | 34 |
| 4.2.6. Western blot .....   | 35 |
| 4.2.7. RNA silencing.....   | 36 |
| 4.2.8. Calcium switch assay .....   | 36 |
| 4.2.9. Cell motility assay.....   | 37 |
| 4.2.10. Quantification and statistics .....   | 37 |
| 5. Results .....  | 39 |
| 5.1. Fulvestrant treatment reorganizes adherens junctions in MCF-7/vBOS cells.....                            | 39 |
| 5.2. Inhibition of ER $\alpha$ signaling induces adherens junction reorganization.....                        | 43 |
| 5.3. Adherens junction reorganization depends on the cortical actomyosin cytoskeleton.....                    | 46 |
| 5.4. Adherens junction reorganization is mediated by Arp2/3, but not by cortactin .....                       | 50 |
| 5.5. Fulvestrant treatment affects the maturation of adherens junctions .....                                 | 53 |
| 5.6. Reorganization of adherens junctions decreases E-cadherin cleavage .....                                 | 55 |
| 5.7. Fulvestrant treatment increases cell stiffness and decreases cell motility .....                         | 57 |
| 5.8. Adherens junction organization and ER $\alpha$ signaling correlate in breast cancer tissue sections..... | 61 |
| 6. Discussion.....  | 63 |
| 6.1. Estrogen levels and ER $\alpha$ signaling inhibition in MCF-7/vBOS cells.....                            | 64 |
| 6.2. The organization(s) of adherens junctions .....  | 66 |
| 6.3. Regulation of adherens junctions through the actomyosin cytoskeleton.....                                | 67 |
| 6.3.1. ER $\alpha$ -dependent mechanisms regulating the actomyosin cytoskeleton .....                         | 68 |
| 6.3.2. Reorganization of adherens junctions through the actomyosin cytoskeleton .....                         | 70 |
| 6.3.3. The role of the actomyosin cytoskeleton in adherens junction maturation.....                           | 72 |
| 6.4. Adherens junction organization – a novel way of regulating E-cadherin cleavage? .....                    | 73 |
| 6.5. The role of intercellular adhesion in the metastatic spread of cancer cells.....                         | 75 |
| 6.6. Clinical implications and conclusion .....   | 78 |
| 7. References .....   | 80 |
| Eidesstattliche Versicherung.....   | 92 |
| Curriculum vitae.....   | 93 |
| Danksagung.....   | 95 |

## List of figures

- Figure 1: Fulvestrant treatment reorganizes adherens junctions in MCF-7/vBOS cells. (pp. 41f.)
- Figure 2: Inhibition of ER $\alpha$  signaling induces adherens junction reorganization. (p. 45)
- Figure 3: Adherens junction reorganization depends on the cortical actomyosin cytoskeleton. (pp. 48f.)
- Figure 4: Adherens junction reorganization is mediated by Arp2/3, but not by cortactin. (p. 52)
- Figure 5: Fulvestrant treatment affects the maturation of adherens junctions. (p. 54)
- Figure 6: Reorganization of adherens junctions decreases E-cadherin cleavage. (p. 56)
- Figure 7: Fulvestrant treatment increases cell stiffness and decreases cell motility. (pp. 59f.)
- Figure 8: Adherens junction organization and ER $\alpha$  signaling correlate in breast cancer tissue sections. (p. 62)
- Figure 9: Schematic representation of events at adherens junctions depending on ER $\alpha$  signaling activity in MCF-7/vBOS breast cancer cells. (p. 63)

## List of tables

- Table 1: List of technical equipment used. (pp. 21f.)
- Table 2: List of commodities used. (pp. 22f.)
- Table 3: List of chemicals and reagents. (pp. 23ff.)
- Table 4: List of cell culture reagents and supplements. (p. 25)
- Table 5: List of drugs for cell treatment. (p. 26)
- Table 6: List of kits used. (p. 27)
- Table 7: Composition of buffers, solutions, and media. (pp. 27f.)
- Table 8: List of primary antibodies. (p. 29)
- Table 9: List of secondary antibodies. (p. 29)
- Table 10: List of primers. (p. 30)
- Table 11: List of small interfering RNAs (siRNAs). (p. 30)
- Table 12: List of software used. (pp. 30f.)

## List of abbreviations

|                          |   |
|--------------------------|---|
| ADAM10                   | A-disintegrin-and-metalloproteinase 10  |
| AJ                       | Adherens junction   |
| APS                      | Ammonium persulfate   |
| Arp2/3                   | Actin-related protein 2/3   |
| BCL2L1                   | B-cell lymphoma 2-like 1  |
| BSA                      | Bovine serum albumin  |
| CDH1                     | Cadherin 1  |
| cDNA                     | Complementary DNA   |
| CK666                    | 2-fluoro-N-[2-(2-methyl-1H-indol-3-yl)ethyl]-benzamide  |
| DAPI                     | 4',6-diamidino-2-phenylindole   |
| DMEM                     | Dulbecco's Modified Eagle's Medium  |
| DNA                      | Deoxyribonucleic acid   |
| E2*                      | 17 $\beta$ -Estradiol   |
| E-cad*                   | E-cadherin  |
| EDTA                     | Ethylenediaminetetraacetic acid   |
| EGTA                     | Ethylene glycol-bis( $\beta$ -aminoethyl ether)-N,N,N',N'-tetraacetic acid  |
| EMT                      | Epithelial-mesenchymal transition   |
| ER                       | Estrogen receptor   |
| ER $\alpha$ / ER $\beta$ | Estrogen receptor $\alpha$ / $\beta$  |
| ESR1                     | Estrogen receptor 1   |
| EtOH*                    | Ethanol   |
| F-actin*                 | Filamentous actin   |
| FCS                      | Fetal calf serum  |
| Fulv*                    | Fulvestrant   |
| GI254023X                | (2R)-N-[(1S)-2,2-dimethyl-1-[(methylamino)carbonyl]propyl]-2-<br>[(1S)-1-(N-hydroxyformamido)ethyl]-5-phenylpentanamide |
| HCl                      | Hydrochloric acid   |
| HER2                     | Human epidermal growth factor receptor 2  |
| IFM*                     | Immunofluorescence microscopy   |
| Lat A*                   | Latrunculin A   |

---

\* Abbreviation only used in figures.

|                         |   |
|-------------------------|---|
| MPP                     | 1,3-bis(4-hydroxyphenyl)-4-methyl-5-[4-(2-piperidinylethoxy)phenol]-1H-pyrazole dihydrochloride |
| mRNA                    | Messenger RNA   |
| NaCl                    | Sodium chloride   |
| PBS                     | Phosphate-buffered saline   |
| phospho-cortactin(Y421) | Tyrosine-421-phosphorylated cortactin   |
| phospho-cSrc(Y416)      | Tyrosine-416-phosphorylated cSrc  |
| phospho-cSrc(Y527)      | Tyrosine-527-phosphorylated cSrc  |
| PHTPP                   | 4-[2-phenyl-5,7-bis(trifluoromethyl)pyrazolo[1,5-a]pyrimidin-3-yl]phenol                        |
| PP2                     | 3-(4-chlorophenyl) 1-(1,1-dimethylethyl)-1H-pyrazolo[3,4-d]pyrimidin-4-amine                    |
| PR                      | Progesterone receptor   |
| qPCR                    | Quantitative real-time polymerase chain reaction  |
| RNA                     | Ribonucleic acid  |
| ROCK                    | Rho-associated coiled-coil-containing protein kinase  |
| SD                      | Standard deviation  |
| SDS                     | Sodium dodecyl sulfate  |
| SFK                     | Src family kinase   |
| siRNA                   | small interfering RNA   |
| TBS / TBST              | Tris-buffered saline / Tris-buffered saline with Triton X-100                                   |
| TEM*                    | Transmission electron microscopy  |
| TEMED                   | Tetramethylenediamine   |
| TFF1                    | Trefoil factor 1  |
| Tris                    | Tris(hydroxymethyl)aminomethane   |
| Y-27632                 | Trans-4-(1-aminoethyl)-N-(4-pyridyl)cyclohexanecarboxamide dihydrochloride                      |
| YWHAZ                   | Tyrosine 3-monooxygenase/tryptophan 5-monooxygenase activation protein zeta                     |
| ZK 164,015              | 2-(4-hydroxyphenyl)-3-methyl-1-[10-(pentylsulfonyl)decyl]-1H-indol-5-ol                         |
| ZO-1                    | Zonula occludens-1  |

---

\* Abbreviation only used in figures.

## 1. Zusammenfassung

Die Therapie mit Antiöstrogenen ist ein integraler Bestandteil in der Behandlung von Östrogenrezeptor  $\alpha$  (ER $\alpha$ )-positivem Brustkrebs, da sie das ER $\alpha$ -abhängige Tumorwachstum hemmt. Im Laufe der letzten Jahre wurde der ER $\alpha$  außerdem mit der Metastasierung von Brustkrebs in Verbindung gebracht, was einen neuen Wirkmechanismus für Antiöstrogene bedeuten könnte. *In-vitro*-Studien legen nahe, dass die ER $\alpha$ -abhängige Herabregulation des Zell-Zell-Adhäsionsproteins E-Cadherin die Metastasierung entscheidend fördert. Allerdings zeigen klinische Studien, dass die Expression von E-Cadherin das Metastasierungsrisiko *in vivo* nur schlecht vorhersagt. Abgesehen von der Expression von E-Cadherin werden Zell-Zell-Adhäsion und folglich das Metastasierungsrisiko wesentlich durch die komplexe Interaktion zwischen E-Cadherin und dem kortikalen Actomyosin-Zytoskelett an Adhärenskontakten reguliert.

In dieser Arbeit untersuchte ich den Einfluss des klinisch angewandten Antiöstrogens Fulvestrant auf Adhärenskontakte in der Brustkrebszelllinie MCF-7/vBOS. Die Hemmung des ER $\alpha$  durch Fulvestrant veränderte nicht die Expression von E-Cadherin, bewirkte aber eine deutliche Umstrukturierung von E-Cadherin-vermittelten Adhärenskontakten. Der Effekt von Fulvestrant und anderen Antiöstrogenen auf Adhärenskontakte konnte spezifisch der Hemmung des ER $\alpha$  zugeordnet werden und war vom kortikalen Actomyosin-Zytoskelett abhängig, welches das primäre Ziel der ER $\alpha$ -Hemmung darstellen könnte. Durch Untersuchung der funktionellen Auswirkungen konnte ich zeigen, dass die Umstrukturierung keine Störung der Adhärenskontakt-vermittelten Zell-Zell-Adhäsion darstellt. Im Gegenteil waren umstrukturierte Adhärenskontakte stabiler, worauf die erniedrigte Spaltung von E-Cadherin hindeutet. Außerdem waren Zellen in einem konfluenten Zellrasen weniger beweglich, was eine erhöhte Zell-Zell-Adhäsion nahelegt. Bei der Untersuchung von Brustkrebsgewebeschnitten beobachtete ich, dass Adhärenskontakte *in vivo* verschiedenartig strukturiert sind. Eine unregelmäßige Strukturierung von Adhärenskontakten korrelierte mit einer niedrigen Aktivität des ER $\alpha$ , was die Bedeutung meiner Beobachtungen in MCF-7/vBOS-Zellen *in vitro* unterstreicht.

Diese Ergebnisse legen nahe, dass die Therapie von Brustkrebs mit Antiöstrogenen die Strukturierung von Adhärenskontakten beeinflussen könnte, wodurch die Zell-Zell-Adhäsion erhöht und die Metastasierung verhindert würde. Obschon weitere Studien notwendig sind, um die klinische Relevanz dieses Effekts zu untersuchen, könnte dies einen neuartigen Wirkmechanismus für die Therapie mit Antiöstrogenen darstellen und ein prädiktives diagnostisches Mittel für das Metastasierungsrisiko von Brustkrebs bieten. Folglich könnten dadurch die Diagnostik, Therapie und Prognose von Brustkrebspatientinnen und -patienten verbessert werden.

## 2. Abstract

Antiestrogen therapy is an integral part of the treatment of estrogen receptor  $\alpha$  (ER $\alpha$ )-positive breast cancer, since it inhibits ER $\alpha$ -dependent tumor growth. In addition, over recent years, ER $\alpha$  signaling has been implicated in the mechanisms of breast cancer metastasis, which might add a new mode of action to antiestrogen therapy. Data from *in vitro* studies suggest that ER $\alpha$ -dependent downregulation of the expression of the cell-cell adhesion protein E-cadherin crucially promotes breast cancer metastasis. However, clinical studies show that E-cadherin expression only poorly predicts the risk of breast cancer metastasis *in vivo*. In addition to E-cadherin expression, cell-cell adhesion and thus the metastatic potential of breast cancer cells are essentially regulated by the complex interaction between E-cadherin and the cortical actomyosin cytoskeleton at the adherens junction (AJ) protein complex.

In my thesis, I studied the impact of the clinical antiestrogen Fulvestrant on AJs using the MCF-7/vBOS breast cancer cell line. ER $\alpha$  inhibition by Fulvestrant did not change E-cadherin expression but induced a distinct reorganization of E-cadherin-mediated AJs. The effect of Fulvestrant and other antiestrogens on AJ organization could be specifically attributed to ER $\alpha$  inhibition. Furthermore, AJ reorganization depended on the cortical actomyosin cytoskeleton which might be the primary target of ER $\alpha$  inhibition. Investigating the functional consequences, I could show that the reorganization of AJs does not represent an impairment of AJ-mediated cell-cell adhesion. On the contrary, reorganized AJs were more stable as indicated by decreased cleavage of E-cadherin. Moreover, cells in a confluent cell monolayer were less motile, suggesting an increase in cell-cell adhesion. Studying breast cancer tissue sections, I observed that AJs were diversely organized *in vivo*. Here, an irregular organization of AJs correlated with low ER $\alpha$  activity, substantiating the data I obtained from the *in vitro* experiments with MCF-7/vBOS cells.

Taken together, these results suggest that antiestrogen therapy might affect AJ organization, thereby increasing cell-cell adhesion and preventing the metastatic spread of breast cancer cells. However, further studies are required to assess the clinical relevance of AJ organization *in vivo*. Altering the organization of AJs could represent a novel mode of action of antiestrogen therapy. Moreover, AJ organization might serve as a diagnostic tool to predict the metastatic risk of breast cancer. Consequently, this could improve the diagnosis, therapy, and prognosis of breast cancer patients.

## 3. Introduction

### 3.1. Breast cancer at a glance

This chapter gives an overview on breast cancer. The principles of diagnosis and treatment are outlined using the guidelines of the American Society of Clinical Oncology<sup>1, 2</sup>, of the European Society for Medical Oncology<sup>3, 4</sup>, and the German guidelines<sup>5, 6</sup>. Special focus lies on the importance of the hormone receptor state and antiestrogen therapy of hormone receptor-positive breast cancer.

#### 3.1.1. Epidemiology and etiology\*

According to the *GLOBOCAN 2012* study, of 14.1 million new cases of cancer per year in total, breast cancer accounts for 1.7 million cases (11.9 %). It is the second most common cancer worldwide in both sexes. Among women, breast cancer is by far the most common malignant disease (25.2 % of all cancer cases) and the first cause for cancer mortality (14.7 % of all cancer deaths). In a more differentiated view, the mortality by breast cancer is slightly exceeded by lung cancer in women in the more developed regions of the world.<sup>7</sup> Corresponding to the data of the worldwide *GLOBOCAN 2012* study, in the European Union, the number of deaths caused by breast cancer was predicted to be exceeded by lung cancer in 2015, being already the case in the United Kingdom and Poland.<sup>8</sup> However, in the latest report of the *German Centre for Cancer Registry Data*, breast cancer is still the most common cancer and accounts for the most deaths by cancer in women in Germany in 2013. In their life time, 1 in 8 women will develop breast cancer.<sup>9</sup>

A variety of risk factors for the development of breast cancer have been identified. Hormonal risk factors are related with high estrogen levels and comprise early menarche, nulliparity, late first birth, late menopause, postmenopausal obesity, and postmenopausal hormone replacement therapy.<sup>10</sup> Interestingly, these risk factors are predominantly although not consistently associated with hormone receptor-positive types of breast cancer.<sup>10, 11</sup> Furthermore, the risk of developing breast cancer is elevated by alcohol consumption, cigarette smoking, obesity, chest radiation, high mammographic breast density, benign and precursor lesions of the breast as well as genetic predisposition.<sup>10</sup>

---

\* As common practice in cancer statistics, cases of non-melanoma skin cancer were excluded in all studies cited in this paragraph.

### 3.1.2. From symptoms to diagnosis

Breast cancer can become apparent by clinical signs such as palpable indurations, lumps, asymmetry of the breast, or retraction, edema, inflammation, or ulceration of the skin and nipple.<sup>12</sup> In case of suspicion, clinical examination should be followed by ultrasound of the breast or mammography, depending on breast density and patient's age. Since breast cancer often does not become clinically apparent until progressed stages of the disease, screening tools for early detection of breast cancer have been established. Therefore, the German and the European guidelines recommend, in addition to yearly inspection and palpation of the breast of women aged 30 years and older, mammography screenings every two years for women from 50 to 70 years of age. Any suspicious lesions detected by breast ultrasound or mammography should be probed by ultrasound-guided or stereotactic core needle or vacuum biopsy to confirm the diagnosis and assess the breast cancer subtype. In suspected locally advanced or metastasized disease, typical sites of haematogenic metastatic spread should be examined by chest x-ray, sonography of the liver, and skeletal scintigraphy. Diagnostics can be complemented by computed tomography scans of the thorax and abdomen, and positron emission tomography.<sup>4, 5</sup>

Lesions of the mammary gland can be classified by analyzing morphological features. Precursor lesions comprise ductal and lobular carcinoma *in situ* (also referred to as ductal and lobular intraepithelial neoplasia).<sup>13, 14</sup> The most common types of invasive lesions are invasive ductal carcinoma (also referred to as invasive carcinoma of no special type) and invasive lobular carcinoma which are further characterized by positive or negative E-cadherin expression, respectively.<sup>14, 15</sup> Furthermore, rare types of breast cancer such as medullary, mucinous, tubular, and papillary carcinoma as well as benign neoplasias of the mammary gland can be differentiated. In addition, morphological analysis of malignant lesions provides information about the level of differentiation of the tumor cells (also referred to as grading of the tumor).<sup>14</sup>

The German<sup>5</sup>, European<sup>4</sup> and American<sup>1</sup> guidelines recommend the assessment of the expression of the estrogen receptor (ER), the progesterone receptor (PR), and the human epidermal growth factor receptor-2 (HER2) in any invasive breast cancer. The ER or PR status is considered positive, if one per-cent of the tumor cell show nuclear expression of ER or PR, respectively.<sup>1, 4, 5</sup> As recommended by the European guideline<sup>4</sup> and the preliminary updated version of the German guideline<sup>6</sup>, invasive breast cancer can further be characterized and classified into intrinsic subtypes such as luminal A, luminal B, HER2-positive, and basal-like/triple-negative, where the luminal A and B subtypes are ER-positive. Consequently, the histological analysis of biopsies of suspicious lesions and of the resected tissue during surgery does not only definitively confirm the diagnosis of breast cancer but sets the course for the subsequent therapeutic regimen.

### 3.1.3. Therapy and prognosis

In general, the therapy of breast cancer is based on surgery, radiotherapy, and systemic therapy, the latter comprising chemo-, endocrine and targeted therapy.<sup>3-5</sup>

First of all, any breast cancer patient without detection of distant metastases should undergo surgical treatment, breast conserving surgery being the preferred option. Alternatively, radical mastectomy is an option, for example, in the case of large or multicentric tumors. Depending on the lymph node status, which is assessed by sentinel lymph node biopsy, subsequent axillary lymph node dissection is indicated. In order to reduce the risk of recurrence, breast conserving surgery should always be followed by radiotherapy of the breast and thorax wall involved. After mastectomy, radiotherapy is recommended in some cases such as large primary tumors, positive lymph node status, and resection margins involved.<sup>4, 5</sup> Furthermore, guidelines recommend palliative radiotherapy of inoperable tumors as well as bone and brain metastases.<sup>3, 5</sup> Surgical treatment should be followed by adjuvant chemotherapy in high-risk situations such as hormone receptor-negative or lymph node-positive disease. Chemotherapy is also indicated for neoadjuvant or palliative treatment of inoperable tumors. Different regimens exist but it is recommended that they contain taxanes and/or anthracyclines.<sup>4, 5</sup>

Adjuvant endocrine therapy is indicated in all ER- or PR-positive cases of breast cancer. If no distant metastases were detected, endocrine therapy should be started after chemotherapy. First-line choice for endocrine therapy is the selective estrogen receptor modulator Tamoxifen in premenopausal women, or aromatase inhibitors such as Anastrozole in postmenopausal women, respectively. Endocrine therapy should be continued for 5 years in both pre- and postmenopausal women.<sup>4, 5</sup>

In metastasized hormone receptor-positive tumors, endocrine therapy is indicated, except in the case of brain metastasis. In premenopausal women, endocrine therapy comprises ovarian suppression or ablation in combination with Tamoxifen. On condition that it was not part of any prior treatment, endocrine therapy should be started with an aromatase inhibitor in postmenopausal women. In both pre- and postmenopausal women, endocrine therapy can be further enhanced by switching from steroidal to non-steroidal aromatase inhibitors or *vice versa*, and by application of ER antagonists, such as Fulvestrant, or high-dose progestogens.<sup>2, 3, 5</sup>

Over the past decade, new targeted therapies have been used in the treatment of breast cancer. In HER2-positive tumors, adjuvant chemotherapy can be complemented with anti-HER2 antibodies such as Trastuzumab and Pertuzumab.<sup>16</sup> Lately, the cyclin-dependent kinase 4/6 inhibitor Palbociclib and the mammalian target of rapamycin inhibitor Everolimus have found

their way into the American<sup>2</sup> and European<sup>3</sup> guidelines for metastasized breast cancer, but they are not yet mentioned in the updated German guidelines<sup>6</sup>.

Taking together the patients' ages and ethnicities as well as clinical stages and receptor statuses, the 5-year survival rate of female breast cancer patients averages 88 % compared to a 66 % 5-year survival rate of all female cancer patients, according to the *German Centre for Cancer Registry Data*<sup>9</sup>, or 89.7 % compared to 67.2 %, according to the *Surveillance, Epidemiology, and End Results* program of the *National Institutes of Health*<sup>17</sup>. However, survival rates differ significantly depending on the clinical stage of the tumor at the time of diagnosis. While the 5-year survival rate is 98.9 % or 85.2 % for patients with local or lymph node-positive disease, respectively, it is only 26.9 % in patients diagnosed with distant metastases.<sup>17</sup> Furthermore, the breast cancer patients' prognosis is influenced by the hormone receptor status of the tumor. Across clinical stages, the 5-year survival rate of ER-positive versus ER-negative breast cancer patients is 91.6 % versus 82.4 %, or 85.8 % versus 76.2 %, depending on positive or negative PR state, respectively.<sup>18</sup>

## **3.2. Estrogen in breast cancer and the effects of antiestrogen therapy**

As shown above, many risk factors contributing to the development of breast cancer are related to high estrogen levels.<sup>10</sup> The assessment of the ER status is the basis for clinically efficient antiestrogen therapy of ER-positive breast cancer<sup>1,2,4,5</sup>, and the prognosis of breast cancer patients depends on the ER status<sup>18</sup>. In the light of this, the effects of estrogen on the initiation, promotion, and progression of breast cancer are generally accepted. In particular, the subtype ER $\alpha$  has been shown to be a key player for estrogen signaling in breast cancer cells.<sup>19, 20</sup> The following paragraphs will outline the mechanisms of ER $\alpha$  signaling, the different types of antiestrogen therapy, and the impact of antiestrogen therapy on ER $\alpha$ -dependent mechanisms in the development and progression of breast cancer.

### **3.2.1. Mechanisms of ER $\alpha$ signaling and antiestrogen therapy**

Endogenous estrogens are the physiological ligands of the ER $\alpha$ . For synthesis of endogenous estrogens, cholesterol is metabolized by different enzymes to the sex steroid precursor androstendione, which can be converted to testosterone. The enzyme aromatase converts androstendione or testosterone to estradiol or estrone, respectively, thereby marking the critical step in estrogen synthesis. Accordingly, aromatase inhibitors can be used to inhibit ER $\alpha$  signaling by lowering endogenous estrogen levels.<sup>21</sup> Since the synthesis of estrogens in the ovaries of

premenopausal women is regulated by the hypothalamic-pituitary-gonadal axis, it can also be inhibited by ovarian ablation or hormonal disruption of the hypothalamic-pituitary-gonadal axis.<sup>22</sup>

Just as other steroid hormone receptors, the ER $\alpha$  belongs to the type I nuclear receptors.<sup>23</sup> This class of nuclear receptors is located in the cytosol and bound to heat shock proteins. Ligand-binding results in heat shock protein dissociation, homo-dimerization of the receptors, and translocation into the nucleus. In the nucleus, the ER $\alpha$  functions as a ligand-dependent transcription factor. It can interact directly with the deoxyribonucleic acid (DNA) by binding to estrogen-responsive elements or indirectly by binding to other DNA-bound transcription factors. Depending on the interaction with different coregulators, the ER $\alpha$  induces or represses gene transcription. In addition, over recent years, studies revealed that the ER $\alpha$  interacts with cytosolic proteins and is therefore involved in non-genomic extranuclear pathways, as well.<sup>19</sup>

ER $\alpha$  activation can be inhibited by different classes of substances. Selective estrogen receptor modulators, such as Tamoxifen, bind to the ligand-binding domain of the ER $\alpha$  and induce conformational changes of the receptor. The conformational state of the ER $\alpha$  affects the recruitment of different ER $\alpha$  coactivators and corepressors. Depending on the set of expressed ER $\alpha$  coregulators, different selective estrogen receptor modulators exert different tissue-specific agonistic or antagonistic effects on ER $\alpha$  signaling.<sup>24</sup> In contrast, complete ER $\alpha$  antagonists, such as Fulvestrant, exert no agonistic activity. Therefore, they are also referred to as ‘pure’ antiestrogens.<sup>25</sup> In addition to competitive antagonism, Fulvestrant disrupts ER $\alpha$  signaling by decreasing ER $\alpha$  protein levels.<sup>26</sup>

ER $\alpha$  signaling can be inhibited by lowering endogenous estrogen levels or by ER $\alpha$  antagonists. In addition, specific inhibition of pathways downstream of extranuclear ER $\alpha$  signaling might become clinically relevant in the future.<sup>27</sup>

### **3.2.2. The role of ER $\alpha$ signaling in breast cancer carcinogenesis**

The ER $\alpha$  has been shown to be critical for the development and maturation of the mammary gland during puberty. Elongation of the ducts, invasion in the underlying fat tissue and formation of the end buds depend on ER $\alpha$  signaling.<sup>19</sup> Furthermore, ER $\alpha$  signaling in interaction with other endocrine pathways is involved in remodeling processes during the menstrual cycle, pregnancy, and lactation.<sup>28, 29</sup>

Given the regulation of proliferation and invasion of mammary epithelial cells during physiological developmental processes, ER $\alpha$  signaling could conceivably be of significant importance in the development and progression of breast cancer, as well. Indeed, many ER $\alpha$  target

genes are associated with proliferation and tumor growth of breast cancer. In addition, ER $\alpha$  signaling directly affects the cell cycle by upregulating cyclin D1, which activates cyclin-dependent kinase 4 and thereby initiates the S phase of the cell cycle. The proliferation-promoting effect of ER $\alpha$  signaling on the one hand promotes tumor growth, inhibition of which is the classical rationale of antiestrogen therapy of breast cancer. On the other hand, a high proliferation rate in precursor lesions increases the probability of transforming mutations, which explains the role of ER $\alpha$  signaling in the development of breast cancer.<sup>19</sup> Moreover, ER $\alpha$  signaling has been proposed to contribute to carcinogenesis by influencing cancer stem cells. Even though ER $\alpha$ -negative, cancer stem cells are stimulated by adjacent ER $\alpha$ -positive cells via paracrine signaling.<sup>30</sup> The role of ER $\alpha$  signaling in breast cancer development led to the recommendation that preventive antiestrogen therapy is an option for young women with increased breast cancer risk.<sup>31</sup>

### **3.2.3. The role of ER $\alpha$ signaling in breast cancer metastasis**

In breast cancer as well as in cancer in general, metastasis is a multi-step process. First, tumor cells invade the surrounding tissue, which is enabled by impaired cell-cell adhesion, degradation of the extracellular matrix, as well as cell motility and migration. In the next step, intravasation into blood and lymphatic vessels generates circulating tumor cells getting disseminated in the human body. Circulating tumor cells adhere to the wall and extravasate out of the vessel – in the blood vessel system preferably in capillary networks where the blood stream lowers. In the organ parenchyma, proliferation of extravasated tumor cells leads to the formation of metastases, a process which is facilitated by the promotion of angiogenesis and vasculogenesis. During the whole process, metastasizing tumor cells need to escape from the immune response, avoid apoptotic signals, and sustain proliferative signaling.<sup>32</sup> All described steps and features have been implicated in the ‘hallmarks of cancer’.<sup>33</sup>

Metastasizing breast cancer cells might acquire critical invasive and migratory features within the context of a cellular program referred to as epithelial-mesenchymal transition (EMT).<sup>34</sup> Physiologically, EMT and its reversal occurs several times during the embryonic development and is crucial for histogenesis and organogenesis.<sup>35</sup> EMT is characterized by the loss of epithelial features such as apico-basal polarity, tight packing of cells, and mechanical rigidity. In turn, cells develop a rather dynamic and less structured mesenchymal phenotype, which is marked by an elongated shape, front-to-back leading edge polarity, and the potential to invade and migrate. The morphological changes during EMT are accompanied by molecular shifts such as a decrease in the

expression of E-cadherin and cytokeratin on one hand and an increased expression of N-cadherin, vimentin, and matrix-metalloproteases on the other.<sup>34</sup>

In breast cancer metastasis, EMT is regulated by ER $\alpha$  signaling and particularly characterized by reduced expression of the epithelial cell-cell adhesion protein E-cadherin. This results in decreased cell-cell adhesion due to disruption of E-cadherin-mediated cell-cell contacts.<sup>20</sup> Active ER $\alpha$  signaling has been shown to downregulate E-cadherin expression which is mediated by the E-cadherin promoter region.<sup>36</sup> Further it could be shown that this region contains a half estrogen-responsive element serving as a binding site for ER $\alpha$ .<sup>37</sup> Correspondingly, EMT can be triggered by ER $\alpha$  signaling.<sup>38</sup> Hence, antiestrogen therapy could have a metastasis-preventing effect by sustaining E-cadherin expression thereby inhibiting EMT. Not only the ER $\alpha$  but also other transcription factors such as Slug and Snail bind to the E-cadherin promoter region. Ligand-activated ER $\alpha$  has been shown to decrease the expression of these repressive transcription factors.<sup>39, 40</sup> Thereby, ER $\alpha$  signaling disinhibits thus indirectly induces E-cadherin expression<sup>39, 40</sup> and might consequently prevent EMT<sup>41</sup>. The EMT-preventing effect of ER $\alpha$  signaling is in line with data showing that lacking expression of ER $\alpha$  in triple-negative breast cancer is a predictor for early metastasis.<sup>42</sup> The discrepancy in the studies investigating the regulation of EMT through ER $\alpha$  signaling has been proposed to be the result of different expression of ER $\alpha$  coregulators.<sup>20</sup>

In human breast cancer patients, E-cadherin expression does not consistently correlate with ER $\alpha$  expression<sup>43-45</sup> substantiating that E-cadherin expression might be regulated in different manners depending on different ER $\alpha$  co-regulators. As described above, low E-cadherin expression is a common used marker for EMT *in vitro*.<sup>20</sup> However, the prognostic and predictive value of the E-cadherin status of the primary tumor for breast cancer metastasis *in vivo* remains questionable in different types of breast cancer.<sup>45-48</sup> Although some studies show a correlation between E-cadherin expression and lymph node metastasis, there is still a significant proportion of E-cadherin-positive lymph node metastases.<sup>44</sup> A possible explanation might be the re-expression of E-cadherin in distant sites within the context of a reversal of EMT.<sup>49</sup> Alternatively, E-cadherin expression levels have been proposed not to be essential for EMT.<sup>50</sup>

Taken together, the impact of ER $\alpha$  signaling on E-cadherin expression as well as the predictive value of E-cadherin expression for breast cancer metastasis remain questionable. Nonetheless, many lines of evidence support the role of ER $\alpha$  signaling *in vitro* and *in vivo*.<sup>20</sup> Given the importance of E-cadherin for the integrity of the mammary gland<sup>51</sup>, other ER $\alpha$ -dependent mechanisms regulating E-cadherin-mediated cell-cell adhesion might exist, which consequently could be affected by antiestrogen therapy.

### **3.3. The adherens junction protein complex**

Cell-cell adhesion does not only depend on the presence or absence of E-cadherin. While mediating the contact to adjacent cells, E-cadherin molecules also interact with the actin cytoskeleton within its own cell – this type of junctions is referred to as AJs. The interaction between E-cadherin and the actin cytoskeleton is coordinated by various associated proteins in order to regulate cell-cell adhesion.<sup>52-54</sup> This offers additional possible mechanisms how E-cadherin-mediated cell-cell adhesion is regulated in breast cancer metastasis.

#### **3.3.1. Structure and function of the E-cadherin protein**

Cadherins are transmembrane proteins mediating cell-cell adhesion in a calcium-dependent manner. E-cadherin is expressed in all epithelial cells of the mammary gland. It is involved in developmental processes and maintenance of tissue integrity.<sup>51</sup>

The extracellular domain of E-cadherin contains five repeating subdomains which can bind calcium ions. Binding of calcium ions changes the conformational state of the extracellular domain and allows homophilic interaction with other E-cadherin molecules. *Trans*-interaction between E-cadherin molecules of adjacent cells mediates cell-cell adhesion. *Cis*-interaction between E-cadherin molecules of the same cell membrane leads to clustering of E-cadherin molecules and strengthens cell-cell adhesion.<sup>54</sup> The short transmembrane domain anchors the E-cadherin molecule in the cell membrane.<sup>51</sup> The intracellular domain binds a variety of proteins which regulate E-cadherin endocytosis, sense mechanical forces, and mediate the interaction with the actin cytoskeleton at the AJ.<sup>54, 55</sup>

As described above, the regulation of E-cadherin transcription involves but is not limited to ER $\alpha$  signaling.<sup>56</sup> E-cadherin turnover is further regulated by endocytosis and recycling to the membrane<sup>52</sup>, and by proteolytical cleavage by proteases such as a-disintegrin-and-metalloproteinase 10 (ADAM10)<sup>57</sup>.

#### **3.3.2. Dynamics of the cortical actomyosin cytoskeleton**

The basic elements of the actin cytoskeleton are globular actin monomers which polymerize into double-stranded helices, also referred to as filamentous actin. Polymerization is followed by ATP hydrolysis and phosphate dissociation from the actin subunits resulting in ADP-bound subunits that slowly depolymerize. However, the constant turnover of actin filaments is essentially regulated by a variety of actin-binding proteins affecting filament polymerization and depolymerization, stability and disassembly, as well as forming crosslinks and branches. By means

of different actin-binding proteins, filamentous actin can form distinct molecular arrangements such as cross-linked, branched, parallel, antiparallel filaments which in turn allow the formation of different cellular structures such as lamellipodia, filopodia, stress-fibers, and the cell cortex.<sup>58</sup>

The cell cortex is a thin layer of straight, cross-linked, and branched actin filaments underlying the cell membrane.<sup>58</sup> The formation of branched actin networks depends on the Actin-related protein 2/3 (Arp2/3) complex and nucleation-promoting factors. The Arp2/3 complex binds to preexisting actin filaments serving as a primer for actin branch polymerization. Nucleation-promoting factors comprise both an Arp2/3-binding domain and an actin monomer-binding domain, thereby accelerating the Arp2/3-induced actin polymerization. This process is further coordinated by scaffolding proteins such as cortactin.<sup>53</sup> Capping proteins limit actin polymerization and increase the degree of branching. However, not only the activity of actin filament polymerization and the degree of branching determine the mechanical properties of the cell cortex. Furthermore, myosin motor proteins are incorporated in the actin network of the cell cortex and build up the mechanical tension of the cortical actomyosin cytoskeleton.<sup>58</sup>

In order to transmit the mechanical properties of the cell cortex to the membrane, the cortical actomyosin cytoskeleton interacts with various membrane proteins.<sup>58</sup> Via a set of adaptor proteins, the cortical actomyosin cytoskeleton interacts with the transmembrane cell-cell adhesion protein E-cadherin at AJs. Thereby, the cortical actomyosin cytoskeleton is able to respond to external mechanical stimuli and regulate E-cadherin-mediated cell-cell adhesion at AJs.<sup>55</sup>

### **3.3.3. Interactions between E-cadherin and the actomyosin cytoskeleton**

The cortical actomyosin cytoskeleton interacts with different membrane protein complexes such as tight junction and AJ complexes. While tight junctions particularly maintain the apico-basal polarization of epithelial cells and regulate paracellular diffusion, AJs are the strongest mediators of intercellular adhesion.<sup>59</sup>

The AJ complex is formed by E-cadherin and a set of adaptor proteins mediating the interaction with the underlying cortical actomyosin cytoskeleton. In the classical view, the intracellular domain of E-cadherin binds  $\beta$ -catenin which binds to  $\alpha$ -catenin which in turn interacts with the actomyosin cytoskeleton. However, although  $\alpha$ -catenin comprises binding domains for both  $\beta$ -catenin and actin filaments, a simultaneous interaction with both of them is questionable.<sup>54</sup> The linkage between E-cadherin and the cortical actomyosin cytoskeleton has been shown to be more complex involving various other associated proteins. These proteins have been implicated in multiple signaling pathways. This enables the AJ complex to sense external mechanical forces

working on E-cadherin and respond with a rearrangement of the actomyosin cytoskeleton, involving the actin-regulating Arp2/3 complex, in order to strengthen cell-cell adhesion.<sup>55</sup> Furthermore, during the formation and maturation of AJs, E-cadherin gets actively recruited to sites of cell-cell contact by means of the cortical actomyosin cytoskeleton, again involving the Arp2/3 complex, as well as cortactin and myosin motor proteins.<sup>52-54</sup>

The ability of the AJ complex to affect cortical actin dynamics and *vice versa* is required for the formation and maintenance of E-cadherin-mediated cell-cell junctions thus for developmental processes and tissue integrity.<sup>53</sup> Consequently, dysregulation of the interplay between E-cadherin and the cortical actomyosin cytoskeleton at AJs might promote invasion and migratory potential of cancer cells.

### **3.4. Aims of the study**

Therapy and prognosis of breast cancer patients has improved over the last decades.<sup>17</sup> However, due to the high prevalence of this disease, it still causes the majority of cancer deaths in women. Furthermore, the prognosis of breast cancer patients in metastasized stages remains poor. Thus, the prediction, prevention, and treatment of breast cancer metastasis are still a challenge.

The ER $\alpha$ -dependent regulation of E-cadherin expression would offer a plausible explanation how estrogens affect cell-cell adhesion and the metastatic potential of breast cancer cells. However, E-cadherin expression alone fails to reliably predict breast cancer metastasis<sup>45-48</sup> suggesting that additional mechanisms exist. Cell-cell adhesion is not only determined by E-cadherin protein levels. Moreover, the complex interaction between E-cadherin and the cortical actomyosin cytoskeleton at AJs essentially regulate cell-cell adhesion.<sup>52-54</sup> Both E-cadherin and the actomyosin cytoskeleton have been shown to be regulated by ER $\alpha$  signaling.<sup>20, 32</sup> Thus, breast cancer metastasis might be affected by ER $\alpha$ -dependent mechanisms that regulate cell-cell adhesion at the level of AJs. Studying these ER $\alpha$ -dependent mechanisms does not only help to better understand the processes of breast cancer metastasis. It is also necessary to assess the impact of antiestrogen treatment, which is an integral part of breast cancer therapy.

In my thesis, I investigated how antiestrogens affect E-cadherin-mediated cell-cell adhesion besides by regulating E-cadherin expression. In particular, I studied if treatment with antiestrogens has an impact on the organization of E-cadherin-mediated AJs in breast cancer cells. The MCF-7/vBOS breast cancer cell line was used as an *in vitro* model system for ER $\alpha$ - and E-cadherin-positive breast cancer. Cells were treated with the potent and clinically used antiestrogen Fulvestrant. The morphology of AJs was studied by immunofluorescence and

transmission electron microscopy. I further investigated the role of the cortical actomyosin cytoskeleton for AJ organization and the functional consequences of AJ organization for cell-cell adhesion. Finally, I studied the organization of AJs in breast cancer tissue sections to evaluate the clinical relevance of my *in vitro* findings in MCF-7/vBOS cells, which might have implications for antiestrogen therapy and breast cancer metastasis *in vivo*.

## 4. Material and methods

### 4.1. Material

#### 4.1.1. Equipment and commodities

Table 1: List of technical equipment used.

| <b>Device</b>                             | <b>Type name</b>        | <b>Manufacturer</b> |
|---|-------------------------|---------------------|
| Analytical balance                        | AX105 DeltaRange        | Mettler Toledo      |
| Aspiration system                         | Vacusafe comfort        | Integra Biosciences |
| Atomic force microscope                   | NanoWizard 1 / 4        | JPK Instruments     |
| Biological safety cabinet                 | Herasafe™ KSP 12        | Thermo Scientific   |
| Blotting chamber                          | Trans-Blot® SD          | BioRad              |
| CCD camera for gel documentation          | CoolSNAP HQ2            | Photometrics        |
| CO <sub>2</sub> incubator                 | Heraeus BBD 6220        | Thermo Scientific   |
| Cooling Block                             | BL°CKICE                | Techne              |
| Cooling centrifuge                        | Heraeus Biofuge primo R | Thermo Scientific   |
| Cooling centrifuge                        | 5424R                   | Eppendorf           |
| Electronic single-/multi-channel pipettes | Xplorer® plus           | Eppendorf           |
| Electrophoresis power supply              | PowerPac200             | BioRad              |
| Electrophoresis system                    | Mini-Protean 3 Cell     | BioRad              |
| Gel documentation system                  |                         | Decon Science Tec   |
| Gradient thermal cycler                   | Mastercycler® nexus     | Eppendorf           |
| Heating block                             | Thermostat 5320         | Eppendorf           |
| Heating oven                              | Heraeus® Function Line  | Thermo Scientific   |
| Inverted fluorescence microscope          | Axio Observer.Z1        | Zeiss               |
| Inverted microscope                       | CKX41                   | Olympus             |
| Laboratory centrifuge                     | Heraeus Labofuge 400    | Thermo Scientific   |
| Microplate incubator                      | THERMOstar              | BMG Labtech         |
| Microplate reader                         | GENios                  | Tecan               |
| Mini centrifuge                           | SU1550                  | Sunlab              |

|   |                                |                          |
|---|--------------------------------|--------------------------|
| Pipette controller                      | accu-jet® pro                  | Brand                    |
| Precision balance                       | Acculab Series                 | Sartorius Group          |
| Real-time PCR system                    | QuantStudio® 7                 | Thermo Fisher Scientific |
| Shaking water bath                      | GFL 1086                       | GFL                      |
| Single-/multi-channel pipettes          | Research® plus<br>Reference® 2 | Eppendorf                |
| Spectrophotometer                       | NanoDrop™ 2000                 | Thermo Fisher Scientific |
| Structured illumination system          | Apotome.2                      | Zeiss                    |
| Transmission electron microscope camera | 4k×4k F416 CMOS camera         | TVIPS                    |
| Transmission electron microscope        | Tecnai Spirit                  | FEI                      |
| Tube roller                             | SRT6                           | Stuart                   |
| Tube shaker                             | Reax top                       | Heidolph                 |
| Tumbling table                          | WT12                           | Biometra                 |
| Vacuum pump                             | EcoVac                         | schuett-biotec           |

Table 2: List of commodities used.

| <b>Name</b>                               | <b>Manufacturer</b>               |
|---|-----------------------------------|
| ACLAR® Fluoropolymer films                | Science Services, Munich, Germany |
| Amersham™ Hybond nitrocellulose membranes | GE Healthcare                     |
| Arrow™ TL1 silicone cantilevers           | Nanoworld                         |
| Blot absorbent filter paper               | Biorad                            |
| Cell culture flasks                       | TPP                               |
| Cover slips                               | Menzel-Gläser                     |
| Falcon™ centrifuge tubes                  | VWR                               |
| FluoroDish cell culture dishes            | WPI                               |
| Microscope slides                         | Menzel-Gläser                     |
| MLCT cantilevers                          | Bruker AFM Probes                 |
| Multi-well plates                         | TPP                               |
| Nalgene™ cryogenic vials                  | Thermo Scientific                 |

|   |                |
|---|----------------|
| Neubauer improved cell counting chamber | Digital Bio    |
| Pipette tips                            | Eppendorf      |
| Polystyrene beads 5 $\mu$ m             | microParticles |
| Reaction tubes                          | Eppendorf      |
| Serological pipettes                    | neoLab         |

#### 4.1.2. Cells and tissue samples

MCF-7 is a stable human breast cancer cell line which originates from cells that were obtained from the pleural effusion of a female patient suffering from metastatic breast cancer.<sup>60</sup> MCF-7/BOS is a highly estrogen-responsive stock of the MCF-7 cell line.<sup>61</sup> The MCF-7/vBOS cell line used in my thesis is a variant which evolved under laboratory conditions from the MCF-7/BOS cell stock kindly provided by *A.M. Soto\** and *C. Sonnenschein\**. Analysis of MCF-7/vBOS cells by the ATCC® Short Tandem Repeat profiling service authenticated the identity of MCF-7/vBOS cells against the MCF-7/ATCC®HTB-22™ reference cell line in the ATCC® database. MCF-7/ACC115 cells used as a control cell line were acquired from the *German Collection of Microorganisms and Cell Cultures*.

*Barbara Ingold-Heppner\*\** and *Carsten Denkert\*\** provided tissue microarrays which contained duplicates of formalin-fixed paraffin-embedded breast cancer tissue sections from human patients with diagnosed invasive ductal carcinoma. The use of tissue samples from breast cancer patients for the generation of tissue microarrays was approved by the ethics committee of the Charité University Hospital Berlin (EA1/139/05).

#### 4.1.3. Chemicals, reagents, and cell culture supplements

Table 3: List of chemicals and reagents.

| Name                                  | Source        |
|---------------------------------------|---------------|
| 4',6-diamidino-2-phenylindole (DAPI)  | Sigma-Aldrich |
| Acetic acid                           | Roth          |
| Acrylamide:Bisacrylamide 37.5:1, 30 % | Biorad        |
| Ammonium persulfate (APS)             | Roth          |
| Bovine serum albumin (BSA)            | Sigma-Aldrich |

\* Tufts University, Boston

\*\* Institute of Pathology, University Hospital Charité, Berlin

|   |                          |
|---|--------------------------|
| Bromophenol blue  | Roth                     |
| Citric acid   | Roth                     |
| cOmplete™ protease inhibitor cocktail   | Roche                    |
| Coomassie blue G-350  | GE Healthcare            |
| Dimethyl sulfoxide (DMSO)   | Roth                     |
| Disodium hydrogen phosphate   | Roth                     |
| Dulbecco's Phosphate Buffered Saline (PBS)<br>(-) Ca <sup>2+</sup> , (-) Mg <sup>2+</sup> | PAN-Biotech              |
| Ethanol   | Roth                     |
| Ethylenediaminetetraacetic acid (EDTA)  | Roth                     |
| Fluorescence Mounting Medium  | Dako                     |
| Formaldehyde 3,7 %  | neoLab                   |
| Glutaraldehyde (Grade I)  | Sigma-Aldrich            |
| Glycine   | Sigma-Aldrich            |
| HiPerFect transfection reagent  | Qiagen                   |
| Hydrochloric acid (HCl)   | Roth                     |
| Laemmli protein sample buffer, 4x   | Biorad                   |
| LR-Gold resin   | Plano                    |
| Methanol  | Roth                     |
| Osmium tetroxide  | Science Services         |
| PageRuler Prestained Protein Ladder   | Thermo Fisher Scientific |
| Phalloidin, FITC-conjugated   | Sigma-Aldrich            |
| Powdered milk, low-fat, blotting grade  | Roth                     |
| PowerUp™ SYBR® Green Master Mix   | Thermo Fisher Scientific |
| Roti®-Free Stripping Buffer   | Roth                     |
| Sodium chloride (NaCl)  | Roth                     |
| Sodium dodecyl sulfate (SDS)  | Biorad                   |
| Sodium orthovanadate  | Sigma-Aldrich            |
| Spurr's resin, Low Viscosity Spurr Kit  | Ted Pella Inc.           |
| Tannic acid   | Science Services         |
| Tetramethylenediamine (TEMED)   | Serva                    |

|  |                     |
|--|---------------------|
| Tris(hydroxymethyl)aminomethane (Tris) | Roth                |
| Triton™ X-100                          | Sigma-Aldrich       |
| Tween-20                               | Roth                |
| Uranyl acetate                         | Sigma-Aldrich       |
| Vectashield® Antifade Mounting Medium  | Vector Laboratories |
| Xylene                                 | VWR                 |
| β-Mercaptoethanol                      | Roth                |

Table 4: List of cell culture reagents and supplements.

| <b>Name</b>   | <b>Source</b>        |
|---|----------------------|
| Biofreeze   | Biochrom             |
| CO <sub>2</sub> Independent Medium  | Gibco                |
| Dulbecco's Modified Eagle Medium (DMEM)<br>(+) 3,7 g/L NaHCO <sub>3</sub> , (+) 1 g/L D-glucose,<br>(+) pyruvate, (+) L-glutamine, (+) phenol red | Biochrom             |
| DMEM<br>(+) 3,7 g/L NaHCO <sub>3</sub> , (+) 1 g/L D-glucose,<br>(+) pyruvate (-) L-glutamine, (-) phenol red                                     | Gibco                |
| Fetal calf serum (FCS), S 0615, LOT 1353 W  | Biochrom             |
| Fibronectin   | Sigma-Aldrich        |
| Gelatine A  | Millipore            |
| GlutaMAX®   | Gibco                |
| Laminin   | Sigma-Aldrich        |
| Opti-MEM™   | Gibco                |
| Penicillin 10,000 U/ml / Streptomycin 10,000 µg/ml  | Biochrom             |
| Trypan blue solution (0.4 %)  | Fluka, Sigma-Aldrich |
| Trypsin   | Biochrom             |

Table 5: List of drugs for cell treatment.

| Name  | CAS-No.     | Source        |
|---|-------------|---------------|
| (2R)-N-[(1S)-2,2-dimethyl-1-[(methylamino)carbonyl]propyl]-2-[(1S)-1-(N-hydroxyformamido)ethyl]-5-phenylpentanamide (GI254023X) | 260264-93-5 | Tocris        |
| 1,3-bis(4-hydroxyphenyl)-4-methyl-5-[4-(2-piperidinyloxy)phenol]-1H-pyrazole dihydrochloride (MPP)                              | 911295-24-4 | Sigma-Aldrich |
| 17 $\beta$ -Estradiol   | 50-28-2     | Serva         |
| 2-(4-hydroxyphenyl)-3-methyl-1-[10-(pentylsulfonyl)decyl]-1H-indol-5-ol (ZK 164,015)  | 177583-70-9 | Tocris        |
| 2-fluoro-N-[2-(2-methyl-1H-indol-3-yl)ethyl]-benzamide (CK666)  | 442633-00-3 | Sigma-Aldrich |
| 3-(4-chlorophenyl) 1-(1,1-dimethylethyl)-1H-pyrazolo[3,4-d]pyrimidin-4-amine (PP2)  | 172889-27-9 | Tocris        |
| 4-[2-phenyl-5,7-bis(trifluoromethyl)pyrazolo[1,5-a]pyrimidin-3-yl]phenol (PHTPP)  | 805239-56-9 | Sigma-Aldrich |
| Cytarabine  | 147-94-4    | Sigma-Aldrich |
| Ethylene glycol-bis( $\beta$ -aminoethyl ether)-N,N,N',N'-tetraacetic acid (EGTA)   | 67-42-5     | Roth          |
| Fulvestrant   | 129453-61-8 | Sigma-Aldrich |
| Jasplakinolide  | 102396-24-7 | Sigma-Aldrich |
| Latrunculin A   | 76343-93-6  | Sigma-Aldrich |
| Tamoxifen   | 10540-29-1  | Sigma-Aldrich |
| Trans-4-(1-aminoethyl)-N-(4-pyridyl)cyclohexanecarboxamide dihydrochloride (Y-27632)  | 129830-38-2 | Sigma-Aldrich |

#### 4.1.4. Kits

Table 6: List of kits used.

| Name  | Manufacturer       |
|---|--------------------|
| High Capacity cDNA Reverse Transcription Kit          | Applied Biosystems |
| Pierce™ BCA Protein Assay Kit                         | Thermo Scientific  |
| RNase-Free DNase Set                                  | Qiagen             |
| RNeasy® Kit   | Qiagen             |
| SuperSignal™ West Femto Maximum Sensitivity Substrate | Thermo Scientific  |

#### 4.1.5. Buffers, solutions, and media

Table 7: Composition of buffers, solutions, and media.

| Name   | Composition   |
|--|---|
| Citrate buffer                                   | A. bidest.  |
|  | 60.4 mM Disodium hydrogen phosphate                       |
|  | 21.4 mM Citric acid                                       |
| Coomassie destaining solution                    | 50 vol% Ethanol   |
|  | 40 vol% A. bidest.  |
|  | 10 vol% Acetic acid                                       |
| Coomassie staining solution                      | 50 vol% A. bidest.  |
|  | 50 vol% Methanol  |
|  | 0.1 wt% Coomassie blue G-350                              |
| Laemmli electrophoresis running buffer           | A. bidest.  |
|  | 192 mM Glycine  |
|  | 25 mM Tris  |
|  | 3,5 mM SDS  |
| Lysis buffer                                     | A. bidest.  |
|  | 5 vol% Glycerin   |
|  | 1 vol% Triton X-100                                       |
|  | 138 mM NaCl   |
|  | 20 mM Tris  |
|  | 5 mM β-Mercaptoethanol                                    |
|  | 4 mM EDTA   |
|  | 1 mM Sodium orthovanadate                                 |
| 1x cOmplete™ protease inhibitor cocktail (Roche) |   |
| Normal-serum medium                              | DMEM, (+) L-glutamine, (+) phenol red                     |
|  | 10 vol% FCS   |
|  | 1 vol% Penicillin 10,000 U/ml / Streptomycin 10,000 µg/ml |

|  |            |  |
|--|------------|--|
| Polyacrylamide separation gel                    |            | A. bidest.   |
|  | 33.3 vol%  | 30 % Acrylamide/ Bisacrylamide 37.5:1              |
|  | 375 mM     | Tris (1.5 M pH 8.8 stock, adjusted with HCl)       |
|  | 3.5 mM     | SDS  |
|  | 0.002 vol% | Bromophenol blue                                   |
|  | 44 µM      | APS (must be added last)                           |
|  | 0.1 vol%   | TEMED (must be added last)                         |
| Polyacrylamide stacking gel                      |            | A. bidest.   |
|  | 16.7 vol%  | 30 % Acrylamide/ Bisacrylamide 37.5:1              |
|  | 125 mM     | Tris (0.5 M pH 6.8 stock, adjusted with HCl)       |
|  | 3.5 mM     | SDS  |
|  | 44 µM      | APS (must be added last)                           |
|  | 0.1 vol%   | TEMED (must be added last)                         |
| Protein transfer buffer                          |            | A. bidest.   |
|  | 10 vol%    | Methanol   |
|  | 150 mM     | Glycine  |
|  | 25 mM      | Tris   |
| Reduced-serum medium                             |            | DMEM, (-) L-glutamine, (-) phenol red              |
|  | 5 vol%     | FCS  |
|  | 1 vol%     | GlutaMAX™ 100x                                     |
|  | 1 vol%     | Penicillin 10,000 U/ml / Streptomycin 10,000 µg/ml |
| Transmission electron microscopy blocking buffer |            | A. bidest.   |
|  | 0,4 wt%    | BSA  |
|  | 155 mM     | NaCl   |
|  | 20 mM      | Tris   |
| Tris/EDTA buffer                                 |            | A. bidest.   |
|  | 40 mM      | Tris   |
|  | 27 mM      | EDTA   |
|  |            | Adjust pH to 9,0 with HCl                          |
| Tris-buffered saline (TBS)                       |            | A. bidest.   |
|  | 150 mM     | NaCl   |
|  | 20 mM      | Tris   |
| Tris-buffered saline with Tween (TBST)           |            | A. bidest.   |
|  | 0.1 vol%   | Tween-20   |
|  | 150 mM     | NaCl   |
|  | 20 mM      | Tris   |

#### 4.1.6. Antibodies

Table 8: List of primary antibodies.

| <b>Name</b>   | <b>Source</b>                |
|---|------------------------------|
| Monoclonal mouse anti-E-cadherin (clone 36)         | BD Transduction Laboratories |
| Monoclonal mouse anti-p120 (clone 98)               | BD Transduction Laboratories |
| Monoclonal mouse anti- $\beta$ -catenin (clone 14)  | BD Transduction Laboratories |
| Monoclonal rabbit anti- $\alpha$ -catenin (EP1739Y) | Abcam                        |
| Polyclonal rabbit anti-cortactin (H-191)            | Santa Cruz Biotechnology     |
| Polyclonal rabbit anti-E-cadherin (H-108)           | Santa Cruz Biotechnology     |
| Polyclonal rabbit anti-ER $\alpha$ (HC-20)          | Santa Cruz Biotechnology     |
| Polyclonal rabbit anti-phospho-cortactin (Tyr466)   | Santa Cruz Biotechnology     |
| Polyclonal rabbit anti-phospho-Src (Tyr416)         | Santa Cruz Biotechnology     |
| Polyclonal rabbit anti-phospho-Src (Tyr527)         | Santa Cruz Biotechnology     |
| Polyclonal rabbit anti-ZO1 (61-7300)                | Invitrogen                   |

Table 9: List of secondary antibodies.

| <b>Name</b>  | <b>Source</b>            |
|--|--------------------------|
| Polyclonal goat anti-Mouse IgG, Alexa Fluor® 488-conjugated  | Jackson ImmunoResearch   |
| Polyclonal goat anti-Mouse IgG, Cy3-conjugated               | Jackson ImmunoResearch   |
| Polyclonal goat anti-Mouse IgG, HRP-conjugated               | Santa Cruz Biotechnology |
| Polyclonal goat anti-Rabbit IgG, 5 nm gold-conjugated        | BBI Solutions            |
| Polyclonal goat anti-Rabbit IgG, Alexa Fluor® 488-conjugated | Jackson ImmunoResearch   |
| Polyclonal goat anti-Rabbit IgG, Cy3-conjugated              | Jackson ImmunoResearch   |
| Polyclonal goat anti-Rabbit IgG, HRP-conjugated              | Santa Cruz Biotechnology |

#### 4.1.7. Oligonucleotides

Table 10: List of primers.

| Target gene  | Sense              | Primer sequence 5' → 3'  |
|--|--------------------|--|
| B-cell lymphoma 2-like 1 (BCL2L1)  | forward<br>reverse | CAG CTT GGA TGG CCA CTT AC<br>TGC TGC ATT GTT CCC ATA GA         |
| Cadherin 1 (CDH1)  | forward<br>reverse | AGG AGC CAG ACA CAT TTA TGG AA<br>GCT GTG TAC GTG CTG TTC TTC AC |
| Trefoil factor 1 (TFF1)  | forward<br>reverse | CAT CGA CGT CCC TCC AGA AGA G<br>CTC TGG GAC TAA TCA CCG TGC TG  |
| Tyrosine 3-monooxygenase/<br>tryptophan 5-monooxygenase<br>activation protein zeta (YWHAZ) | forward<br>reverse | ACT TTT GGT ACA TTG TGG CTT CAA<br>CCG CCA GGA CAA ACC AGT AT    |

Table 11: List of small interfering RNAs (siRNAs).

| Name  | Source |
|---|--------|
| FlexiTube GeneSolution for Estrogen receptor 1 (ESR1) | Qiagen |
| Negative control siRNA                                | Qiagen |

#### 4.1.8. Software

Table 12: List of software used.

| Name                          | Source                   |
|-------------------------------|--------------------------|
| Adobe Illustrator             | Adobe Systems            |
| Chemotaxis and Migration Tool | Ibidi                    |
| Excel                         | Microsoft                |
| Fiji                          | open source              |
| GraphPad Prism 5/6            | GraphPad Software        |
| JPK Data Processing Software  | JPK Instruments          |
| Magellan™                     | Tecan                    |
| NanoDrop™ software            | Thermo Fisher Scientific |
| Powerpoint                    | Microsoft                |

|                       |                          |
|-----------------------|--------------------------|
| QuantStudio® software | Thermo Fisher Scientific |
| SPM software          | JPK Instruments          |
| Word                  | Microsoft                |
| ZEN pro               | Zeiss                    |

## 4.2. Methods

### 4.2.1. Cell culture and treatment

Aliquots of MCF-7/vBOS and MCF-7/ACC115 cells were stored in Biofreeze freezing medium in liquid nitrogen. Cells were routinely cultured in normal-serum medium containing 10 % FCS in cell culture flasks at 37°C, 5 % CO<sub>2</sub> and 95 % humidity. FCS contained 6.8 × 10<sup>-11</sup> M 17β-estradiol. The clinical relevance of the resulting 17β-estradiol levels under maintenance and experimental conditions will be discussed in section 6.1.

When reaching 70-80 % confluence, cells were trypsinized and split. For cell counting, trypsinized cells were stained with trypan blue solution and counted using a Neubauer improved cell counting chamber. The number of cell passages was limited to 8-10 in order to reduce passage-dependent variations between experiments. Cells were regularly tested for mycoplasma contamination using the GATC MYOPLASMACHECK testing service (GATC Biotech).

For all experiments, cells were seeded in reduced-serum medium containing 5 % FCS. Drug treatment was started when cells reached about 70-80 % confluence. If not stated otherwise, Fulvestrant treatment was performed at a concentration of 10<sup>-8</sup> M for 48 hours. During drug treatment, the cell culture medium was exchanged on a daily basis. Drugs were dissolved in ethanol or DMSO.

For coating experiments, surface coating was carried out prior to cell seeding. For this, 0.1 % gelatine A, 0.5 µg/ml fibronectin, or 2.0 µg/ml laminin was given into the wells of a multi-well plate, respectively. After incubation for 30 min, 1 h, or 4 h, respectively, the wells were rinsed once with PBS. Cells were then seeded, cultured, and treated as described above.

### 4.2.2. Immunofluorescence microscopy

Cells were seeded in 6-well plates on sterilized coverslips, cultured and treated as described above. After treatment, cells were washed two times with PBS and fixed with 3.7 % formaldehyde for 15 min. Afterwards, cells were permeabilized with 0.2 % Triton X-100 for 30 min and unspecific antibody binding sites were blocked with 5 % FCS for 60 min. The

subsequent incubation with the primary antibody was carried out overnight at 4°C or for 2 h at room temperature. The incubation with the secondary antibody was carried out for 1 h at room temperature. For incubation with primary and secondary antibodies, antibodies were diluted in 1.5 % BSA in PBS in order to reduce unspecific antibody binding. For actin filament visualization, cells were incubated with fluorophore-conjugated phalloidin for 1 h at room temperature after fixation, permeabilization and blocking as described above. Cell nuclei were visualized by incubation with 20 ng/ml DAPI in PBS for 15 min. If not stated otherwise, all incubation steps were followed by washing the cells three times for 5 mins with PBS.

*Barbara Ingold-Heppner\** and *Carsten Denkert\** provided tissue microarrays which contained duplicates of formalin-fixed paraffin-embedded breast cancer tissue sections of about 1.5 mm diameter each from human patients with diagnosed invasive ductal carcinoma. Prior to immunostaining, paraffin-embedded sections were deparaffinized by incubation with xylene for 5 min three times. Subsequently, the sections were rehydrated in serial dilutions of ethanol in water (100 %, 70 %, 0 %) for 5 min at room temperature. To unmask epitopes, sections were incubated with citrate buffer for 15 min at room temperature and Tris/EDTA buffer for 20 min at 100°C. Unspecific antibody binding sites were blocked with 1 % BSA in PBS for 1 h at room temperature. Afterwards, tissue sections were incubated with primary and secondary antibodies as described above.

After immunostaining, coverslips were washed with distilled water and mounted in Dako or VectaShield® mounting medium on microscope slides. Immunofluorescence images were acquired using an Axio Observer.Z1 widefield microscope (Zeiss), which was equipped with an Apotome.2 device for optical sectioning by structured illumination (Zeiss).

#### **4.2.3. Transmission electron microscopy**

Cells were seeded on sterilized ACLAR® fluoropolymer films (Science Services, Munich, Germany) and cultured and treated as described above. The subsequent preparation of the cells for transmission electron microscopy and image acquisition was performed by *Beatrix Fauler\*\** and *Thorsten Mielke\*\**.

First, 5 % glutaraldehyde (Grade I) in PBS was given to the cell culture medium, resulting in a final concentration of 2.5 % glutaraldehyde. This way, cells were fixed for 1 h. Subsequently, cells were post-fixed with 0.5 % osmium tetroxide in PBS for 1 h followed by 0.1 % tannic acid

---

\* Institute of Pathology, University Hospital Charité, Berlin

\*\* Max Planck Institute for Molecular Genetics, Berlin

in PBS for 30 min. Cells were contrasted in 2 % uranyl acetate for 1.5 h. Afterwards, cells were dehydrated in serial dilutions of ethanol in water (30 %, 50 %, 70 %, 90 %, 96 %, 100 %) for 10-15 min. All incubation steps were performed at room temperature. After dehydration, cells were embedded in Spurr's resin and polymerized for 3 d at 60°C. Cells embedded on ACLAR® fluoropolymer films were subjected to ultrathin sectioning for image acquisition by transmission electron microscopy.

For immuno-transmission electron microscopy, 8 % paraformaldehyde / 0.4 % glutaraldehyde in PBS was given to the cell culture medium resulting in final concentrations of 4 % paraformaldehyde / 0.2 % glutaraldehyde. This way, cells were fixed for 30 min and subsequently post-fixed with 0.1 % tannic acid in PBS for 30 min. Afterwards, cells were dehydrated in serial dilutions of ethanol in water as described above. All incubation steps were performed at room temperature. Samples were embedded in LR-Gold resin and polymerized at 4°C under a 350 W lamp for 3 d. Cells embedded on ACLAR® fluoropolymer films were subjected to ultrathin sectioning. Sections were incubated with transmission electron microscopy blocking buffer for 1 h in order to block unspecific antibody binding sites. Sections were then incubated with the primary antibody in transmission electron microscopy blocking buffer overnight at 4°C. Sections were washed and incubated with the gold-conjugated secondary antibody in transmission electron microscopy blocking buffer for 2 h at room temperature. After antibody incubation, sections were post-contrasted with 2 % uranyl acetate for 2 min and lead citrate for 1 min at room temperature.

Transmission electron microscopy images were acquired using a Tecnai Spirit transmission electron microscope (FEI) operated at 120 kV, which was equipped with a 4kx4k F416 CMOS camera (TVIPS).

#### **4.2.4. Atomic force microscopy**

Cells were seeded in petri dishes, cultured and treated as described above. Afterwards, atomic force microscopy was performed by *Anna Taubenberger*\*.

For atomic force microscopy indentation measurements, reduced-serum medium was exchanged for CO<sub>2</sub> Independent Medium. Measurements were performed at 37°C using the NanoWizard 1 or 4 (JPK Instruments). First, polystyrene beads (diameter 5 µm) were attached to tipless cantilevers using epoxy glue. This ensured well-defined indenter geometry and decreased

---

\* BIOTEC, Biotechnological Center TU Dresden

the local stress on the cell surface during indentation. The system was calibrated using built-in procedures of the SPM software (JPK Instruments). For indentation measurements, the cantilever was positioned above the confluent monolayer. It was then lowered at a speed of 10  $\mu\text{m/s}$  onto the cell surface. Upon contact with the cell surface, the cantilever got deflected, which was detected by altered laser beam reflection. The deflection of the cantilever indicated the forces generated by the tip-surface interaction. Force-distance curves were calculated using a force setpoint of 2.5 nN. Measurements from 3 to 4 different positions on the surface of 40-80 cells were collected for each experiment. Force-distance curves were transformed and fitted according to *Radmacher*<sup>62</sup> and *Sneddon*<sup>63</sup> using the JPK Data Processing software (JPK Instruments). The apparent elastic (Young's) moduli were calculated to describe the resistance of the cell surface to elastic deformation. Assuming that the cell volume was not altered by cantilever indentation, a Poisson ratio of 0.5 was assumed for calculating the apparent elastic (Young's) modulus.

To measure the spatial distribution of the apparent elastic (Young's) moduli across the cell monolayer, the cell surface was probed with a cantilever comprising a pyramid-shaped tip. This allowed a spatial resolution of 1  $\mu\text{m}$ . Atomic force microscopy indentation measurements were performed and apparent elastic (Young's) moduli were calculated as described above.

#### **4.2.5. Quantitative real-time polymerase chain reaction**

Cells were seeded in multi-well plates, cultured and treated as described above. Ribonucleic acid (RNA) was extracted and isolated using the RNeasy Kit (Qiagen) according to the manufacturer's protocol including a DNA digestion step. The concentration of the RNA yield was determined using a NanoDrop<sup>TM</sup> spectrophotometer. RNA was stored at  $-80^{\circ}\text{C}$ . Prior to quantitative real-time polymerase chain reaction (qPCR), RNA was transcribed to complementary DNA (cDNA) by reverse transcription using the High Capacity cDNA Reverse Transcription Kit (Applied Biosystems). cDNA was stored at  $-20^{\circ}\text{C}$ .

Master mixes were prepared using the PowerUp<sup>TM</sup> SYBR<sup>®</sup> Green Master Mix (Thermo Fisher Scientific) according to the manufacturer's protocol. qPCR was performed using the QuantStudio<sup>®</sup> 7 Real-time PCR system (Thermo Fisher Scientific). The cycling mode started with two holding stages at  $50^{\circ}\text{C}$  and  $95^{\circ}\text{C}$  for 2 min each for polymerase activation which were followed by 40 amplification cycles of 1 s at  $95^{\circ}\text{C}$  and 30 s at  $60^{\circ}\text{C}$  each. Definition of the threshold level and calculation of  $C_T$ -values was conducted by the built-in QuantStudio<sup>®</sup> software. Relative gene expression was calculated according to the  $\Delta\Delta C_T$  method. *YWHAZ* served as housekeeping gene.<sup>64</sup>

#### 4.2.6. Western blot

Cells were seeded in multi-well plates or cell culture flasks, cultured and treated as described above. For protein extraction, cells were scraped in ice-cold PBS and centrifuged for 1 min at 13.000 g. The cell pellet was then incubated with lysis buffer for 20 min on ice. Lysed cells were again centrifuged for 10 min at 13.000 g. The supernatant was diluted 1:1 in glycerin to prevent protein precipitation during long-term storage. Samples were stored at -20°C.

Protein concentration was determined using the Pierce™ BCA Protein Assay Kit (Thermo Scientific) according to the manufacturer's protocol by means of a microplate reader (Tecan) and the Magellan™ software. Proteins were separated by SDS- polyacrylamide gel electrophoresis. For this, equal protein amounts were diluted in Laemmli protein sample buffer, denatured at 95°C for 3 min, and loaded on polyacrylamide gels. Polyacrylamide gels consisted of a 5 % stacking gel and a 10 % separation gel. Electrophoresis was run at 120 min for about 90 minutes in Laemmli electrophoresis running buffer. After electrophoresis, the separated proteins were transferred to nitrocellulose membranes by semi-dry blotting. For this purpose, gels were placed between filter papers soaked with protein transfer buffer. Protein transfer was performed in a semi-dry blotting chamber at 25 V for 90 to 120 minutes.

Nitrocellulose membranes were incubated with 6 % low-fat milk powder in TBS to block unspecific antibody binding sites. Afterwards, membranes were incubated with the primary antibody overnight at 4°C and incubated with the secondary antibody for 1 h at room temperature. Incubation with antibodies was carried out in the presence of 0.6 % low-fat milk powder in TBS in order to reduce unspecific antibody binding. All incubation steps were followed by washing the membrane three times with TBST and three times with TBS for 5 min each. For detection of protein bands, membranes were incubated with the chemiluminescent substrate SuperSignal West Femto Maximum Sensitivity Substrate (Thermo Scientific) according to the manufacturer's protocol. Detection of protein bands was performed using a gel documentation system (Decon DC Science Lec) equipped with a CCD camera (CoolSNAP HQ2, Photometrics).

For detection of another protein on the same membrane, membranes were incubated in Roti®-Free Stripping Buffer (Roth) for 30 min at room temperature to remove bound antibodies. Subsequently, membranes were washed, incubated with the primary and secondary antibody, and protein bands were detected as described above.

After detection of protein bands, membranes were subjected to Coomassie total protein staining according to *Welinder et Ekblad*<sup>65</sup>. In short, nitrocellulose membranes were stained with Coomassie staining solution while subjected to slight shaking for 1 min at room temperature. Membranes were then washed with Coomassie destaining solution for 30 minutes at room

temperature while subjected to permanent shaking in order to reduce Coomassie background staining. Afterwards, membranes were dried and scanned at 600 dpi.

Densitometric quantification of protein bands and total protein lanes was performed using the Fiji software. Coomassie total protein staining served as loading control for normalization of protein bands detected by chemiluminescence.

#### **4.2.7. RNA silencing**

Cells were seeded in multi-well plates and cultured in reduced-serum medium. For immunofluorescence microscopy after RNA silencing, cells were seeded on coverslips in 24-well plates. For protein extraction and western blot analysis after RNA silencing, cells were seeded in 6-well plates.

After reaching 70-80 % confluence, cells were transfected with siRNA. For this purpose, siRNA (FlexiTube GeneSolution, Qiagen) was diluted in OptiMEM cell culture medium to a final concentration of 10 to 20 nM. HiPerFect transfection reagent (Qiagen) was then added according to the manufacturer's protocol. This mixture was given to the cells cultured as described above. Cells were now incubated in the presence of siRNA for 24 h under cell culture conditions. Afterwards, cells were washed once with PBS and further cultured in reduced-serum medium for another 72 h. Finally, cells were subjected to immunofluorescence microscopy (see section 4.2.2), or protein extraction and western blot analysis (see section 4.2.6).

#### **4.2.8. Calcium switch assay**

Cells were seeded on coverslips, cultivated, and treated as described above. The Ca<sup>2+</sup>-dependent homophilic interaction of E-cadherin molecules was transiently impaired by the Ca<sup>2+</sup>-chelating agent EGTA. For this purpose, after treatment, cells were washed with PBS once and incubated with reduced-serum medium containing  $8 \times 10^{-3}$  M EGTA for 2 h under cell culture conditions in order to disrupt E-cadherin-mediated cell-cell contacts and induce cell rounding. The EGTA-containing reduced-serum medium was then removed and exchanged for EGTA-free reduced-serum medium to allow the renewed formation of E-cadherin-mediated cell-cell contacts. Coverslips were fixed with 3.7 % formaldehyde directly before and after the incubation with EGTA-containing reduced-serum, and at different time points after the exchange for EGTA-free reduced serum medium. Fixed coverslips were further subjected to immunostaining and immunofluorescence imaging (see section 4.2.2).

#### 4.2.9. Cell motility assay

Cells were seeded in 12-well plates, cultured, and treated as described above. After treatment, the cell monolayer in each well was wounded by one straight scratch with a yellow pipette tip. After the scratch, cells were further treated in reduced-serum medium for another 3 days. To reduce the effects of cell proliferation during the cell motility assay,  $10^{-5}$  M Cytarabine was added to the reduced-serum medium starting 1 h before the scratch. Cytarabine exerts its antiproliferative effect by inhibiting DNA replication without affecting RNA synthesis.<sup>66</sup>

Finally, 12-well plates were sealed with Parafilm® film and observed by phase contrast microscopy over the course of 6 h at room temperature. Phase contrast images of regions near the scratch were taken every 5-10 min. Phase contrast images were acquired using an Axio Observer.Z1 widefield microscope (Zeiss) equipped with a motorized scanning table. For analysis of cell motility, three  $300 \times 300$   $\mu\text{m}$  regions per sample close to the border of the scratch were selected randomly. Each region was divided into 9 quadrants. The movements of one cell per quadrant were tracked manually using the Fiji software plugin MTrack ( $10 \pm 3$  tracking points per cell depending on cell velocity). The accumulated distance of cell movements was calculated using the Fiji software plugin MTrack. Trajectory plots of cell movements were generated using the Chemotaxis and Migration Tool software (Ibidi).

#### 4.2.10. Quantification and statistics

All graphs were created and statistical analyses were performed using the GraphPad Prism 5/6 software. In bar diagrams, bars and lines represent the mean value and standard deviation (SD), respectively. In boxplots, boxes indicate the lower quartile, median, and upper quartile. Whiskers represent the 10<sup>th</sup> and 90<sup>th</sup> percentile. Dots represent outliers. In dot plots, lines indicate mean values  $\pm$  SD. Dots represent single values.

Gene expression data obtained by qPCR was analyzed by one-way ANOVA testing with Dunnett's correction for multiple comparisons. Statistical analyses were performed on  $\Delta C_T$  values. Apparent elastic (Young's) moduli data obtained by atomic force microscopy and cell motility data were analyzed using the two-tailed Mann Whitney U-test.

Protein expression data obtained by western blot analyses was normalized to Coomassie total protein staining and solvent control. Polyacrylamide gel electrophoresis and transfer to nitrocellulose membranes were performed separately for each biological replicate. Since absolute protein expression values from different membranes are not comparable among each other, only relative protein expression values were used to calculate mean values and SD. However, this way,

the relative protein expression value of the solvent control is always exactly 1. Consequently, no statistical testing was performed on protein expression data.

Analysis of breast cancer tissue samples was performed on 13 tissue samples containing a significant amount of E-cadherin-positive breast cancer cells, which were selected manually from the tissue microarray. Per tissue sample, 6-10 individual cells were selected randomly for the assessment of E-cadherin-mediated cell-cell contacts and ER $\alpha$  localization. In the set of 121 individual breast cancer cells, the organization of E-cadherin-mediated cell-cell contacts (regular versus irregular) and ER $\alpha$  localization (cytosolic versus nuclear) were assessed separately by three observers independent from each other. Contingency tables were analyzed using the Fisher's test.

## 5. Results

### 5.1. Fulvestrant treatment reorganizes adherens junctions in MCF-7/vBOS cells

In breast cancer metastasis, the importance of E-cadherin protein levels and its dependence on ER $\alpha$  signaling remain questionable (see section 3.2.3). Thus, other ER $\alpha$ -dependent mechanisms regulating cell-cell adhesion might exist. Cell-cell adhesion is regulated essentially by the complex interaction between E-cadherin and the cortical actomyosin cytoskeleton at AJs.<sup>52-54</sup> This interplay and the consequences for cell-cell adhesion and metastatic potential might be affected by ER $\alpha$  signaling and consequently by antiestrogen therapy of breast cancer.

To investigate if antiestrogen treatment has an impact on cell-cell contacts in breast cancer, cells of the breast cancer cell line MCF-7/vBOS were treated with the potent antiestrogen Fulvestrant. Cell morphology was visualized by phase contrast microscopy. Both solvent control and Fulvestrant-treated MCF-7/vBOS cells formed a confluent cobblestone-like monolayer of cells. However, cell-cell contacts of Fulvestrant-treated cells appeared highly refractive in phase contrast microscopy (Fig. 1A), indicating that Fulvestrant treatment changed the morphology of cell-cell contacts in MCF-7/vBOS cells. To test if the observed morphological changes could be attributed to E-cadherin-mediated cell-cell contacts, MCF-7/vBOS cells were treated with Fulvestrant for 48 hours and subsequently immunostained for E-cadherin. Solvent control cells exhibited a continuous, partly spot-like E-cadherin staining along basolateral membranes. Interestingly, upon Fulvestrant treatment, E-cadherin staining revealed discontinuous reticular, partly even honeycombed structures (Fig. 1B).

Both solvent control and Fulvestrant-treated cells displayed a strong immunostaining of E-cadherin. Since contradictory data has been published with regard to the effect of antiestrogen treatment on E-cadherin expression<sup>36, 37, 39, 40</sup>, messenger RNA (mRNA) levels of the E-cadherin-coding *CDH1* gene and E-cadherin protein levels were quantified using qPCR and western blot analysis, respectively. Interestingly, neither *CDH1* mRNA levels nor E-cadherin protein levels were altered upon Fulvestrant treatment (Fig. 1C+D). This suggests that Fulvestrant does not alter E-cadherin expression while affecting the organization of E-cadherin-mediated cell-cell contacts in MCF-7/vBOS cells.

Further characterization revealed that the effect of Fulvestrant on the organization of E-cadherin-mediated cell-cell contacts appeared only after 24 to 48 hours and became even more distinct after ongoing treatment (Fig. 1E). The altered organization of E-cadherin-mediated cell-cell contacts was stable for more than 24 hours in the absence of Fulvestrant and reversible after

longer periods of time (Fig. 1F). None of the different surface coatings tested perturbed the effect of Fulvestrant treatment on E-cadherin-mediated cell-cell contacts (Fig. 1G). These results further substantiate a specific effect of Fulvestrant treatment on the organization of E-cadherin-mediated cell-cell contacts in MCF-7/vBOS cells.

In order to more precisely resolve the morphology of E-cadherin-mediated cell-cell contacts upon Fulvestrant treatment, MCF-7/vBOS cells were analyzed using transmission electron microscopy in cooperation with *Thorsten Mielke\** and *Beatrix Fauler\**. Conventional transmission electron microscopy showed that solvent control cells form continuous cell-cell contacts (Fig. 1H, arrowheads). In contrast, Fulvestrant-treated cells exhibited spatially restricted cell-cell contacts, where the adjacent cell membranes in between diverged from each other (Fig. 1H). Immuno-gold labelling of E-cadherin in Fulvestrant-treated cells revealed that E-cadherin protein is located predominantly at the spatially restricted cell-cell contacts (Fig. 1J). Since transmission electron microscopy visualizes a cross-section of the cell monolayer, this corresponds to the observations in immunofluorescence microscopy (Fig. 1K).

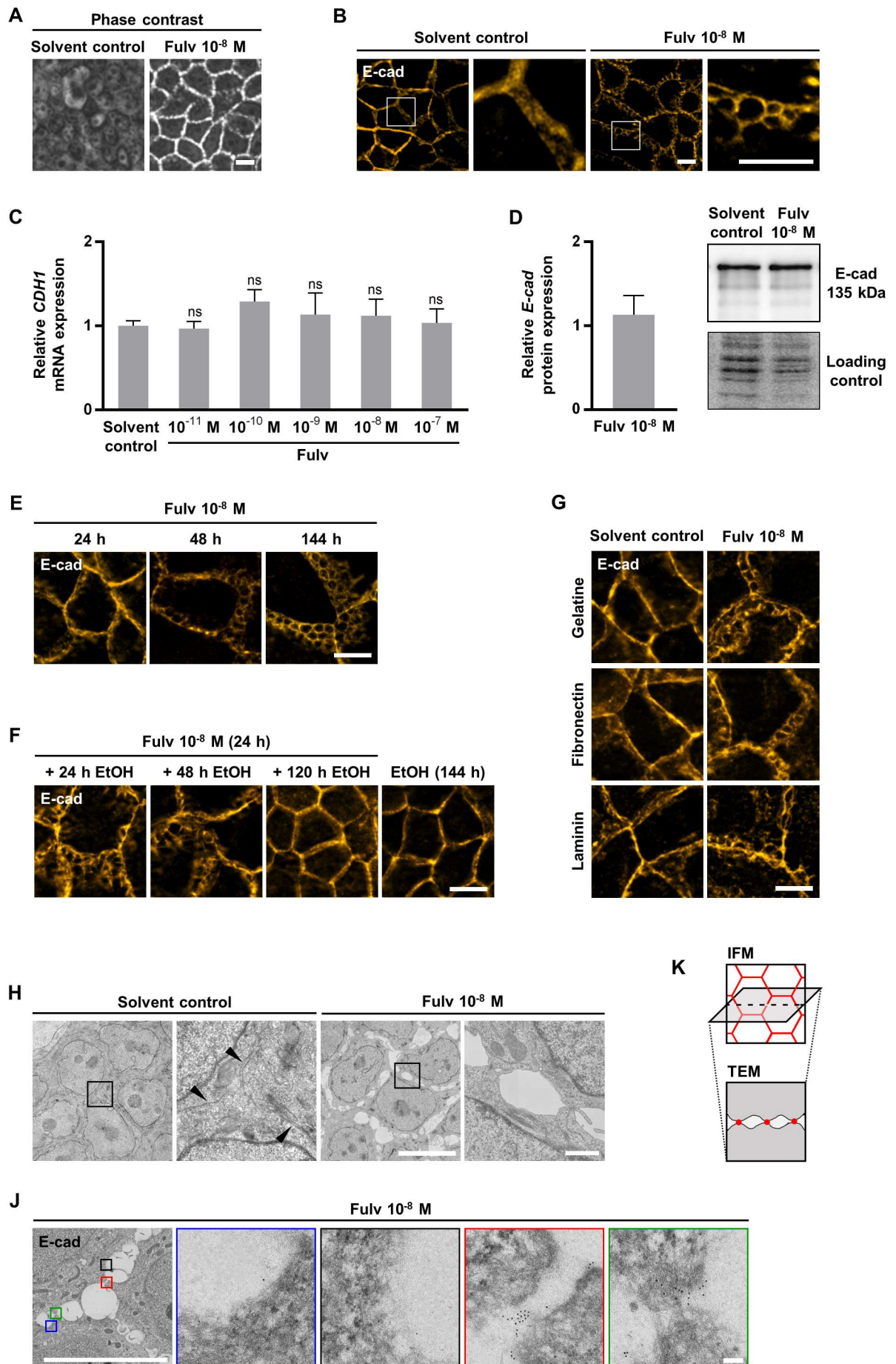
To test if the effect of Fulvestrant on the organization of E-cadherin-mediated cell-cell contacts marks a reorganization of AJ complexes, the co-localization of E-cadherin with other AJ components was investigated. For this purpose, MCF-7/vBOS cells immunostained for E-cadherin were co-immunostained for other AJ proteins such as  $\alpha$ -catenin,  $\beta$ -catenin, and p120, or co-phalloidin-stained to visualize actin filaments. It is worth noting that in both solvent control and Fulvestrant-treated cells, E-cadherin strongly co-localized with other AJ proteins (Fig. 1L) as well as cortical actin filaments (Fig. 1M). These results suggest that MCF-7/vBOS cells exhibit intact AJs which are distinctly reorganized upon Fulvestrant treatment.

Not only AJs but also tight junctions interact with the cortical actomyosin cytoskeleton, forming a circular apical belt.<sup>67</sup> Immunostaining of the zonula occludens-1 (ZO-1) protein served as a marker for tight junctions in MCF-7/vBOS cells. As expected, in solvent control cells, ZO-1 staining marked a thin belt of tight junctions that did not co-localize with AJs as marked by E-cadherin co-immunostaining. Interestingly, despite the distinct reorganization of AJs in Fulvestrant-treated cells, the morphology of ZO-1 staining did not differ from solvent control cells (Fig. 1N). This indicates that Fulvestrant treatment does neither generally affect actin-associated protein complexes nor severely perturb the apico-basal polarity of MCF-7/vBOS cells.

Together, these results suggest that Fulvestrant treatment induces a specific reorganization of AJs in MCF-7/vBOS cells which is not accompanied by altered E-cadherin protein levels.

---

\* Max Planck Institute for Molecular Genetics, Berlin



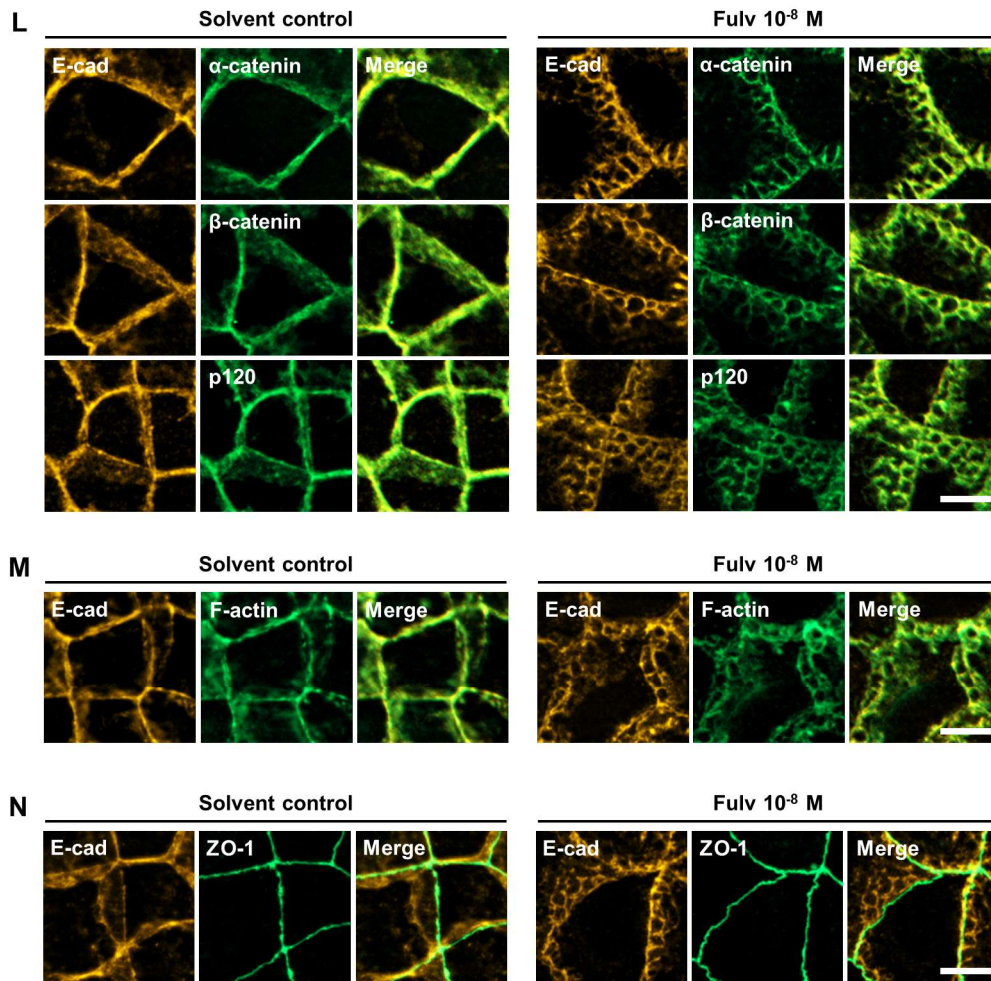


**Figure 1: Fulvestrant treatment reorganizes adherens junctions in MCF-7/vBOS cells.**

(A+B) MCF-7/vBOS cells were treated with Fulvestrant (Fulv)  $10^{-8}$  M for 48 hours. Cells were then (A) visualized by phase contrast microscopy, or (B) immunostained for E-cadherin (E-cad) and imaged by immunofluorescence microscopy. White boxes indicate enlarged areas. (C) MCF-7/vBOS cells were treated with different concentrations of Fulvestrant for 48 hours. Relative *CDHI* mRNA levels were quantified by qPCR,  $n = 3$ , mean  $\pm$  SD, ns = not significant. (D) MCF-7/vBOS cells were treated with Fulvestrant  $10^{-8}$  M for 48 hours. E-cadherin protein levels were quantified by western blot analysis,  $n = 3$ , mean  $\pm$  SD. Loading control, Coomassie. (E) MCF-7/vBOS cells were treated with Fulvestrant  $10^{-8}$  M for different periods of time. Immunostaining of E-cadherin. (F) MCF-7/vBOS cells were treated with Fulvestrant  $10^{-8}$  M for 24 hours and then treated with solvent control (ethanol, EtOH) for different periods of time. Immunostaining of E-cadherin. (G) MCF-7/vBOS cells were seeded on differently coated cover slips and subsequently treated with Fulvestrant  $10^{-8}$  M for 48 hours. Immunostaining of E-cadherin. (H) Transmission electron microscopy of MCF-7/vBOS cells treated with Fulvestrant  $10^{-8}$  M for 48 hours. Black boxes indicate enlarged areas. Scale bars, 10 and 1  $\mu$ m. (J) Transmission electron microscopy with immuno-gold labeling of E-cadherin of MCF-7/vBOS cells treated with Fulvestrant  $10^{-8}$  M for 48 hours. Boxes indicate enlarged areas. Scale bars, 10 and 0.1  $\mu$ m. (K) Schematic representation of the morphology of E-cadherin-mediated cell-cell contacts in immunofluorescence microscopy (IFM) and transmission electron microscopy (TEM). E-cadherin-mediated cell-cell contacts, red. (L-N) MCF-7/vBOS cells were treated with Fulvestrant  $10^{-8}$  M for 48 hours, immunostained for E-cadherin and (L) co-immunostained for  $\alpha$ -catenin,  $\beta$ -catenin, and p120, (M) co-phalloidin-stained for actin filaments (F-actin), or (N) co-immunostained for ZO-1. (A-G, L-N) Scale bars, 10  $\mu$ m.

## 5.2. Inhibition of ER $\alpha$ signaling induces adherens junction reorganization

Fulvestrant is a well-characterized and clinically used antiestrogen. It exerts its antiestrogenic potential via a competitive antagonism at the ligand-binding site of the ER and via decreasing ER protein levels.<sup>26</sup> 17 $\beta$ -estradiol is one of the strongest endogenous ER agonists.<sup>21</sup>

To test if the reorganization of AJs upon treatment with Fulvestrant is a specific effect related to inhibition of ER $\alpha$  signaling, MCF-7/vBOS cells were treated with different concentrations of Fulvestrant. ER $\alpha$  signaling was monitored by quantification of the typical ER $\alpha$  target genes *BCL2L1* and *TFF1*.<sup>68</sup> Immunostaining of E-cadherin served as a marker for AJs. As expected, Fulvestrant treatment resulted in concentration-dependent upregulation of *BCL2L1* and downregulation of *TFF1* mRNA levels. Interestingly, Fulvestrant treatment induced AJ reorganization in a dose-dependent manner which correlated well with the regulation of ER $\alpha$  target genes (Fig. 2A). Furthermore, treatment with a fixed concentration of Fulvestrant 10<sup>-8</sup> M and co-treatment with different concentrations of 17 $\beta$ -estradiol could prevent the effect of Fulvestrant on AJ organization. Again, this correlated with ER $\alpha$  target gene regulation (Fig. 2B). These results suggest that the reorganization of AJs upon Fulvestrant treatment of MCF-7/vBOS cells is caused by ER $\alpha$  inhibition. However, other ER subtypes might be involved as well.

In order to further substantiate the role of ER $\alpha$  inhibition for AJ reorganization in MCF-7/vBOS cells, cells were treated with other drugs inhibiting ER $\alpha$  signaling. Tamoxifen is a selective estrogen receptor modulator which is also clinically used for breast cancer therapy.<sup>24</sup> In addition, cells were treated with substances not approved for human application such as the selective ER $\alpha$  antagonist MPP<sup>69</sup> and the ER antagonist ZK 164,015<sup>70</sup>. The selective estrogen receptor  $\beta$  (ER $\beta$ ) antagonist PHTPP served as negative control.<sup>71</sup> Treatment of MCF-7/vBOS cells with Tamoxifen, MPP, and ZK 164,015 resulted in AJ reorganization in a dose-dependent manner (Fig. 2C-E). In the case of Tamoxifen and MPP, treatment for periods of time longer than 48 hours was required to obtain the specific phenotype of reorganized AJs (Fig. 2C+D). Treatment with PHTPP did not cause AJ reorganization in MCF-7/vBOS cells (Fig. 2F). This indicates that AJ reorganization is an effect which is specific to ER $\alpha$  inhibition.

To study if disruption of ER $\alpha$  signaling activity alone is sufficient to induce AJ reorganization, ER $\alpha$  knockdown experiments were conducted on MCF-7/vBOS cells. For this purpose, cells were transfected with siRNA against the ER $\alpha$ -coding gene *ESR1*. To ensure the specificity of ER $\alpha$  knockdown, three different siRNA samples against *ESR1* were used. An unspecific control siRNA sample served as negative control. ER $\alpha$  knockdown efficacy was monitored by assessing ER $\alpha$  protein levels by western blot analysis. Interestingly, all *ESR1*-

specific siRNA samples tested were able to induce AJ reorganization in MCF-7/vBOS cells (Fig. 2G). Correspondingly, transfection of all *ESR1*-specific siRNA samples resulted in reduced ER $\alpha$  protein levels (Fig. 2H). Unspecific control siRNA had no effect on ER $\alpha$  protein levels nor on AJ organization (Fig. 2G+H). Groups of cells expressing ER $\alpha$  despite ER $\alpha$  knockdown did not exhibit AJ reorganization (Fig. 2J, crosses), while cells with low ER $\alpha$  protein levels displayed reorganized AJs (Fig. 2J, stars). Although the latter could not be consistently observed, ER $\alpha$  knockdown experiments strongly suggest that the disruption of ER $\alpha$  signaling alone is sufficient to induce AJ reorganization in MCF-7/vBOS cells.

Taken together, these results demonstrate that AJ reorganization in MCF-7/vBOS is not specific to the treatment with Fulvestrant. Instead, AJ reorganization is also induced by other antiestrogens via the inhibition of ER $\alpha$  signaling.

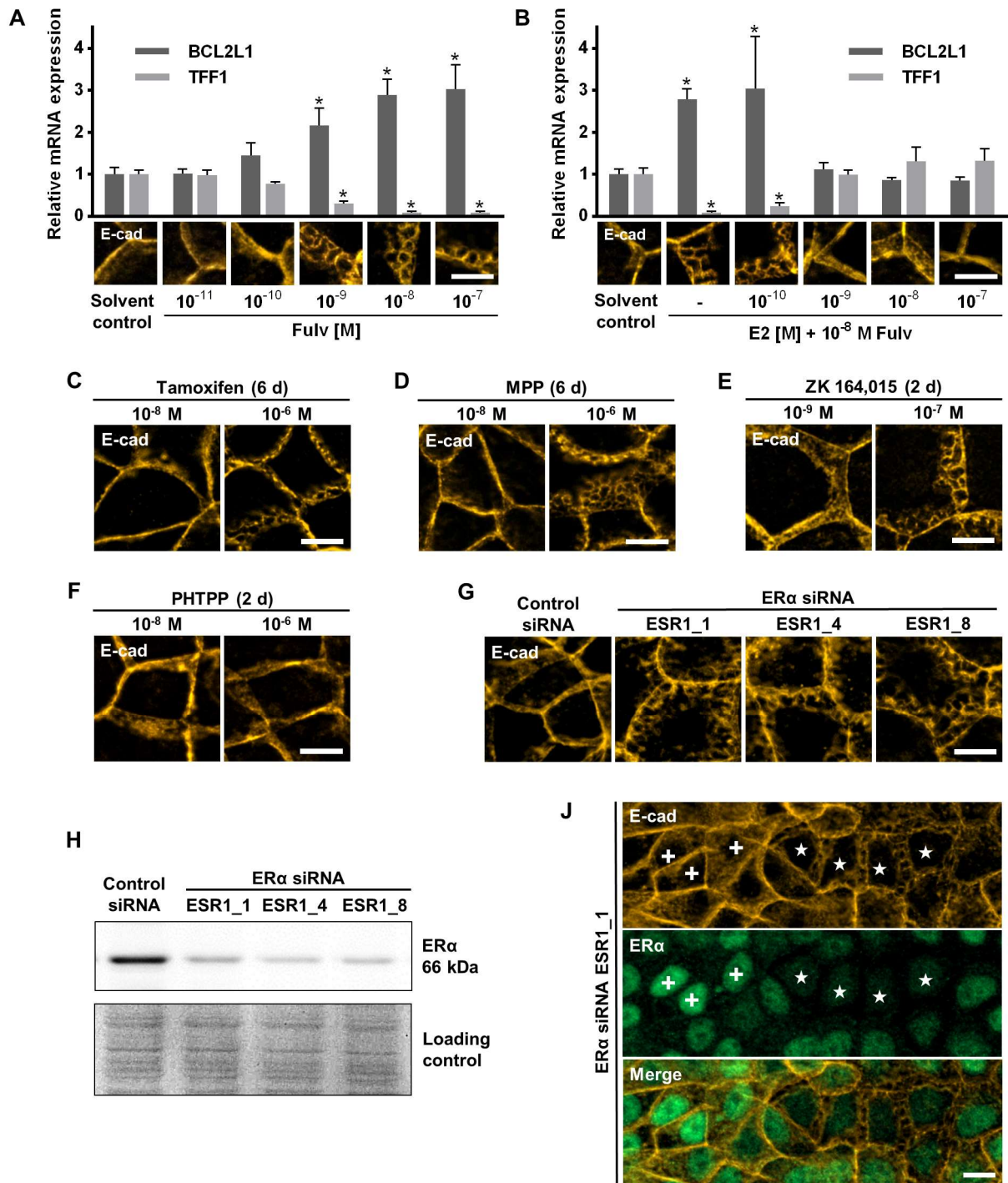


## Figure 2: Inhibition of ER $\alpha$ signaling induces adherens junction reorganization.

(A) MCF-7/vBOS cells were treated with different concentrations of Fulvestrant (Fulv) for 48 hours or (B) with Fulvestrant 10<sup>-8</sup> M and different concentrations of 17 $\beta$ -estradiol for 48 hours.<sup>§</sup> (A+B) Quantification of mRNA levels of typical ER $\alpha$  target genes by qPCR, n = 3, mean  $\pm$  SD, \* = p < 0.01. Corresponding immunostaining of E-cadherin (E-cad). (C-F) MCF-7/vBOS cells were treated with different ER antagonists at indicated concentrations for indicated periods of time. (G-J) MCF-7/vBOS cells were transfected with control siRNA and different siRNA samples against the *ESR1* gene and then cultured for 72 hours. (G) Immunostaining of E-cadherin. (H) Western blot of ER $\alpha$  protein. Loading control, Coomassie. (J) Co-immunostaining of E-cadherin and ER $\alpha$ . (A-J) Scale bars, 10  $\mu$ m.

<sup>§</sup> Samples kindly provided by Marja Kornhuber, Federal Institute for Risk Assessment.

### **5.3. Adherens junction reorganization depends on the cortical actomyosin cytoskeleton**

Proteins of the AJ complex and actin filaments displayed a strong co-localization in MCF-7/vBOS cells, indicating intact AJs in both untreated and Fulvestrant-treated cells (see Fig.1L+M). Dynamics of the cortical actomyosin cytoskeleton actively regulate the assembly of AJs during the formation and maturation of cell-cell contacts.<sup>52</sup> Therefore, AJ reorganization in MCF-7/vBOS cells upon Fulvestrant treatment might be affected by the cortical actomyosin cytoskeleton.

Since the dynamics of the cortical actomyosin cytoskeleton are strongly influenced by polymerization and depolymerization of actin filaments<sup>58</sup>, the impact of these processes on AJ reorganization was studied by pharmacological modulation. Polymerization of actin filaments was inhibited using latrunculin A which binds to actin monomers and prevents their polymerization.<sup>72</sup> In turn, jasplakinolide binds to actin filaments and inhibits their depolymerization.<sup>73</sup> MCF-7/vBOS cells were treated with Fulvestrant  $10^{-8}$  M and simultaneously co-treated with latrunculin A or jasplakinolide for 48 hours, respectively. Actin filaments were visualized by fluorophore-conjugated phalloidin. Immunostaining of E-cadherin served as a marker for AJs.

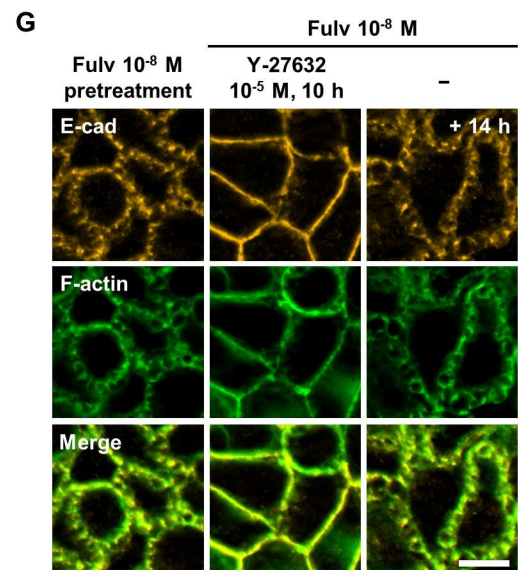
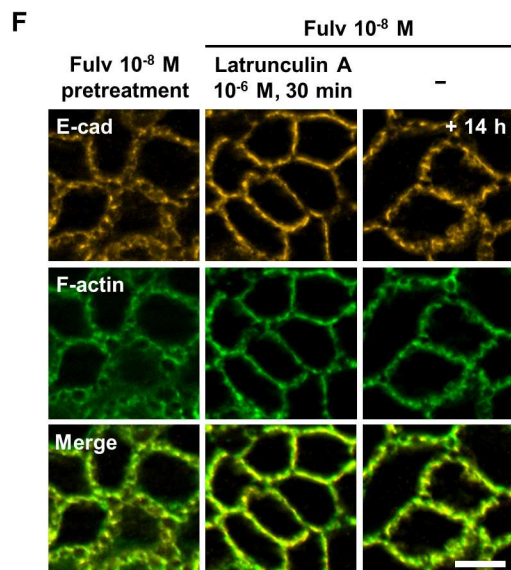
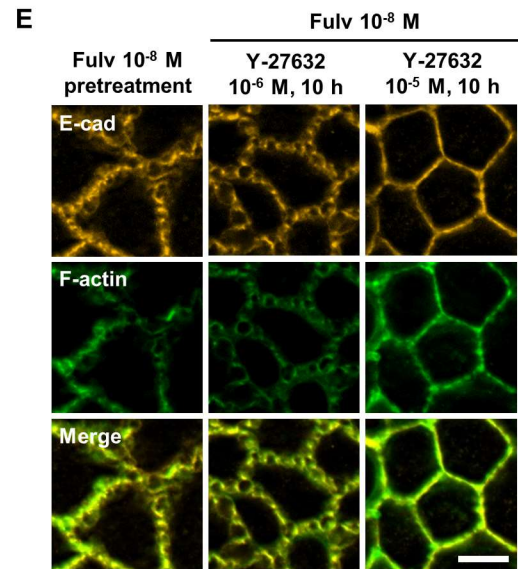
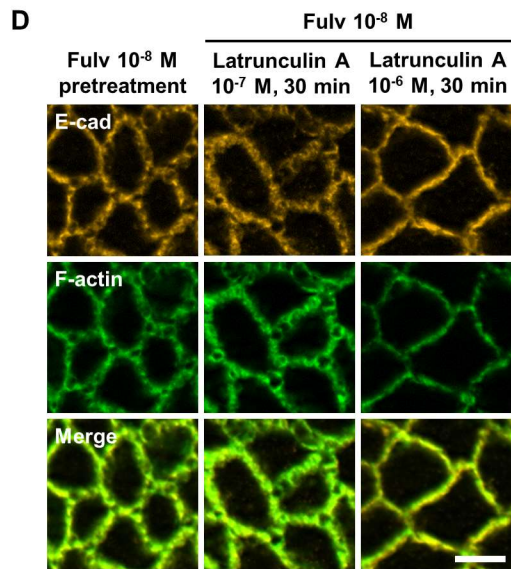
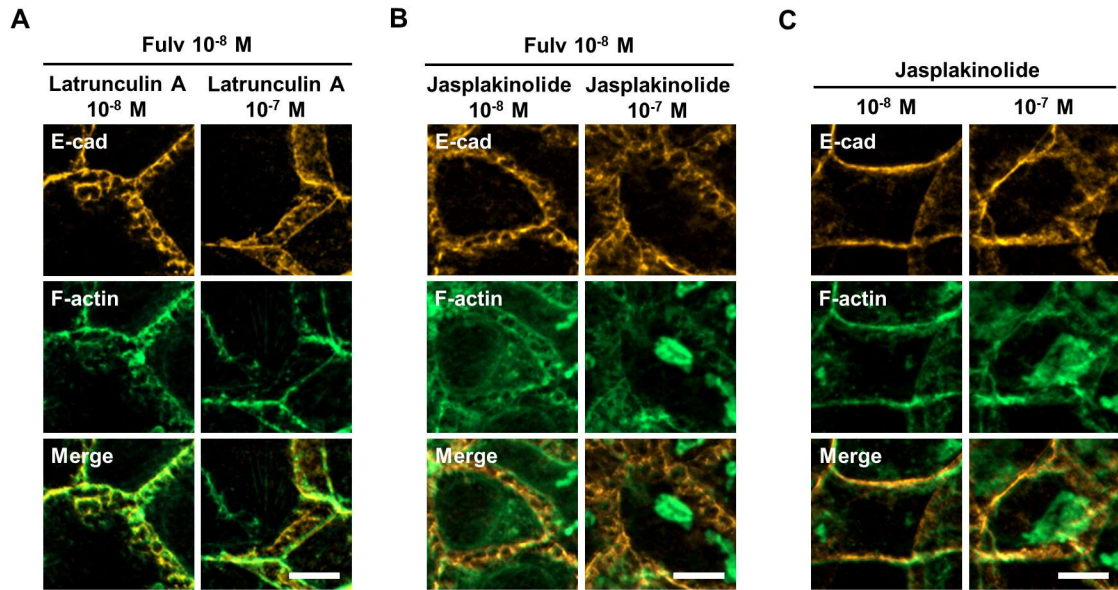
As expected, co-treatment with high concentrations of latrunculin A led to complete depolymerization of actin filaments and resulted in cell death (data not shown). However, co-treatment with lower concentrations did not result in complete depolymerization of actin filaments but distinctly attenuated AJ reorganization in a dose-dependent manner (Fig. 3A). In contrast, inhibition of actin filament depolymerization by co-treatment with jasplakinolide did not perturb the reorganization of AJs upon Fulvestrant treatment (Fig. 3B). In addition, treatment of MCF-7/vBOS cells with jasplakinolide alone was not able to induce AJ reorganization (Fig. 3C). These results indicate that adequate polymerization of actin filaments is required for AJ reorganization in Fulvestrant-treated MCF-7/vBOS cells. However, promoting actin filament polymerization by inhibiting depolymerization alone is not sufficient to reorganize AJs.

In order to investigate the role of the cortical actomyosin cytoskeleton for maintenance of reorganized AJs and to reduce possible cytotoxic side effects of long-term co-treatment with latrunculin A, actomyosin dynamics of pretreated MCF-7/vBOS cells already exhibiting reorganized AJs were modulated. As described above, polymerization of actin filaments was inhibited by latrunculin A. In addition, cells were treated with Y-27632 which is an inhibitor of the rho-associated coiled-coil-containing protein kinase (ROCK). ROCK is an effector kinase of the small GTPase Rho A that regulates both actin filament polymerization and contractility of the

actomyosin network.<sup>74</sup> Again, fluorophore-conjugated phalloidin and immunostaining of E-cadherin were used to visualize actin filaments and AJs, respectively.

MCF-7/vBOS cells pretreated with Fulvestrant  $10^{-8}$  M for 48 hours consistently exhibited reorganized AJs. Short-term treatment with either latrunculin A or Y-27632 was able to largely dissolve AJ reorganization in a dose-dependent manner (Fig. 3D+E). After latrunculin or Y-27632 was washed out and cells were further cultivated, reorganization of AJs redeveloped within several hours (Fig. 3F+G). Interestingly, the redevelopment of reorganized AJs did not require further Fulvestrant treatment (Fig. 3H+J). These experiments demonstrate that not only the formation but also the maintenance of AJ reorganization upon Fulvestrant treatment of MCF-7/vBOS cells requires sufficient actin filament polymerization and might also depend on sufficient contractility of the actomyosin cytoskeleton. Furthermore, abolishment of AJ reorganization by modulation of actomyosin dynamics appears to be a reversible process. Redevelopment of AJ reorganization was independent from ongoing Fulvestrant treatment, corresponding to the observation that AJ reorganization is rather stable over the course of time (see Fig. 1F).

The fact that modulation of actin dynamics interferes with the formation and maintenance of AJ reorganization suggests that the cortical actomyosin cytoskeleton is essentially involved in AJ reorganization. Given the importance of the actomyosin cytoskeleton for AJ assembly, it is conceivable that Fulvestrant treatment might primarily affect signaling pathways regulating the cortical actomyosin cytoskeleton which could induce AJ reorganization in MCF-7/vBOS cells.



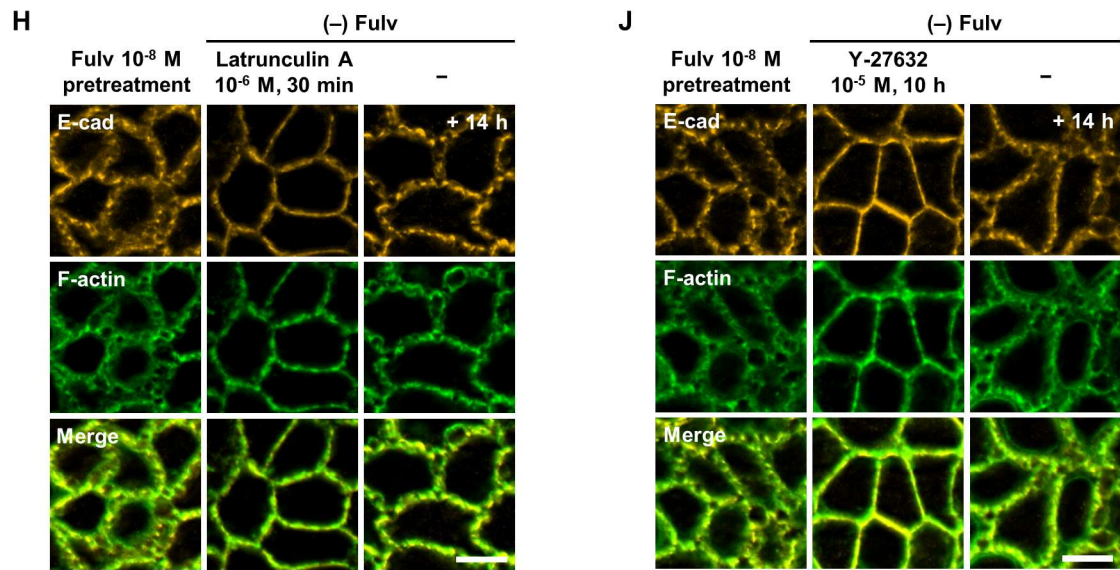


**Figure 3: Adherens junction reorganization depends on the cortical actomyosin cytoskeleton.** (A+B) MCF-7/vBOS cells were treated with Fulvestrant (Fulv)  $10^{-8}$  M and simultaneously co-treated with (A) the actin polymerization inhibitor latrunculin A, or (B) the actin depolymerization inhibitor jasplakinolide for 48 hours. (C) MCF-7/vBOS cells were treated with jasplakinolide for 48 hours. (D+E) MCF-7/vBOS cells were pretreated with Fulvestrant  $10^{-8}$  M for 48 hours. Subsequently, cells were treated with different concentrations of (D) latrunculin A for 30 min, or (E) the ROCK inhibitor Y-27632 for 10 hours. (F+G) MCF-7/vBOS cells were pretreated with Fulvestrant  $10^{-8}$  M for 48 hours. Subsequently, cells were treated with (F) latrunculin A  $10^{-6}$  M for 30 min, or (G) Y-27632  $10^{-5}$  M for 10 hours, and afterwards further cultured in medium containing Fulvestrant  $10^{-8}$  M. (H+J) MCF-7/vBOS cells were pretreated with Fulvestrant  $10^{-8}$  M for 48 hours. Subsequently, cells were treated with (H) latrunculin A  $10^{-6}$  M for 30 min, or (J) Y-27632  $10^{-5}$  M for 10 hours, and afterwards further cultured in Fulvestrant-free medium. (A-J) Immunostaining of E-cadherin (E-cad) and co-phalloidin-staining of actin filaments (F-actin). Scale bars, 10  $\mu$ m.

#### **5.4. Adherens junction reorganization is mediated by Arp2/3, but not by cortactin**

Fulvestrant treatment induces AJ reorganization via inhibition of ER $\alpha$  signaling in MCF-7/vBOS cells. AJ reorganization depends on the dynamics of the actomyosin cytoskeleton. Hence, Fulvestrant treatment might induce AJ reorganization in MCF-7/vBOS cells via ER $\alpha$ -dependent mechanisms regulating the cortical actomyosin cytoskeleton. The Arp2/3 complex is essential for the generation of branched actin networks as found in the cell cortex and has been shown to be particularly involved in actin assembly at AJs.<sup>53</sup> Therefore, Arp2/3 activity might play a role in AJ reorganization in MCF-7/vBOS cells upon Fulvestrant treatment.

To assess the role of Arp2/3 activity for AJ organization, MCF-7/vBOS cells were treated with the Arp2/3 inhibitor CK666. CK666 inhibits the Arp2/3-initiated formation of branched actin networks by stabilizing the Arp2/3 complex in an inactive conformational state.<sup>75</sup> Co-treatment of MCF-7/vBOS cells with Fulvestrant 10<sup>-8</sup> M and different concentration of CK666 for 48 hours showed that CK666 co-treatment attenuated AJ reorganization in a dose-dependent manner (Fig. 4A). This suggests that formation of reorganized AJs in Fulvestrant-treated MCF-7/vBOS cells depends on the activity of the Arp2/3 complex.

The activity of the Arp2/3 complex is regulated by other actin-regulating proteins such as cortactin. Cortactin activity is regulated by different tyrosine and serine/threonine kinases.<sup>76</sup> Tyrosine phosphorylation of cortactin by Src family kinases (SFKs) has been shown to affect the organization of AJs in MCF-7 cells.<sup>77</sup> Accordingly, this mechanism might be important in AJ reorganization in MCF-7/vBOS cells upon Fulvestrant treatment. Co-immunostaining of E-cadherin and cortactin of MCF-7/vBOS cells treated with Fulvestrant 10<sup>-8</sup> M for 48 hours revealed that both solvent control and Fulvestrant-treated cells expressed cortactin. Under both conditions, cortactin was located both in the cytosol and at cell membranes. The morphological changes of AJs upon Fulvestrant treatment, as visualized by E-cadherin staining, could partly be recapitulated in cortactin staining as well (Fig. 4B). In order to study the effects of cortactin on AJ organization in MCF-7/vBOS cells, cortactin tyrosine phosphorylation via SFKs was inhibited by treatment of cells with the SFK inhibitor PP2<sup>78</sup>. Interestingly, PP2 treatment altered the organization of AJs in a way that very closely resembled AJ reorganization upon Fulvestrant treatment (Fig. 4C). While AJ reorganization induced by Fulvestrant could be prevented by simultaneous co-treatment with 17 $\beta$ -estradiol (see also Fig. 2B), 17 $\beta$ -estradiol co-treatment could not prevent AJ reorganization upon PP2 treatment (Fig. 4D). This suggests that PP2 treatment is unlikely to directly interfere with ER $\alpha$  signaling.

Instead, PP2 has been reported to specifically inhibit SFKs.<sup>78</sup> The functional state of SFKs was assessed by investigation of different phosphorylation sites of the SFK c-Src by western blot analyses. Tyrosine-416-phosphorylation has been shown to activate c-Src, while tyrosine-527-phosphorylation decreases c-Src activity.<sup>79</sup> As expected, treatment with the SFK inhibitor PP2 decreased relative levels of active tyrosine-416-phosphorylated c-Src (phospho-cSrc(Y416)) in MCF-7/vBOS cells (Fig. 4E). However, relative levels of inactive tyrosine-527-phosphorylated c-Src (phospho-cSrc(Y527)) were also decreased upon PP2 treatment (Fig. 4F). In contrast, Fulvestrant treatment affected neither the relative levels of phospho-cSrc(Y416) nor of phospho-cSrc(Y527) (Fig. 4E+F). Note that the significance of these results is limited since total protein levels of c-Src were not measured. Thus, the effects of PP2 and Fulvestrant treatment on c-Src activity remain vague in MCF-7/vBOS cells.

To directly study the effect of PP2 and Fulvestrant on cortactin phosphorylation, relative levels of tyrosine-421-phosphorylated cortactin (phospho-cortactin(Y421)) were determined. Here, PP2 treatment distinctly reduced the relative levels of phospho-cortactin(Y421), which were by tendency increased upon Fulvestrant treatment (Fig. 4G). Despite contradictory regulation of c-Src phosphorylation, altered AJ organization induced by PP2 was accompanied by a distinct decrease of phospho-cortactin(Y421). In contrast, Fulvestrant induced AJ reorganization without affecting phospho-cortactin(Y421) levels. Although total protein levels of cortactin were not determined, these results suggest that AJ reorganization is accompanied by reduced cortactin tyrosine phosphorylation upon PP2 treatment, but not upon Fulvestrant treatment.

Together, these results indicate that AJ reorganization upon Fulvestrant treatment of MCF-7/vBOS cells depends on the activity of the Arp2/3 protein complex but might be independent from tyrosine phosphorylation of the Arp2/3-regulating protein cortactin.

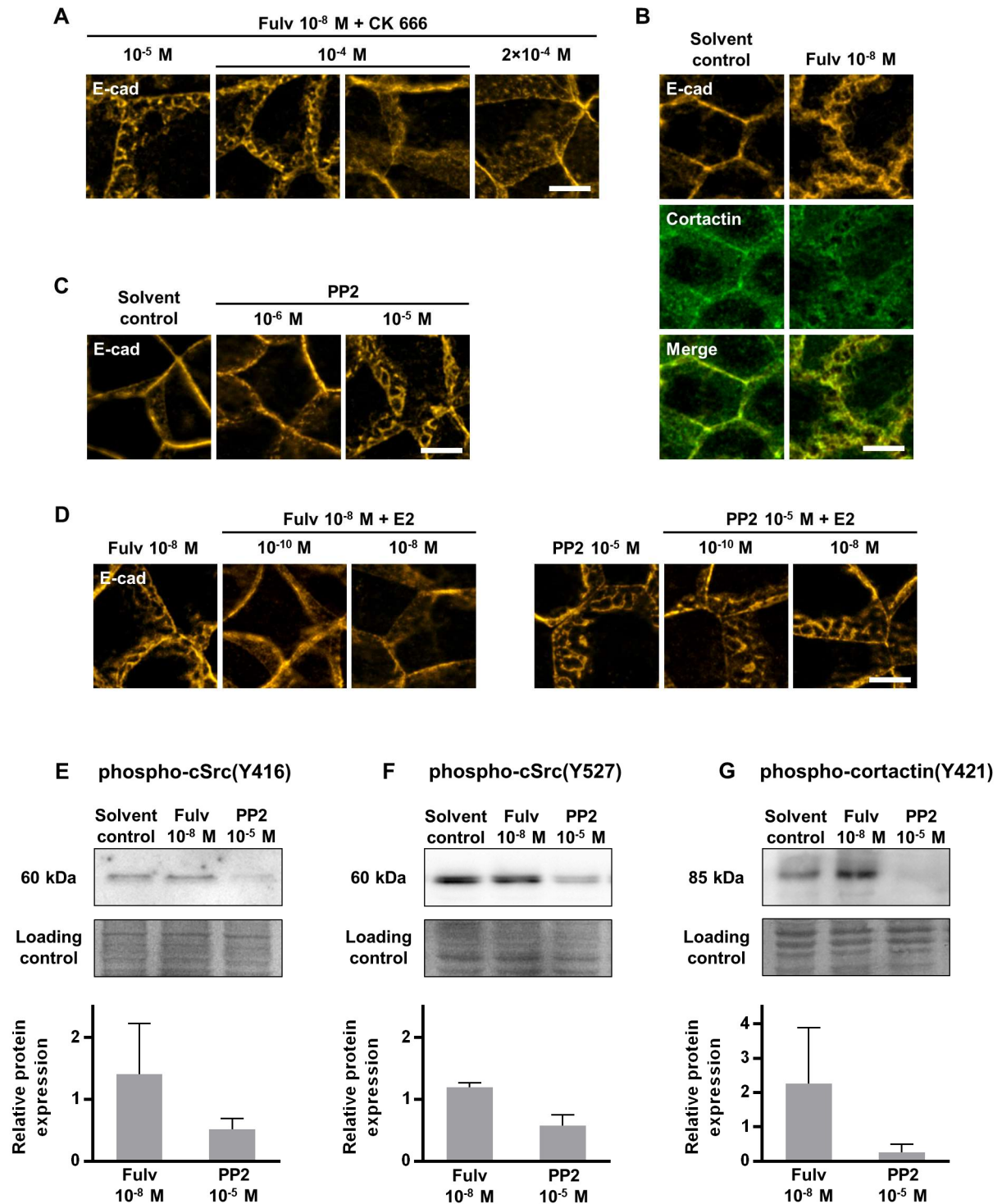


**Figure 4: Adherens junction reorganization is mediated by Arp2/3, but not by cortactin.**

(A) MCF-7/vBOS cells were treated with Fulvestrant (Fulv)  $10^{-8}$  M and co-treated with the Arp2/3 inhibitor CK666 for 48 hours. Immunostaining of E-cadherin (E-cad). (B) MCF-7/vBOS cells were treated with Fulvestrant  $10^{-8}$  M for 48 hours. Co-immunostaining of E-cadherin and cortactin. (C) MCF-7/vBOS cells were treated with different concentrations of the SFK inhibitor PP2 for 48 hours. Immunostaining of E-cadherin. (D) MCF-7/vBOS cells were treated with either Fulvestrant  $10^{-8}$  M or PP2  $10^{-5}$  M, and co-treated with  $17\beta$ -estradiol, respectively, for 48 hours. Immunostaining of E-cadherin. (E-G) MCF-7/vBOS cells were treated with either Fulvestrant  $10^{-8}$  M or PP2  $10^{-5}$  M for 48 hours. Western blot analysis and relative protein levels of (E) phospho-cSrc(Y416), (F) phospho-cSrc(Y527), and (G) phospho-cortactin(Y421). (A-D) Scale bars, 10  $\mu$ m. (E-G) n = 3, mean  $\pm$  SD. Loading control, Coomassie.

## 5.5. Fulvestrant treatment affects the maturation of adherens junctions

The cortical actomyosin cytoskeleton is essential for the initiation, expansion, and maturation of cell-cell contacts mediated by AJs.<sup>52</sup> Since Fulvestrant treatment of MCF-7/vBOS cells leads to an actomyosin-dependent reorganization of AJs, actomyosin-dependent processes during the formation of cell-cell contacts might be affected as well. To investigate this, the process of cell-cell contact formation was recapitulated by calcium switch experiments. The homophilic interaction of E-cadherin molecules requires calcium ions.<sup>51</sup> E-cadherin-mediated AJs were disrupted by treatment with the calcium-chelating agent EGTA in order to deplete the medium of calcium ions. After disruption of AJs, the calcium-depleted medium was exchanged for fresh calcium-containing medium to enable homophilic E-cadherin interaction. The subsequent *de novo* formation of E-cadherin-mediated cell-cell contacts was monitored by immunostainings of E-cadherin at different time points. (Fig. 5A)

As expected, upon EGTA treatment, solvent control cells rounded and displayed diffuse E-cadherin staining all over the cell membrane, indicating disrupted AJs. After switching back to calcium-containing medium, cells re-established a confluent monolayer and displayed E-cadherin staining exclusively at basolateral cell membranes, marking the re-establishment of cell-cell contacts based on AJs (Fig. 5B(1)). In Fulvestrant-pretreated cells exhibiting reorganized AJs, EGTA treatment disrupted AJs and switching back to calcium-containing medium led to redevelopment of cell-cell contacts as well. However, initially formed AJs were not reorganized but uniformly distributed like in solvent control cells. Reorganization of AJs appeared only after several hours (Fig. 5B(3)). It is worth noting that the reorganization of AJs after the calcium switch did not require ongoing Fulvestrant treatment (Fig. 5B(2)). Cells treated with Fulvestrant only after the calcium switch developed reorganization of AJs only after a longer period of time (Fig. 5B(4)). This indicates that the pretreatment with Fulvestrant is crucial for the reorganization of AJs after the calcium switch. This corresponds to the observation that the reorganization of AJs is rather stable over the course of time (see Fig. 1F).

Taken together, the results from the calcium switch experiments show that AJ reorganization depends on homophilic E-cadherin interactions. Fulvestrant treatment did not impair the *de novo* formation of cell-cell contacts after disruption of AJs. Interestingly, AJ reorganization did not appear in early-formed cell-cell contacts but only after several hours in matured cell-cell contacts. This indicates that Fulvestrant treatment might induce AJ reorganization via pathways that regulate the cortical actomyosin cytoskeleton not in early steps of cell-cell contact formation, but in later steps of cell-cell contact maturation.

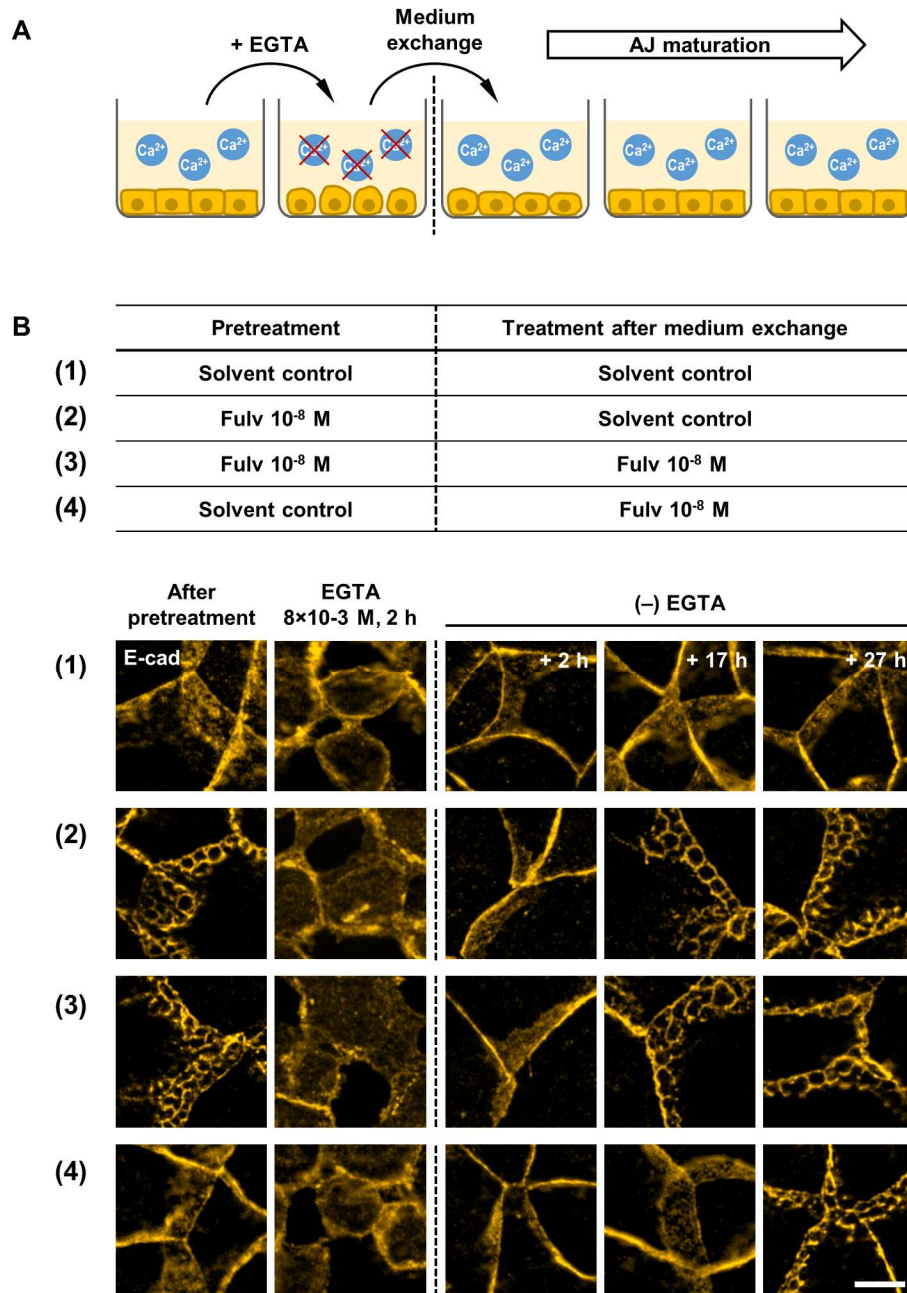


**Figure 5: Fulvestrant treatment affects the maturation of adherens junctions.**

(A) Schematic representation of calcium switch experiments in order to mimic the formation and maturation of AJs. (B) MCF-7/vBOS cells were pretreated with solvent control or Fulvestrant (Fulv)  $10^{-8}$  M for 48 hours. Subsequently, cells were treated with EGTA  $8 \times 10^{-3}$  M for 2 hours. Afterwards, calcium-depleted medium was exchanged for calcium-containing medium and cells were further cultivated in the presence or absence of Fulvestrant  $10^{-8}$  M. Table shows treatment of cells before and after the medium exchange. Cells were fixed and immunostained for E-cadherin (E-cad) at the indicated time points. Scale bar, 10  $\mu$ m.

## 5.6. Reorganization of adherens junctions decreases E-cadherin cleavage

Fulvestrant treatment causes AJ reorganization via ER $\alpha$  inhibition. Thereby, it might primarily affect the dynamics of the cortical actomyosin cytoskeleton and in particular the regulation of mature AJs. The stability and function of mature AJs can be regulated by proteolytical cleavage of E-cadherin. Different proteases such as ADAM10 have been shown to be involved in E-cadherin cleavage. ADAM10 cleaves E-cadherin at a distinct extracellular site near the transmembrane domain, generating an extracellular 80 kDa fragment and an intracellular 38 kDa fragment.<sup>57</sup>

To investigate if AJ reorganization alters E-cadherin cleavage, western blot analyses were performed using antibodies detecting the extracellular or intracellular domain of E-cadherin, respectively. MCF-7/vBOS cells were treated either with Fulvestrant  $10^{-8}$  M or with the ADAM10 inhibitor GI254023X  $5 \times 10^{-6}$  M for 48 hours, respectively. In solvent control cells, both the 80 kDa and 38 kDa fragment were detectable, indicating a constitutive cleavage of E-cadherin in MCF-7/vBOS cells. As expected, treatment with the ADAM10 inhibitor GI254023X distinctly suppressed E-cadherin cleavage, resulting in a significant decrease in the levels of both E-cadherin fragments. It is worth noting that treatment with Fulvestrant decreased levels of E-cadherin fragments to a similar extent (Fig. 6A), suggesting that Fulvestrant treatment prevents E-cadherin cleavage by ADAM 10. However, no distinct increase of 135 kDa full-length E-cadherin could be observed (Fig. 6A).

To test if the inhibition of E-cadherin cleavage affects the organization of AJs in MCF-7/vBOS cells, cells were treated with GI254023X and immunostained for E-cadherin to visualize AJs. However, the dose-dependent inhibition of E-cadherin cleavage by GI254023X did not alter the organization of AJs in MCF-7/vBOS cells (Fig. 6B). This indicates that inhibition of ADAM10-mediated E-cadherin cleavage does not affect AJ organization in MCF-7/vBOS cells.

To study if, in turn, AJ organization affects E-cadherin cleavage, the formation of AJ reorganization upon Fulvestrant treatment was prevented by simultaneous co-treatment with the actin polymerization inhibitor latrunculin A as described before (see Fig. 3A). Interestingly, co-treatment with latrunculin A increased levels of the 38 kDa E-cadherin fragment, although not completely restoring the levels of E-cadherin fragments (Fig. 6C). This suggests that AJ reorganization reduces the cleavage of E-cadherin in MCF-7/vBOS cells.

Together, these results show that Fulvestrant treatment suppresses E-cadherin cleavage. Prevention of Fulvestrant-induced AJ reorganization partly restored E-cadherin cleavage, suggesting that E-cadherin cleavage is regulated by AJ organization. Thus, Fulvestrant treatment might stabilize AJs by reducing E-cadherin cleavage by reorganizing AJs in MCF-7/vBOS cells.

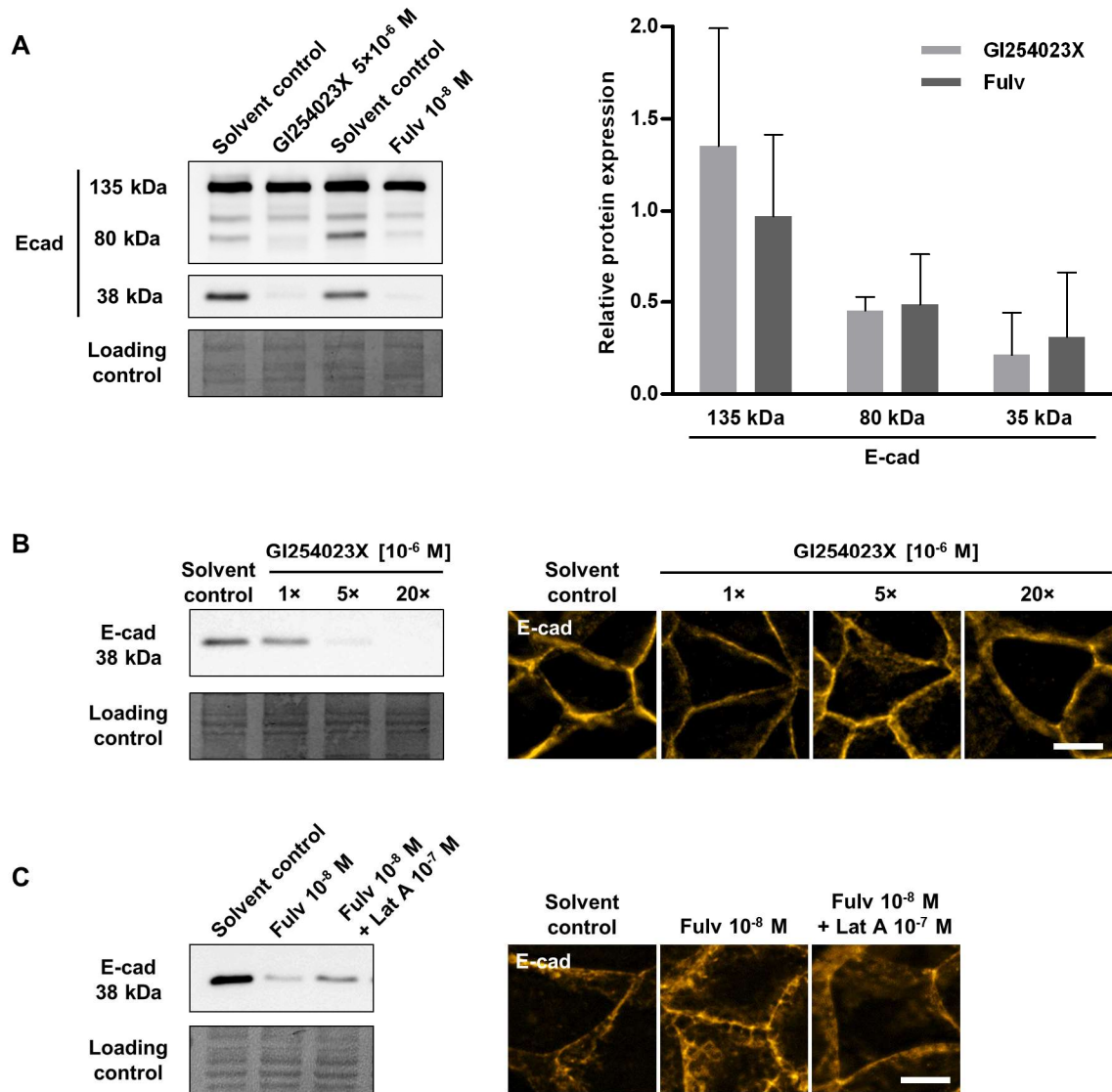


**Figure 6: Reorganization of adherens junctions decreases E-cadherin cleavage.**

(A) MCF-7/vBOS were treated with either the ADAM10 inhibitor GI254023X  $5 \times 10^{-6}$  M or Fulvestrant (Fulv)  $10^{-8}$  M for 48 hours, respectively. Relative protein levels of E-cadherin (E-cad) fragments were quantified by western blot analysis,  $n = 3$ , mean  $\pm$  SD. Loading control, Coomassie. (B) MCF-7/vBOS cells were treated with different concentrations of GI254023X for 48 hours. Western blot of the 38 kDa intracellular E-cadherin fragment. Corresponding immunostaining of E-cadherin. (C) MCF-7/vBOS cells were treated with Fulvestrant  $10^{-8}$  M and simultaneously co-treated with latrunculin A (Lat A)  $10^{-7}$  M for 48 hours. Western blot of the 38 kDa intracellular E-cadherin fragment. Corresponding immunostaining of E-cadherin. (B+C) Scale bars, 10  $\mu$ m.

## 5.7. Fulvestrant treatment increases cell stiffness and decreases cell motility

The actomyosin-dependent reorganization of mature AJs upon Fulvestrant treatment reduced E-cadherin cleavage in MCF-7/vBOS cells, which might stabilize AJs. In order to further investigate the functional consequences of AJ reorganization, the effects on cellular biomechanical properties and cell-cell adhesion were assessed.

In order to attribute possible effects of Fulvestrant treatment to AJ reorganization, MCF-7/vBOS cells were compared with MCF-7/ACC115 serving as control cell line. To visualize the effects of Fulvestrant treatment on AJs in MCF-7/ACC115 cells, cells were treated with Fulvestrant for 48 hours and subsequently immunostained for E-cadherin serving as a marker for AJs. In contrast to MCF-7/vBOS cells, no alterations in AJ organization were observed in MCF-7/ACC115 upon Fulvestrant treatment (Fig. 7A). To ensure the responsiveness of MCF-7/ACC115 cells to ER $\alpha$  inhibition by Fulvestrant, transcription of the published ER $\alpha$  target genes *TFF1* and *BCL2L1* was quantified. Comparable to MCF-7/vBOS cells, in MCF-7/ACC115 cells, Fulvestrant treatment decreased mRNA levels of *TFF1* and increased mRNA levels of *BCL2L1*. However, MCF-7/vBOS and MCF-7/ACC115 cells differed in the extent of ER $\alpha$  target gene regulation (Fig. 7B). Since responding to ER $\alpha$  inhibition without developing AJ reorganization, MCF-7/ACC115 is a suitable control cell line to study if possible functional consequences of Fulvestrant treatment are related to AJ reorganization.

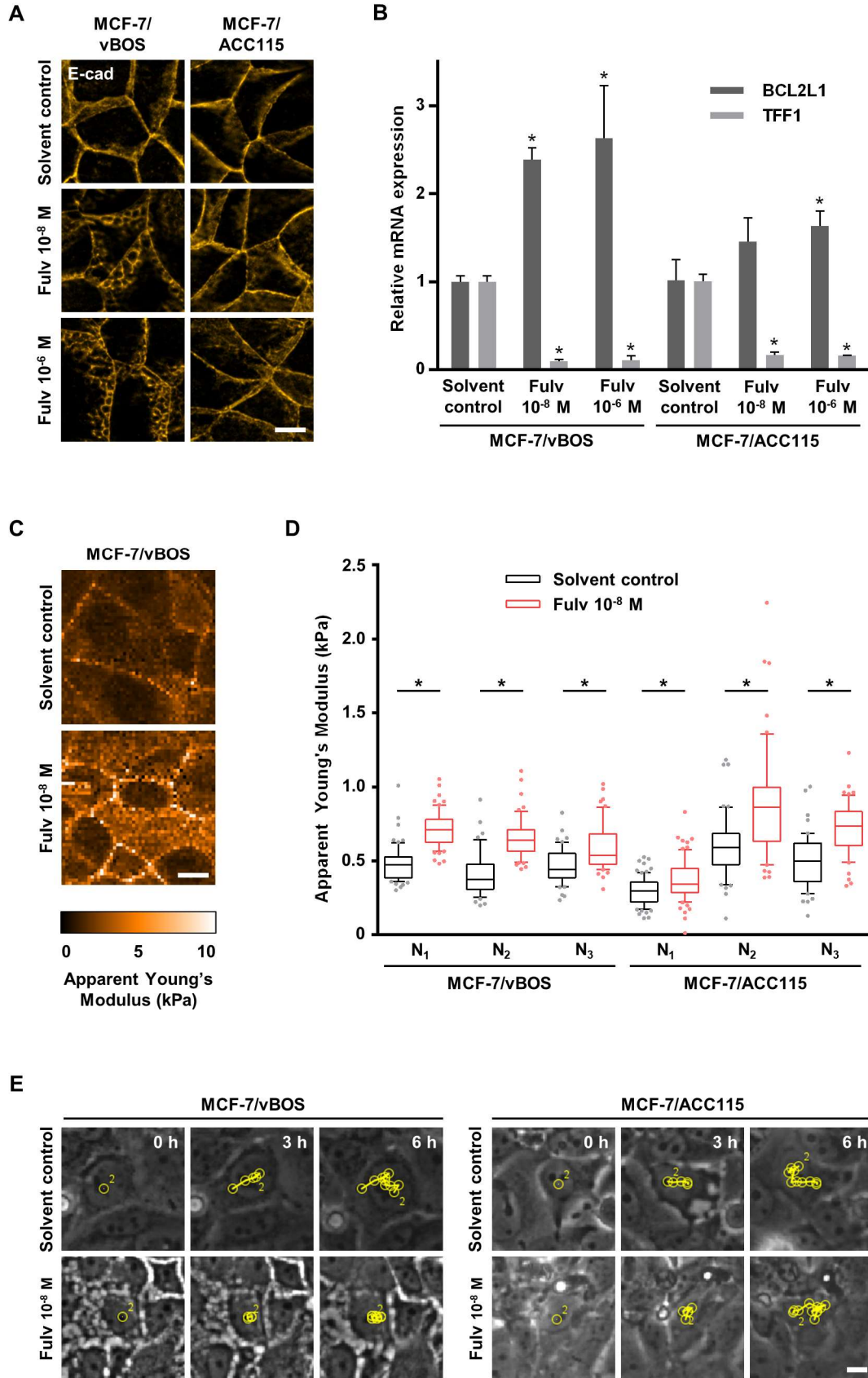
Since AJ reorganization depends on the cortical actomyosin cytoskeleton, Fulvestrant treatment might primarily affect pathways regulating actomyosin dynamics. The functional state of the actomyosin cytoskeleton determines biomechanical properties of the cell such as cell stiffness.<sup>80</sup> Accordingly, Fulvestrant treatment might change the biomechanical properties of MCF-7/vBOS cells. To test this, MCF-7/vBOS and MCF-7/ACC115 cells were treated with Fulvestrant  $10^{-8}$  M for 48 hours. Subsequently, cell stiffness was measured by atomic force microscopy in cooperation with *Anna Taubenberger*\*. Interestingly, Fulvestrant treatment increased cell stiffness in MCF-7/vBOS cells, particularly in the regions of cell-cell junctions (Fig. 7C). Quantification of cell stiffness throughout the surface of the cell monolayer revealed a significant increase in cell stiffness upon Fulvestrant treatment. However, this was not specific to MCF-7/vBOS cells but was also the case in MCF-7/ACC115 cells (Fig. 7D). This indicates that the increase of cell stiffness in Fulvestrant-treated MCF-7/vBOS cells treatment might not be related to AJ reorganization.

---

\* BIOTEC, Biotechnological Center TU Dresden

Assuming that movements of individual cells in a confluent monolayer of cells require dynamic break-up and redevelopment of cell-cell contacts, increased intercellular adhesion would result in lower cell motility under confluent conditions. To study cell motility as a proxy for intercellular adhesion, cell motility assays were performed on MCF-7/vBOS and MCF-7/ACC115 cells. For this purpose, the monolayer of confluent solvent control and pretreated cells was scratched with a pipette tip to provide space for cell movements and cells were cultured and treated for three more days. Subsequently, the confluent region near the scratch was imaged by phase contrast microscopy over the course of time. Phase contrast images were used to track the movements of a representative number of cells by using the Fiji plugin MTrack (Fig. 7E). Trajectory plots of both MCF-7/vBOS and MCF-7/ACC115 cells show cell movements of no certain direction within the confluent monolayer. However, in MCF-7/vBOS cells, Fulvestrant-treated cells were rather immobile compared to the solvent control. In contrast, Fulvestrant treatment did not change the mobility of MCF-7/ACC115 cells (Fig. 7F). Quantification of trajectory length of the tracked cells revealed that solvent control cells covered a significantly longer distance than Fulvestrant-treated MCF-7/vBOS cells, while there was no significant difference between solvent control and Fulvestrant-treated MCF-7/ACC115 cells (Fig. 7G). The decrease of cell motility within the confluent monolayer suggests that Fulvestrant treatment increases intercellular adhesion in MCF-7/vBOS cells.

Fulvestrant treatment increased cell stiffness in both MCF-7/vBOS and MCF-7/ACC115 cells. In MCF-7/vBOS cells, Fulvestrant treatment additionally decreased cell motility, suggesting increased cell-cell adhesion. Both cell stiffness and intercellular adhesion might affect the metastatic potential of breast cancer cells. However, only the increase in intercellular adhesion might be a functional consequence of Fulvestrant-induced AJ reorganization in MCF-7/vBOS cells.



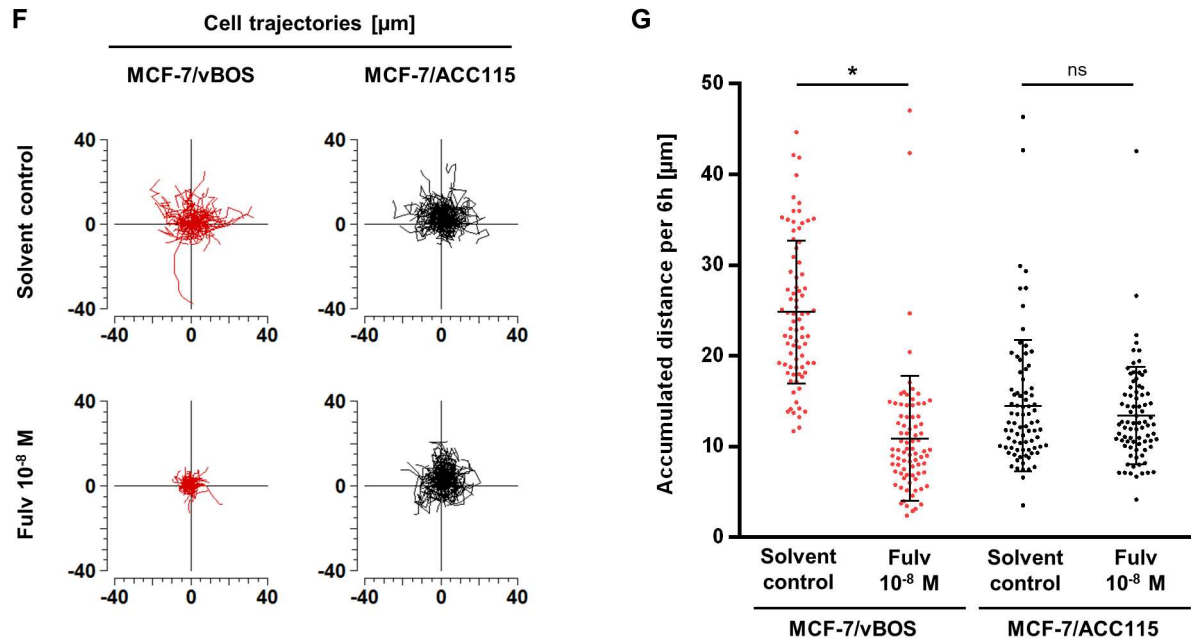


**Figure 7: Fulvestrant treatment increases cell stiffness and decreases cell motility.**

(A+B) MCF-7/vBOS and MCF-7/ACC115 cells were treated with Fulvestrant (Fulv) for 48 hours. (A) Immunostaining of E-cadherin (E-cad). (B) Quantification of mRNA levels of typical ER $\alpha$  target genes by qPCR,  $n = 3$ , mean  $\pm$  SD, \* =  $p < 0.05$ . (C) Cell stiffness distribution map generated by atomic force microscopy of MCF-7/vBOS cells treated with Fulvestrant  $10^{-8}$  M for 48 hours. (D) MCF-7/vBOS and MCF-7/ACC115 cells were treated with Fulvestrant for 48 hours. Quantification of cell stiffness (Apparent Young's Modulus), depicted are individual biological replicates ( $N_1, N_2, N_3$ ). 40-80 cells per biological replicate, \* =  $p < 0.01$ . Boxes, lower quartile, median, and upper quartile. Whiskers, 10<sup>th</sup> and 90<sup>th</sup> percentile. (E-G) MCF-7/vBOS and MCF-7/ACC115 cells were pretreated with Fulvestrant  $10^{-8}$  M for 48 hours. The monolayer was scratched with a pipette tip and cells were further treated for 72 hours, now in the presence of cytarabine  $10^{-5}$  M in order to inhibit proliferation. Subsequently, confluent regions near the scratch were imaged by phase contrast microscopy over the course of 6 hours. (E) Tracking of cell movements using the plugin MTrack of the Fiji software. (F) Trajectory plots of 81 tracked cells per condition generated using the Chemotaxis and Migration Tool software. (G) Quantification of accumulated distance using the plugin MTrack of the Fiji software,  $n = 3$ , 27 cells per biological replicate, mean  $\pm$  SD, \* =  $p < 0.01$ , ns = not significant. (A+C+E) Scale bars, 10  $\mu\text{m}$ .

## 5.8. Adherens junction organization and ER $\alpha$ signaling correlate in breast cancer tissue sections

AJ reorganization upon Fulvestrant treatment decreased cell motility, suggesting an increase in intercellular adhesion. This might affect the risk of metastatic spread of E-cadherin-positive breast cancer cells *in vivo*. While lobular invasive carcinomas lose E-cadherin expression in most cases, invasive ductal carcinomas of the breast often retain E-cadherin expression.<sup>15</sup>

To study if the reorganization of AJs observed in MCF-7/vBOS cells can also be recapitulated *in vivo*, the organization of AJs was assessed by immunofluorescence microscopy of tissue microarrays kindly provided by *Barbara Ingold-Heppner\** and *Carsten Denkert\**. Tissue microarrays contained tissue sections from patients with diagnosed invasive ductal carcinoma (for the approval by the ethics committee see section 4.1.2). Immunostaining of E-cadherin served as a marker for AJs. As expected for invasive ductal carcinoma cells, most tissue samples expressed E-cadherin. It is worth noting that the organization of E-cadherin-mediated cell-cell contacts varied between the patients and within the sections. Besides cells exhibiting regular continuous cell-cell contacts, cells exhibiting irregular discontinuous E-cadherin-mediated cell-cell contacts could also be observed (Fig. 8A). This shows that AJs might be diversely organized *in vivo*.

In MCF-7/vBOS cells, ER $\alpha$  inhibition by Fulvestrant treatment induced AJ reorganization. Due to the very limited availability of tissue samples from patients undergoing antiestrogen therapy, ER $\alpha$  localization was used as a surrogate for ER $\alpha$  signaling activity to study the correlation between ER $\alpha$  and AJ reorganization *in vivo*. Since ligand-activated ER $\alpha$  translocates into the nucleus<sup>19</sup>, nuclear or cytosolic ER $\alpha$  localization might indicate high or low ER $\alpha$  signaling activity, respectively. The organization of E-cadherin-mediated cell-cell contacts (regular versus irregular) and the localization of ER $\alpha$  (nuclear versus cytosolic) were separately assessed by three observers independent from each other. To account for the heterogeneity of tumor cells *in vivo*, 6 to 10 randomly selected individual cells from each of 13 tissue samples were assessed separately. Interestingly, the appearance of irregular discontinuous E-cadherin-mediated cell-cell contacts correlated with primarily cytoplasmic ER $\alpha$  localization (Fig. 8B+C). This indicates that low ER $\alpha$  signaling activity correlates with irregular AJ organization in breast cancer cells *in vivo*.

Together these results show that AJs are diversely organized in breast cancer cells *in vivo* and might be regulated by ER $\alpha$  signaling activity. Thus, the organization of AJs and possible consequences for breast cancer metastasis might be affected by antiestrogen treatment *in vivo*.

---

\* Institute of Pathology, University Hospital Charité, Berlin

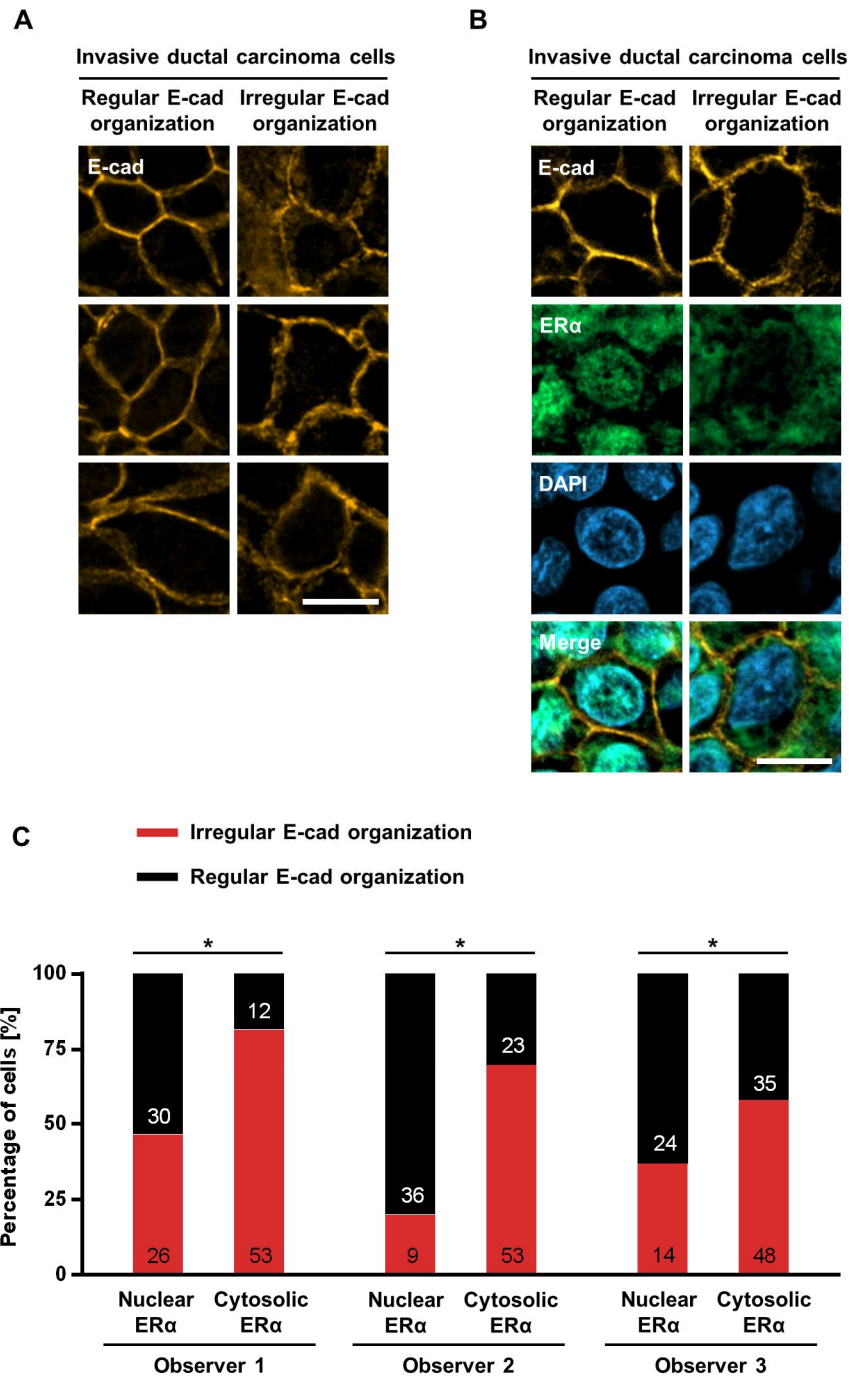


**Figure 8: Adherens junction organization and ER $\alpha$  signaling correlate in breast cancer tissue sections.**

(A) Samples of invasive ductal carcinoma were immunostained for E-cadherin (E-cad). Depicted are examples of cells exhibiting E-cadherin-mediated cell-cell contacts in regular or irregular organization, respectively. (B) Invasive ductal carcinoma cells were co-immunostained for E-cadherin and ER $\alpha$ . Depicted are cells exhibiting regular or irregular organized E-cadherin-mediated cell-cell contacts, and nuclear or cytosolic ER $\alpha$  localization, respectively. DAPI staining served to visualize cell nuclei. (C) E-cadherin organization and ER $\alpha$  localization was assessed by three observers. 6-10 cells of each of 13 tissue samples were assessed. Depicted are the relative proportions of cells displaying regular or irregular E-cadherin organization in dependence on ER $\alpha$  localization. Numbers in bars indicate absolute cell numbers. Contingency tables were analyzed using the Fisher's test, \* =  $p < 0.05$ . (A+B) Scale bars, 10  $\mu$ m.

## 6. Discussion

In my thesis, I studied estrogenic effects on the organization of E-cadherin-mediated AJs in the MCF-7/vBOS breast cancer cell line. I was able to show that treatment with antiestrogens such as Fulvestrant induced a specific ER $\alpha$ -dependent reorganization of AJs. This alteration of AJ organization was not accompanied by altered E-cadherin protein levels. Instead, the Fulvestrant-induced AJ reorganization essentially depended on the cortical actomyosin cytoskeleton. Despite the distinct reorganization of mature AJs, the formation of new E-cadherin-mediated cell-cell contacts was not perturbed. Fulvestrant treatment reduced the cleavage of E-cadherin, which could partly be attributed to AJ reorganization and suggests a higher stability of AJs. Correspondingly, AJ reorganization correlated with decreased cell motility, indicating an increase in intercellular adhesion. Additionally, Fulvestrant treatment increased cell stiffness. Intercellular adhesion and cell stiffness might be of importance in breast cancer metastasis. *In vivo*, I observed that breast cancer cells exhibited diversely organized AJs which correlated with ER $\alpha$  localization. This suggests that the effects of AJ reorganization on cell-cell adhesion which I found in MCF-7/vBOS cells *in vitro* might be of clinical relevance.

Together, these results point toward an ER $\alpha$ -dependent regulation of AJ organization in breast cancer cells which might affect cell-cell adhesion without significant alterations of E-cadherin expression. This could improve our current understanding of breast cancer metastasis *in vivo* and might imply a metastasis-preventing effect for antiestrogen therapy. (Fig. 9)

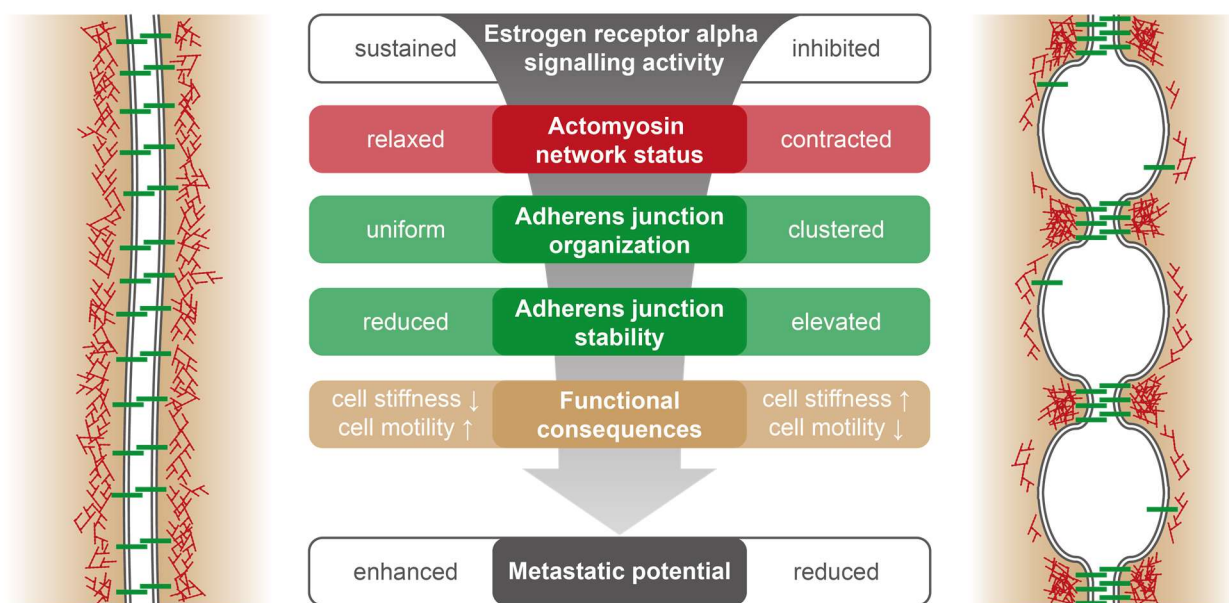


**Figure 9: Schematic representation of events at adherens junctions depending on ER $\alpha$  signaling activity in MCF-7/vBOS breast cancer cells.**

E-cadherin, green. Cortical actomyosin cytoskeleton, red. Cell membrane, double line. Cytosol, brown.

## 6.1. Estrogen levels and ER $\alpha$ signaling inhibition in MCF-7/vBOS cells

Studying the effects of antiestrogens on E-cadherin-mediated cell-cell adhesion, I found that treatment of MCF-7/vBOS cells with Fulvestrant and other antiestrogens induced a distinct reorganization of AJs (see section 6.2). The original cell lines (MCF-7 and MCF-7/BOS) of the MCF-7/vBOS cell line I used in my experiments have been shown to respond to estrogen stimuli.<sup>60, 61</sup> I monitored the estrogen responsiveness of MCF-7/vBOS by the transcription of typical ER $\alpha$  target genes such as *BCL2L1* and *TFE1*. These genes have been shown to be down- and upregulated, respectively, upon activation of the ER $\alpha$  by the potent estrogen 17 $\beta$ -estradiol.<sup>68</sup> Correspondingly, I observed an inverse regulation when the serum estrogen of the cell culture medium was counteracted by Fulvestrant treatment. The combination of genes responding with both up- and downregulation in my experiments reduced the risk of mistaking unspecific effects on the gene transcription machinery for specific effects of ER $\alpha$  inhibition. My results attest the estrogen responsiveness of MCF-7/vBOS cells.

In addition, it was important to assess if MCF-7/vBOS cells respond to clinically relevant levels of estrogens and antiestrogens in order to obtain *in vitro* data that reflect the conditions *in vivo*. For the cultivation of MCF-7/vBOS cells, I supplemented the cell culture medium with low-estrogen serum, resulting in a concentration of 6.8 or  $3.4 \times 10^{-12}$  M 17 $\beta$ -estradiol in maintenance or experimental conditions, respectively. These levels of 17 $\beta$ -estradiol correspond to physiological postmenopausal serum 17 $\beta$ -estradiol levels which start at  $18.0 \pm 4.8 \times 10^{-12}$  M and fall to  $4.8 \pm 1.1 \times 10^{-12}$  M in women less and more than 5 years after menopause, respectively.<sup>81</sup> Steady-state Fulvestrant plasma levels peak at  $2.3 \pm 1.4 \times 10^{-8}$  M and fall to  $1.3 \pm 0.3 \times 10^{-8}$  M over the course of the regular dosing interval of one month.<sup>82</sup> I observed that the treatment with Fulvestrant induced the reorganization of AJs at a minimum concentration of  $10^{-9}$  M. The fixed concentration of  $10^{-8}$  M which I used in most experiments well reflects the steady-state plasma levels of breast cancer patients receiving monthly Fulvestrant treatment. I further found that the Fulvestrant-induced AJ reorganization in MCF-7/vBOS cells could be prevented by co-treatment with a 10-fold lower concentration of 17 $\beta$ -estradiol. This corresponds to the published relative ER $\alpha$ -binding affinities of both compounds.<sup>69, 83</sup> The fact that MCF-7/vBOS cells respond to clinically relevant concentrations of Fulvestrant in the presence of physiological concentrations of 17 $\beta$ -estradiol makes this cell line a suitable *in vitro* system to study the effects of antiestrogen treatment.

In order to attribute the Fulvestrant-induced effect on AJ organization specifically to ER $\alpha$  inhibition, I treated MCF-7/vBOS cells with different ER inhibitors such as Fulvestrant,

Tamoxifen, ZK 164,015, MPP, and PHTPP. Previous characterization revealed that MCF-7/vBOS cells strongly express ER $\alpha$  while ER $\beta$  is expressed only at very low levels (data not shown). Nonetheless, it is important to take into account the selectivity of the antiestrogens used. The selectivity of Fulvestrant and Tamoxifen for ER $\alpha$  versus ER $\beta$  is poor.<sup>69</sup> For the ER antagonist ZK 164,015 no data could be found in the literature. For this reason, the induction of AJ reorganization upon treatment with these substances cannot be related specifically to ER $\alpha$  inhibition. Only MPP can be considered as a highly selective ER $\alpha$  antagonist.<sup>69</sup> Hence, the effect of MPP treatment on AJ organization suggests that AJ reorganization is specific to ER $\alpha$  inhibition. Corresponding to this and to the expression levels of ER $\alpha$  and ER $\beta$ , the selective ER $\beta$  inhibitor PHTPP<sup>71</sup> did not alter the organization of AJs in MCF-7/vBOS cells. However, the use of pharmacological inhibitors is often limited by the specificity to their target protein. Moreover, other ER subtypes expressed in breast cancer cells<sup>84</sup> might influence the organization of AJs in MCF-7/vBOS cells. Therefore, I performed ER $\alpha$  knockdown experiments. This way, I could show that the reduction of ER $\alpha$  protein levels is sufficient to cause AJ reorganization in MCF-7/vBOS cells. This strongly attributes AJ reorganization to the disruption of ER $\alpha$  signaling. The use of different siRNA samples targeting different regions of the ER $\alpha$ -coding *ESR1* gene reduced the risk of misinterpreting off-target effects and thus increased the specificity of my ER $\alpha$  knockdown experiments.

The different antiestrogens I used to treat MCF-7/vBOS cells induced AJ reorganization after different periods of time. However, this did not correlate with the ER $\alpha$  binding affinities of the substances published in the literature.<sup>69</sup> The different kinetics could possibly be explained by different modes of action. For instance, Fulvestrant acts not only as a competitive antagonist but also decreases ER $\alpha$  protein levels<sup>26</sup> which might explain its higher effectiveness in altering the organization of AJs in MCF-7/vBOS cells.

Estrogens promote the development and progression of ER-positive breast cancer, and antiestrogen therapy is an integral part of the therapeutic regimen.<sup>19</sup> Beside its proliferation-promoting effect<sup>19</sup>, ER $\alpha$  signaling has been implicated in breast cancer metastasis as well. Here, the ER $\alpha$ -dependent downregulation of E-cadherin has been suggested to impair cell-cell adhesion, thereby increasing the risk of metastasis.<sup>20</sup> However, contradictory ER $\alpha$ -dependent mechanisms have been identified, resulting in both up-<sup>39, 40</sup> and downregulation<sup>36, 37</sup> of E-cadherin. In MCF-7/vBOS cells, I did not find any effects of Fulvestrant treatment on E-cadherin expression, although other ER $\alpha$  target genes such as *BCL2L1* and *TFF1*<sup>68</sup> were regulated as expected. For cell culture and experiments, I used physiological concentrations of 17 $\beta$ -estradiol, while many studies on the ER $\alpha$ -dependent regulation of E-cadherin expression do not state the final estrogen levels in

the cell culture media.<sup>36, 37, 39, 40</sup> Since the importance of ER $\alpha$  signaling for E-cadherin expression remains vague, other mechanisms might exist that regulate E-cadherin-mediated cell-cell adhesion. Possibly, ER $\alpha$  signaling does not only regulate the transcription or translation of E-cadherin. In addition, it could exert post-translational effects on E-cadherin such as its function in interplay with other proteins which together form the AJ protein complex.

## 6.2. The organization(s) of adherens junctions

AJs are defined as E-cadherin-mediated cell-cell contacts that interact with the cortical actomyosin cytoskeleton via various E-cadherin-associated proteins such as  $\alpha$ -catenin,  $\beta$ -catenin, and p120.<sup>52</sup> Confluent epithelial cells exhibit an apical and a lateral compartment of AJs. The apical compartment forms a belt-like structure underneath the tight junction ring and is also referred to as linear contacts or *zonula adherens*. The lateral compartment consists of multiple spot-like *puncta* at the basolateral cell membrane.<sup>85</sup> Consistent with published data<sup>85, 86</sup>, I observed that basolateral AJs formed various spot-like structures which were homogeneously distributed along the basolateral cell membrane in MCF-7/vBOS cells under control conditions. In contrast, I found that Fulvestrant-treated MCF-7/vBOS cells displayed AJs which were reorganized in a very specific manner into reticular, partly even honeycombed or sponge-like structures. Fulvestrant treatment affected the organization of the whole AJ protein complex since I could show that E-cadherin co-localized with actin filaments and AJ proteins such as  $\alpha$ -catenin,  $\beta$ -catenin, and p120. *Wu et al.* showed that both the apical and lateral compartment of AJs contribute to cell-cell adhesion.<sup>86</sup> Therefore, the effects of Fulvestrant on the organization of basolateral AJs might represent a way to regulate cell-cell adhesion.

*DePasquale et al.* might have observed a resembling rearrangement of cell-cell contacts in MCF-7 cells cultured in estrogen-deprived medium. In their study, rearranged cell-cell contacts were marked by staining for actin filaments and the AJ protein plakoglobin. In addition, cells displayed morphological changes of cell-cell contacts in transmission electron microscopy when cultured in estrogen-deprived medium.<sup>87</sup> In MCF-7/vBOS cells, I visualized the reorganization of AJs by actin filament staining. In transmission electron microscopy, I observed similar morphological changes of cell-cell contacts. Moreover, I was able to detect E-cadherin molecules at these contact sites. Despite the lack of E-cadherin immunostaining, further characterization of the cell-cell contact rearrangement and its functional consequences for intercellular adhesion in the study of *DePasquale et al.*<sup>87</sup>, their observations might resemble the effect of Fulvestrant treatment on AJ organization which I observed in MCF-7/vBOS cells.

Other groups described phenotypes of AJ reorganization comparable with those found in Fulvestrant-treated MCF-7/vBOS cells. *Fernández-Martín et al.* observed reticular VE-cadherin-based AJs in endothelial cells<sup>88</sup>, *Lee et al.* and *Ren et al.* showed that E-cadherin-based AJs in epithelial cells adopt a reticular phenotype upon perturbation of different mechanisms regulating the cortical actomyosin cytoskeleton<sup>77,89</sup>. Even though the findings in these studies are not related to ER $\alpha$  signaling, they all show a significant impact of the actomyosin cytoskeleton on AJ organization. The underlying mechanisms and possible similarities to my findings in MCF-7/vBOS cells will be discussed in section 6.3.2.

AJs have been proposed to not only differ in their morphology but also in their molecular composition. Apical and lateral AJs might interact with the cortical actomyosin cytoskeleton via different sets of adaptor proteins.<sup>85</sup> Likewise, the tight junction protein complex is linked to the apical actomyosin ring via other adaptor proteins than the AJ protein complex.<sup>67</sup> The resulting different interaction with the cortical actomyosin cytoskeleton could explain why Fulvestrant treatment significantly reorganized AJs at basolateral cell membranes while not affecting the organization of tight junctions in MCF-7/vBOS cells.

In the light of this, further characterization of the AJ protein complex in MCF-7/vBOS cells is necessary. For instance, it needs to be tested if genetic alterations of E-cadherin and other AJ proteins or quantitative changes in their expression levels alter the organization and function of the AJ protein complex. This especially includes the interaction with the cortical actomyosin cytoskeleton which might play a pivotal role in reorganizing AJs in Fulvestrant-treated MCF-7/vBOS cells.

### **6.3. Regulation of adherens junctions through the actomyosin cytoskeleton**

When studying how ER $\alpha$  inhibition by antiestrogen treatment causes AJ reorganization in MCF-7/vBOS cells, the role of the actomyosin cytoskeleton was of particular interest because of the complex interaction between E-cadherin and the cortical actomyosin cytoskeleton at AJs.<sup>52-54</sup> I modulated the actomyosin cytoskeleton by direct inhibition of actin polymerization using latrunculin A as well as by indirect inhibition of actin polymerization and actomyosin contractility using the ROCK inhibitor Y-27632. Thereby, I found that modulating the actomyosin cytoskeleton interfered with the reorganization of AJs upon Fulvestrant treatment of MCF-7/vBOS cells. These data indicate a strong dependence of AJ reorganization on the actomyosin cytoskeleton. However, it remains to be shown if changes of the actomyosin cytoskeleton alone are sufficient to induce the observed AJ reorganization in Fulvestrant-treated MCF-7/vBOS cells. Given the importance of

the cortical actomyosin cytoskeleton for the regulation of AJ-mediated cell-cell adhesion<sup>53</sup>, it is likely that Fulvestrant treatment primarily affects the actomyosin cytoskeleton and thereby secondarily induces AJ reorganization in MCF-7/vBOS cells. In the following sections, I will discuss ER $\alpha$ -dependent mechanisms that regulate the actomyosin cytoskeleton and how the actomyosin cytoskeleton can affect the organization of AJs.

### 6.3.1. ER $\alpha$ -dependent mechanisms regulating the actomyosin cytoskeleton

The small GTPase RhoA is an important regulator of the actomyosin cytoskeleton regulating both the myosin-dependent contractility of the actomyosin network and the polymerization of actin filaments via effectors such as the kinase ROCK.<sup>74</sup> *Giretti et al.* showed that extranuclear ER $\alpha$  signaling induces a remodeling of the actomyosin cytoskeleton via the RhoA/ROCK pathway in T-47D and MCF-7 breast cancer cells. In their study, activated ER $\alpha$  recruited and activated ROCK-2.<sup>90</sup> This resulted in increased actin polymerization and phosphorylation of moesin<sup>90</sup>, a member of the ezrin-radixin-moesin protein family which link the actomyosin cytoskeleton to different membrane proteins<sup>91</sup>. Via actin filament polymerization and moesin phosphorylation, extranuclear ER $\alpha$  signaling promoted breast cancer cell migration and invasion. This effect was reversed by treatment with different ER antagonists such as Fulvestrant and Tamoxifen.<sup>90</sup> Correspondingly, *Zheng et al.* demonstrated the activation of ezrin, another member of the ezrin-radixin-moesin protein family, via extranuclear ER $\alpha$  activation and the RhoA/ROCK pathway in T-47D breast cancer cells. Again, the resulting increase in migration and invasion of breast cancer cells was inhibited by Fulvestrant treatment.<sup>92</sup> In addition, *Sanchez et al.* identified a mechanism where extranuclear ER $\alpha$  signaling promotes actin polymerization via phosphorylation of the focal adhesion kinase in T-47D breast cancer cells. This caused the phosphorylation of the nucleation-promoting factor N-WASP, which activated actin polymerization via the Arp2/3 protein complex.<sup>93</sup> Recently, the scaffolding protein Paxillin has been implicated in this pathway. The promoting effects on cell migration and invasion were reversed by treatment with the selective estrogen receptor modulator Raloxifene.<sup>94</sup>

These studies show that ER $\alpha$  signaling can affect the actomyosin cytoskeleton. Counteracting these effects by treatment with antiestrogens reduced the migratory potential of breast cancer cells *in vitro*. However, whether remodeling of the actomyosin cytoskeleton had an impact on AJs was not studied.<sup>90, 92-94</sup> The activation of extranuclear ER $\alpha$  signaling initiated non-genomic pathways, causing rapid changes of the actomyosin cytoskeleton within minutes.<sup>90, 92-94</sup> In contrast, the effects I observed on AJ reorganization in MCF-7/vBOS cells required

inhibition of ER $\alpha$  signaling by Fulvestrant for more than 24 hours and were stable over the course of time after cessation of treatment. The fact that Fulvestrant decreases ER $\alpha$  protein levels only after several hours<sup>95, 96</sup> might influence the temporal delay in the induction of AJ reorganization. However, other drugs that do not affect ER $\alpha$  protein levels, such as Tamoxifen<sup>24</sup> and MPP<sup>69</sup>, required an even longer treatment to induce AJ reorganization. In the light of these results, it is unlikely that rapid non-genomic regulations of the actomyosin cytoskeleton induced by extranuclear ER $\alpha$  signaling are involved in the reorganization of AJs in MCF-7/vBOS cells. Instead, nuclear ER $\alpha$  signaling would explain the temporal delay of AJ reorganization upon antiestrogen treatment. ER $\alpha$ -dependent genomic effects on the transcription and translation of proteins regulating the dynamics of the cortical actomyosin cytoskeleton might affect the organization of AJs in MCF-7/vBOS cells.

Indeed, estrogen treatment has been shown to change the expression of many genes coding for proteins that regulate the actomyosin cytoskeleton. *Huan et al.* performed global gene expression analyses on MCF-7 cells treated with 17 $\beta$ -estradiol. Pathway enrichment analyses revealed various patterns of differentially expressed genes including pathways regulating the actin cytoskeleton. In their study, global gene expression was assessed at different time points. Interestingly, changes in pathways regulating the actin cytoskeleton occurred only after 48 hours of treatment with 17 $\beta$ -estradiol.<sup>97</sup> This corresponds to my observation that AJ reorganization in MCF-7/vBOS cells required between 24 and 48 hours of Fulvestrant treatment. However, the study by *Huan et al.* did not differentiate whether gene transcription was regulated by ER $\alpha$  or ER $\beta$ <sup>97</sup>, while I found that AJ reorganization was a specific effect of ER $\alpha$  inhibition in MCF-7/vBOS cells.

With regard to the impact of nuclear ER $\alpha$  signaling, several lines of evidence suggest that the dysregulation of ER $\alpha$  coregulators contributes to breast cancer metastasis while less is known about the contribution of distinct ER $\alpha$  target genes.<sup>20</sup> Possibly, the investigation of critical ER $\alpha$  coregulators and identification of their target genes might help to unravel the underlying mechanism leading to AJ reorganization in MCF-7/vBOS cells.

As shown above, the actomyosin cytoskeleton can be regulated via both extranuclear and nuclear ER $\alpha$  signaling. However, no effects on AJ organization have been described in the current literature so far. Hence, pathways regulating the actomyosin cytoskeleton that are not yet related to ER $\alpha$  signaling might affect the organization of AJs in MCF-7/vBOS cells treated with antiestrogens such as Fulvestrant.

### 6.3.2. Reorganization of adherens junctions through the actomyosin cytoskeleton

Studies have shown that the actomyosin cytoskeleton can be regulated by nuclear and extranuclear ER $\alpha$  signaling<sup>90, 92-94, 97</sup>. However, the impact of these mechanisms on AJ organization remains elusive. Few other studies, albeit not focusing on ER $\alpha$  signaling, could identify mechanisms that reorganize AJs<sup>77, 88, 89</sup> in a manner similar to that of the phenotype which I found in MCF-7/vBOS cells upon Fulvestrant treatment.

*Fernandéz-Martín et al.* studied AJs in endothelial cells. Here, AJs are mediated by the vascular cadherin subtype VE-cadherin. Interestingly, in endothelial cells, AJs partly formed reticular structures<sup>88</sup> resembling the reorganized AJs in MCF-7/vBOS cells upon Fulvestrant treatment. However, while VE-cadherin co-localized with other AJ proteins, it did not co-localize with actin filaments at these reticular structures.<sup>88</sup> In contrast, I could show that E-cadherin co-localized with both AJ proteins and actin filaments even in Fulvestrant-treated MCF-7/vBOS cells exhibiting reorganized AJs. Treatment of endothelial cells with thrombin abolished the reticular organization of AJs which could be rescued by the ROCK-inhibitor Y-27632.<sup>88</sup> These results are contrary to my findings that the ROCK-inhibitor Y-27632 itself abolishes AJ reorganization in Fulvestrant-treated MCF-7/vBOS cells. Nonetheless, the results of *Fernandéz-Martín et al.*<sup>88</sup> give a hint that RhoA/ROCK signaling might be involved in the actomyosin-dependent regulation of AJ organization in MCF-7/vBOS cells. As described above in section 6.3.1, extranuclear ER $\alpha$  signaling has already been shown to regulate the actomyosin cytoskeleton via the RhoA/ROCK pathway.<sup>90</sup>

Besides the regulation via RhoA/ROCK signaling<sup>74</sup>, the dynamics of the actomyosin cytoskeleton essentially depends on the activity of the Arp2/3 protein complex (see section 3.3.2). Together with nucleation-promoting factors, it generates the branched actin network of the cell cortex.<sup>58</sup> *Lee et al.* found that the Arp2/3 complex and the nucleation-promoting factor WAVE2 are recruited to E-cadherin-mediated AJs by the transmembrane protein neogenin in Caco-2 cells. By regulating the Arp2/3-dependent actin assembly at AJs, as the authors conclude, neogenin maintains AJ stability. After neogenin knockdown, Caco-2 cells failed to recruit Arp2/3 and WAVE2 to the cell membrane.<sup>89</sup> Interestingly, this resulted in an altered organization of AJs<sup>89</sup> which resembled the reorganized AJs I observed in Fulvestrant-treated MCF-7/vBOS cells. However, I found that AJ reorganization in MCF-7/vBOS cells did not result from a lack of Arp2/3 activity but can be dissolved by use of the Arp2/3 inhibitor CK666. *Lee et al.* interpret the altered phenotype after neogenin knockdown as a disruption of AJs.<sup>89</sup> In contrast, my findings suggest that AJ reorganization increases cell-cell adhesion of MCF-7/vBOS cells as I will discuss in sections 6.4 and 6.5.

In addition to neogenin<sup>89</sup>, the activity of the Arp2/3 complex can be regulated by other proteins such as cortactin. This scaffolding protein binds actin filaments, the Arp2/3 complex, and nucleation-promoting factors. Thereby, cortactin activates the Arp2/3 complex and stabilizes actin filaments in branched actin networks. The activity of cortactin can be regulated by tyrosine phosphorylation.<sup>76</sup> *Ren et al.* found that cortactin gets increasingly tyrosine-phosphorylated by SFKs once MCF-7 cells established E-cadherin-mediated AJs.<sup>77</sup> Interestingly, cells expressing a phosphorylation-incompetent cortactin mutant or cells treated with the SFK inhibitor PP2 exhibited a reorganization of AJs<sup>77</sup> similar to that I observed in MCF-7/vBOS cells upon Fulvestrant treatment. In MCF-7/vBOS cells, I could reproduce the effect of SFK inhibition by PP2 on AJ organization as shown by *Ren et al.*<sup>77</sup>. Correspondingly, PP2 treatment distinctly decreased the level of phospho-cortactin(Y421). In contrast, although limited by the lack of total cortactin protein quantification, my results suggest that Fulvestrant treatment did not affect cortactin tyrosine-phosphorylation. Since both PP2 and Fulvestrant treatment induced a similar phenotype of AJ reorganization, AJ reorganization in Fulvestrant-treated MCF-7/vBOS cells might depend on similar but still different mechanisms than those described by *Ren et al.*<sup>77</sup>. I found that PP2 treatment reduced the levels of both phospho-cSrc(Y416) and phospho-cSrc(Y527) which have been shown to activate and inhibit c-Src activity, respectively.<sup>79</sup> These contradictory findings need to be supplemented with total c-Src protein quantification. In addition, SFKs other than c-Src might be targeted by PP2 and Fulvestrant treatment in MCF-7/vBOS cells. Furthermore, other cortactin phosphorylation sites than the investigated tyrosine-421 site should be analyzed because a variety of tyrosine or serine phosphorylation, and even acetylation sites have been shown to regulate cortactin activity.<sup>76</sup> Analysis of these other modifications and the quantification of total protein levels of cortactin could help to evaluate the importance of cortactin for AJ reorganization in MCF-7/vBOS cells upon ER $\alpha$  inhibition by Fulvestrant.

Both neogenin and cortactin regulate the activity of the Arp2/3 complex<sup>77, 89</sup> which, in turn, essentially determines the dynamics of the cortical actomyosin cytoskeleton<sup>53, 58</sup>. The perturbation of both neogenin and cortactin activity reorganizes AJs<sup>77, 89</sup> in a manner similar to the one I observed in Fulvestrant-treated MCF-7/vBOS cells. Thus, ER $\alpha$  inhibition by Fulvestrant might interfere with similar or comparable pathways regulating the cortical actomyosin cytoskeleton. Therefore, the impact of ER $\alpha$  signaling on these pathways need to be further studied in detail. In MCF-7/vBOS cells, antiestrogen treatment could alter the transcription of proteins involved in these pathways via nuclear ER $\alpha$  signaling, as I discussed in section 6.3.1. Given the fact that the cortical actomyosin cytoskeleton plays an important role not only in the organization but also in

the formation of AJs, both the development and maturation of AJ-mediated cell-cell contacts might be affected by antiestrogen treatment of MCF-7/vBOS cells.

### **6.3.3. The role of the actomyosin cytoskeleton in adherens junction maturation**

The actomyosin cytoskeleton plays a crucial role in the formation and subsequent maturation of AJs.<sup>52</sup> Fulvestrant treatment might affect these processes in MCF-7/vBOS cells, since I was able to show that Fulvestrant-induced AJ reorganization depends on the actomyosin cytoskeleton. In my experiments, I recapitulated the formation and subsequent maturation of AJs by transient disruption of the calcium-dependent homophilic interaction of E-cadherin molecules by transient calcium depletion. After transient disruption of cell-cell contacts, Fulvestrant-treated MCF-7/vBOS cells were fully able to establish new E-cadherin-mediated cell-cell contacts, indicating that Fulvestrant treatment does not perturb the *de novo* formation of AJs. Interestingly, upon *de novo* formation of cell-cell contacts, AJ reorganization did only appear with temporal delay. This suggests that the changes of the actomyosin cytoskeleton by Fulvestrant causing AJ reorganization might be predominantly important during the maturation of AJs.

Indeed, during the multistep process of AJ formation and maturation, different proteins regulate the dynamics of the actomyosin cytoskeleton. In short, local activation of the small GTPase Rac induces membrane protrusions by actin polymerization in order to set up initial cell-cell contacts. Rac-dependent activation of actin-regulating proteins such as the Arp2/3 complex and cortactin leads to remodeling of the cortical actomyosin cytoskeleton and increases initially formed cell-cell contacts. The small GTPase RhoA regulates further maturation and maintenance of AJs, for instance by activating the myosin-dependent contractility of the cortical actomyosin cytoskeleton to drive E-cadherin clustering.<sup>52</sup>

This process requires different pathways regulating the actomyosin cytoskeleton to be switched on and off in a coordinated fashion. Conceivably, alterations of this coordinated sequence might affect the organization of AJs. For instance, as already described in the preceding section, the actin-regulating protein cortactin gets increasingly tyrosine-phosphorylated and thus activated upon the formation of E-cadherin-mediated cell-cell contacts.<sup>77</sup> Inhibition of cortactin tyrosine-phosphorylation significantly changes AJ organization<sup>77</sup> which might be the consequence of impaired AJ maturation. Correspondingly, Fulvestrant treatment might affect mechanisms regulating the actomyosin cytoskeleton in particular during the maturation of AJs, thereby inducing AJ reorganization in MCF-7/vBOS cells. However, the distinct pathways remain to be elucidated. Here, it has to be taken into account that calcium ions do not only perturb the

homophilic interaction between E-cadherin molecules. Calcium ions are also an intracellular second messenger which regulates different signaling pathways.<sup>98</sup> Hence, calcium-dependent signaling pathways might be influenced by calcium depletion by EGTA treatment as well. More specific results can be obtained by monitoring the formation of cell-cell contacts of cells reseeded after Fulvestrant pretreatment or by using E-cadherin antibodies to transiently perturb E-cadherin-mediated cell-cell adhesion.

The formation and maturation of AJ-mediated cell-cell contacts are important in the maintenance of epithelial integrity.<sup>52</sup> In MCF-7/vBOS cells, antiestrogen treatment might alter these processes, resulting in AJ reorganization. Since the function of AJs might depend on how AJs are organized in the cell membrane, Fulvestrant-induced AJ reorganization could alter the strength of cell-cell adhesion in MCF-7/vBOS cells.

#### **6.4. Adherens junction organization – a novel way of regulating E-cadherin cleavage?**

I observed that the organization of AJs was distinctly altered upon treatment of MCF-7/vBOS cells with Fulvestrant. This might be the consequence of alterations of the cortical actomyosin cytoskeleton. *Wu et al.* reported that the interplay between E-cadherin and the cortical actomyosin cytoskeleton at AJs contributes to intercellular adhesion not only at the apical *zonula adherens* but also along the lateral cell membrane.<sup>86</sup> Therefore, the AJ reorganization I observed along the lateral membrane of Fulvestrant-treated MCF-7/vBOS cells might have an effect on cell-cell adhesion.

*Maretzky et al.* showed that the stability of cell-cell adhesion is regulated by the proteolytical cleavage of E-cadherin by ADAM10 at a distinct site near the transmembrane domain, generating an extracellular 80 kDa and an intracellular 38 kDa fragment.<sup>99</sup> In MCF-7/vBOS cells, I found that Fulvestrant treatment reduced the constitutive cleavage of E-cadherin into 80 kDa and 38 kDa fragments. Interestingly, both the ADAM10 inhibitor GI254023X and Fulvestrant reduced the amounts of both E-cadherin fragments to comparable levels. This suggests that Fulvestrant treatment suppresses the ADAM10-mediated E-cadherin cleavage in MCF-7/vBOS cells.

Besides ADAM10, a few other proteinases also catalyze the proteolytical cleavage of E-cadherin<sup>57</sup> and might therefore be relevant in MCF-7/vBOS cells. In addition, the authors *David et Rajasekaran* question in their review about the clinical importance of E-cadherin cleavage whether the incorporation in AJs might affect the cleavage of E-cadherin as well.<sup>57</sup> Here, the reorganization of AJs and the concomitant suppression of E-cadherin cleavage in Fulvestrant-

treated MCF-7/vBOS cells might offer a plausible hint. I was able to show that the prevention of Fulvestrant-induced AJ reorganization by modulation of the actomyosin cytoskeleton by latrunculin A to some extent restored the cleavage of E-cadherin in MCF-7/vBOS cells. This suggests that the reduced E-cadherin cleavage upon Fulvestrant treatment is partly caused by AJ reorganization. *David et Rajasekaran* propose that small intercellular distances prevent the cleavage of AJ-associated E-cadherin by soluble proteases.<sup>57</sup> In addition, I propose that E-cadherin molecules which are densely packed and immobilized at AJs could be less accessible for soluble and membrane-bound proteases. This might further reduce the proteolytical cleavage of AJ-associated E-cadherin. Upon Fulvestrant treatment, I found that the area of cell-cell contacts was distinctly reduced in MCF-7/vBOS cells, while full-length E-cadherin protein levels did not change. Hence, in reorganized AJs, E-cadherin molecules might be packed more densely, since an equal amount of E-cadherin protein spreads over a reduced area of cell-cell contacts. Consequently, the higher density of E-cadherin in reorganized AJs might prevent E-cadherin molecules from being cleaved in Fulvestrant-treated MCF-7/vBOS cells. This assumption is further underlined by the results of *Schmidt et al.* who show that E-cadherin cleavage by the protease HtrA is increased upon impairment of homophilic E-cadherin *cis* and *trans* interactions by calcium depletion.<sup>100</sup> As *Yap et al.* report, *cis* and *trans* interactions are required to form E-cadherin clusters.<sup>101</sup> Calcium depletion might interfere with E-cadherin clustering at AJs, thereby facilitating the proteolytical cleavage of E-cadherin. To substantiate my preliminary results on the effect of AJ organization on the cleavage of E-cadherin, further experiments are necessary. The dose-dependent effects of Fulvestrant and concomitant latrunculin A treatment have to be studied by quantitative assessment of the levels of both E-cadherin fragments. It would be helpful to study if AJ reorganization upon PP2 treatment (see section 6.3.2) is also associated with suppressed E-cadherin cleavage. Furthermore, the activity and expression of ADAM10 and other E-cadherin-cleaving proteinases need to be assessed upon Fulvestrant treatment of MCF-7/vBOS cells.

Although Fulvestrant treatment reduced the cleavage of E-cadherin in MCF-7/vBOS cells, the levels of full-length E-cadherin were not affected in my experiments. This could be explained by the low rate of constitutive E-cadherin cleavage compared to the large pool of full-length E-cadherin. The effect of inhibition of E-cadherin cleavage on full-length E-cadherin levels could be too small to be detected by western blot analysis. Alternatively, the expression of E-cadherin might adapt to the rate of E-cadherin cleavage via negative feedback mechanisms, generating a constant level of full-length E-cadherin in MCF-7/vBOS cells. Moreover, besides proteolytical cleavage, E-cadherin levels at the cell membrane are regulated by endocytosis of E-cadherin and

recycling back to the membrane.<sup>102</sup> As shown by *de Beco et al.*, endocytosis also occurs at mature AJs.<sup>103</sup> It remains to be investigated if Fulvestrant treatment affects E-cadherin endocytosis and if this, in turn, has an impact on AJ organization in MCF-7/vBOS cells.

However, *David et Rajasekaran* report that the clinical relevance of E-cadherin cleavage does not only result from lower levels of full-length E-cadherin. Instead, the generated extracellular 80 kDa fragment referred to as soluble E-cadherin seems to be of significant clinical importance. Homophilic interaction of soluble E-cadherin with full-length E-cadherin further reduces the pool of adhesion-competent E-cadherin, thereby decreasing intercellular adhesion and increasing metastatic potential of cancer cells. Metastatic spread can further be facilitated by soluble E-cadherin trapped in the extracellular matrix serving as anchoring points for migrating cancer cells. In addition, just as full-length E-cadherin, soluble E-cadherin interacts with different members of the epidermal growth factor receptor family, thereby activating growth and survival pathways in cancer cells.<sup>57</sup> Accordingly, for different types of cancer, the level of soluble E-cadherin in patient's sera has been shown to correlate with invasive disease and poor prognosis.<sup>104</sup>

I found that Fulvestrant treatment of MCF-7/vBOS cells reduced the constitutive proteolytical cleavage of E-cadherin. The dense packing of E-cadherin molecules in reorganized AJs might contribute to this effect. This would offer a functional effect of the organization of AJs on the strength of intercellular adhesion. By lowering the levels of soluble E-cadherin and strengthening cell-cell adhesion, antiestrogens might reduce the metastatic potential of breast cancer cells.

## **6.5. The role of intercellular adhesion in the metastatic spread of cancer cells**

Fulvestrant treatment might strengthen cell-cell adhesion by inhibiting the proteolytical cleavage of E-cadherin. However, using transmission electron microscopy, I observed that the area of E-cadherin-mediated cell-cell contacts was distinctly reduced in Fulvestrant-treated MCF-7/vBOS cells. This might, in contrast, impair the strength of intercellular adhesion and could promote metastasis *in vivo*. To better understand the effects of AJ reorganization upon Fulvestrant treatment on intercellular adhesion in MCF-7/vBOS cells, I investigated the motility of individual cells under confluent conditions. Assuming that this form of cell motility depends on the ability of cells to break up intercellular contacts in order to build up new contacts with adjacent cells, cell motility can be used to indirectly assess intercellular adhesion. Interestingly, MCF-7/vBOS cells responded to Fulvestrant treatment with decreased cell motility, indicating increased intercellular adhesion.

In contrast, Fulvestrant treatment did not alter the cell motility in MCF-7/ACC115 cells. This cell line responded to ER $\alpha$  inhibition by Fulvestrant as shown by regulation of the ER $\alpha$  target genes *BCL2L1* and *TFF1* (see also section 6.1) but did not show any alteration of AJ organization. Hence, decreased cell motility correlated with the appearance of AJ reorganization. Although not completely excluding the possibility of other Fulvestrant-induced effects, these results suggest that AJ reorganization might increase cell-cell adhesion, thereby decreasing cell motility. The Fulvestrant-induced increase of cell-cell adhesion might have an impact on the metastatic potential of breast cancer cells.

In the context of metastasis, two different types of cancer cell migration can be distinguished: single and collective cell migration. Single cells lack cell-cell contacts to adjacent cells and exclusively interact with the extracellular matrix via integrins.<sup>105</sup> This might be the case in metastasizing breast cancer cells after loss of E-cadherin expression in the context of EMT.<sup>20</sup> In a group of collectively migrating cells, cells not only interact with the extracellular matrix but also adhere to each other via cadherin-mediated AJs.<sup>105</sup> This offers a possible mechanism for the metastatic spread of breast cancer cells with sustained E-cadherin expression such as MCF-7/vBOS cells.

However, AJs exhibit more functions than only making a group of migrating cells stick together. Moreover, AJs are capable of sensing external forces which allows them to distribute mechanical tension within the group. Thereby, collectively migrating cells adopt a front-rear polarity that results in more efficient migration.<sup>105</sup> *Ladoux et al.* studied the formation of N-cadherin-based AJs on N-cadherin-coated substrates of different rigidity. Observing that AJs are larger on a stiffer substrate, the authors of the study conclude that cells respond to high external tension with actomyosin rearrangement leading to the formation of large AJ clusters.<sup>106</sup> *Yap et al.* review the importance of cadherin clustering in order to stabilize and strengthen AJs. In their review, the authors differentiate between nano- and microclusters, which do not only differ in their size. Instead, while nanoclusters develop independently from cadherin-mediated cell-cell contacts, the formation of microclusters depends on parameters such as homophilic cadherin interaction and the actomyosin cytoskeleton.<sup>101</sup> In MCF-7/vBOS cells, the Fulvestrant-induced reorganization of E-cadherin-mediated AJs is accompanied by a decrease in cell-cell contact area as shown by transmission electron microscopy. However, considering that Fulvestrant treatment did not change total E-cadherin protein levels, AJ reorganization might represent an increased microclustering of E-cadherin. Corresponding to *Yap et al.*<sup>101</sup>, I found that AJ reorganization depends on homophilic E-cadherin interaction and the actomyosin cytoskeleton, since it was perturbed by impairment of E-cadherin interaction or modulation of actomyosin dynamics, respectively. Thus, increased

microclustering of E-cadherin might offer an explanation how AJ reorganization strengthens cell-cell adhesion.

Although not specific to AJ reorganization, I found that Fulvestrant treatment increased the cell stiffness of MCF-7/vBOS cells as measured by atomic force microscopy. However, the causal relation to AJ reorganization remains unclear. Regarding the above-mentioned study by *Ladoux et al.* where high external stiffness increased AJ clustering<sup>106</sup>, E-cadherin clustering in the context of AJ reorganization might be a secondary effect in response to increased mechanical tension within the cell layer of MCF-7/vBOS cells upon Fulvestrant treatment. Alternatively, AJ reorganization could be a primary effect of Fulvestrant treatment which secondarily increases the mechanical tension in the cell layer. Thus, AJ reorganization might result in or from altered mechanical properties such as increased cell stiffness of Fulvestrant-treated MCF-7/vBOS cells. Considering that Fulvestrant treatment did not induce AJ reorganization but increased cell stiffness in MCF-7/ACC115 cells, these effects might also be independent from each other. Interestingly, the mechanical properties of cancer cells have been shown to correlate with their metastatic potential. For different cell types, it has been shown that cancer cells are softer, while corresponding non-malignant cells of the same tissue are stiffer.<sup>107</sup> This is also the case in different breast cancer cell lines.<sup>108-110</sup> Thus, further studies investigating the effects of antiestrogens such as Fulvestrant on the mechanical properties of breast cancer cells are necessary. Measuring the cell stiffness in PP2-treated MCF-7/vBOS cells (see section 6.3.2) could help to evaluate the contribution of AJ reorganization to increased cell stiffness. The use of molecular tension sensors as shown by *Borghini et al.*<sup>111</sup> would allow to assess the mechanical forces at E-cadherin-based cell-cell contacts in dependence on the organization of AJs.

With regard to the metastatic potential of breast cancer cells, ER $\alpha$  signaling is supposed to promote metastasis which could consequently be prevented by antiestrogen treatment.<sup>20</sup> However, *Lymperatou et al.* showed that different drugs used in antiestrogen therapy might affect cell migration differently.<sup>112</sup> Interestingly, many *in vitro* studies only assess two-dimensional cell migration, thereby neglecting the importance of the three-dimensional spaced tumor microenvironment with its complex biochemical composition and mechanical properties.<sup>113</sup> Experiments considering these parameters are necessary to better evaluate the effect of AJ organization on the metastatic potential of breast cancer cells.

The reorganization of AJs I observed in Fulvestrant-treated MCF-7/vBOS cells appears to be accompanied by increased E-cadherin microclustering. As indicated by decreased cell motility, this might strengthen cell-cell adhesion. This offers a possible way how antiestrogen treatment increases intercellular adhesion without affecting E-cadherin protein levels in breast cancer cells.

However, it remains to be shown *in vivo* if and how the organization of AJs affects intercellular adhesion and cell migration and to what extent this is regulated by ER $\alpha$  inhibition through antiestrogen therapy.

## 6.6. Clinical implications and conclusion

In MCF-7/vBOS cells, I found that Fulvestrant treatment induced a distinct reorganization of AJs which might have functional consequences for the strength of cell-cell adhesion. To investigate the clinical relevance of my *in vitro* findings in the invasive ductal carcinoma cell line MCF-7/vBOS, I first studied how AJs are organized *in vivo* using tissue sections from breast cancer patients. For this purpose, I investigated tissue samples from patients with diagnosed invasive ductal carcinoma, a subtype of breast cancer which often retains E-cadherin expression.<sup>15</sup> As in studying the organization of AJs in MCF-7/vBOS cells, I used structured illumination microscopy which allowed an enhanced resolution compared to conventional fluorescence microscopy. This way, I was able to observe that AJs are organized in different ways in tissue samples from invasive ductal carcinoma breast cancer patients. AJ reorganization in MCF-7/vBOS cells was induced by treatment with antiestrogens such as Fulvestrant which inhibited ER $\alpha$  signaling. To investigate the relation between the organization of AJs and ER $\alpha$  signaling *in vivo*, I used the translocation of the ER $\alpha$  into the nucleus<sup>19</sup> as a proxy for ER $\alpha$  signaling activity. Studying tissue sections from invasive ductal carcinoma patients, I found that an irregular, discontinuous organization of AJs correlated with cytosolic ER $\alpha$  localization, indicating low ER $\alpha$  signaling activity. These results show that breast cancer cells *in vivo* display different morphologies of AJ organization which might correlate with ER $\alpha$  signaling. Considering my findings in MCF-7/vBOS cells about the effects of Fulvestrant-induced AJ reorganization on the strength of intercellular adhesion, the organization of AJs *in vivo* might have clinically relevant consequences. Therefore, future studies should focus on the assessment of AJ organization *in vivo* by immunofluorescence microscopy and enhanced resolution imaging techniques.

To investigate the clinical relevance of AJ organization, further studies are needed which comprise tissue samples from a much larger study population than I investigated. Since I observed AJ reorganization in MCF-7/vBOS cell after Fulvestrant treatment, tissue samples from patients undergoing antiestrogen therapy might display alterations in the organization of AJs in cancer cells. Here, it has to be taken into account that ongoing antiestrogen therapy might change the behavior of tumor cells, since it favors the selection of ER $\alpha$ -independent clones. However, alterations of AJ organization might also develop independently from antiestrogen therapy, as I

observed diversely organized AJs in tissue samples from patients who have not yet undergone any treatment with antiestrogens.

For the assessment of the clinical consequences of AJ organization, it will be necessary to correlate AJ organization with clinical parameters such as the presence of metastases, the response to antiestrogen therapy, and the patient's survival. If the clinical importance of AJ organization could be confirmed, this would offer a new tool to predict the metastatic risk and prognosis of breast cancer patients. With regard to the heterogeneity of tumors, it might be the case that AJ organization is regulated by ER $\alpha$  signaling in some patients while not in others, for instance due to different expression of ER $\alpha$  coregulators. Assessment of the tumor-specific effect of ER $\alpha$  inhibition on AJ organization might provide a predictive tool for the individual therapeutic response and would consequently allow a personalization of antiestrogen therapy.

Nowadays, immunostaining of E-cadherin serves to better distinguish between invasive lobular and invasive ductal carcinoma of the breast which are typically characterized by negative and positive E-cadherin expression, respectively.<sup>15</sup> However, the use of peroxidase staining in histopathological diagnostics does not allow to visualize the organization of AJs in such detail as immunofluorescence microscopy. To further study AJ organization *in vivo*, automated image analysis by machine learning tools could offer a more precise and less biased method of assessing AJ organization than the manual assessment by human observers. Identification of mechanistic pathways behind AJ reorganization could help to find marker proteins to predict the metastatic risk using tissue samples from breast cancer patients.

And lastly, elucidating the molecular events causing AJ organization as well as its cell-biological and clinical consequences might help to improve our current understanding of breast cancer metastasis. *In vitro* models describing the ER $\alpha$ -dependent regulation of E-cadherin expression do not reflect the *in vivo* situation, where E-cadherin expression levels only poorly predict the metastatic risk of breast cancer cells. In MCF-7/vBOS cells, ER $\alpha$  signaling does not affect E-cadherin expression levels, making it a suitable model system for studying alternative mechanisms. I found that Fulvestrant treatment of MCF-7/vBOS cells caused a distinct reorganization of E-cadherin-mediated AJs which might stabilize AJs and increase intercellular adhesion. These findings could provide a novel mode of action for antiestrogen treatment. Besides inhibiting breast cancer cell proliferation, antiestrogens might also exert metastasis-preventing effects by regulating the organization of AJs. In addition, the organization of AJs could have a predictive and prognostic value in breast cancer, for instance to assess the risk of metastasis. Hence, my work and subsequent studies might help to take research a small step forward in the big challenge of improving the diagnosis, therapy, and prognosis of breast cancer patients.

## 7. References

- 1 Hammond ME, Hayes DF, Dowsett M, Allred DC, Hagerty KL, Badve S, Fitzgibbons PL, Francis G, Goldstein NS, Hayes M, Hicks DG, Lester S, Love R, Mangu PB, McShane L, Miller K, Osborne CK, Paik S, Perlmutter J, Rhodes A, Sasano H, Schwartz JN, Sweep FC, Taube S, Torlakovic EE, Valenstein P, Viale G, Visscher D, Wheeler T, Williams RB, Wittliff JL, and Wolff AC, *American Society of Clinical Oncology/College Of American Pathologists guideline recommendations for immunohistochemical testing of estrogen and progesterone receptors in breast cancer*. J Clin Oncol, 2010. 28(16): p. 2784-95.
- 2 Rugo HS, Rumble RB, Macrae E, Barton DL, Connolly HK, Dickler MN, Fallowfield L, Fowble B, Ingle JN, Jahanzeb M, Johnston SR, Korde LA, Khatcheressian JL, Mehta RS, Muss HB, and Burstein HJ, *Endocrine Therapy for Hormone Receptor-Positive Metastatic Breast Cancer: American Society of Clinical Oncology Guideline*. J Clin Oncol, 2016. 34(25): p. 3069-103.
- 3 Cardoso F, Costa A, Senkus E, Aapro M, Andre F, Barrios CH, Bergh J, Bhattacharyya G, Biganzoli L, Cardoso MJ, Carey L, Corneliussen-James D, Curigliano G, Dieras V, El Saghir N, Eniu A, Fallowfield L, Fenech D, Francis P, Gelmon K, Gennari A, Harbeck N, Hudis C, Kaufman B, Krop I, Mayer M, Meijer H, Mertz S, Ohno S, Pagani O, Papadopoulos E, Peccatori F, Pernault-Llorca F, Piccart MJ, Pierga JY, Rugo H, Shockney L, Sledge G, Swain S, Thomssen C, Tutt A, Vorobiof D, Xu B, Norton L, and Winer E, *3rd ESO-ESMO International Consensus Guidelines for Advanced Breast Cancer (ABC 3)*. Ann Oncol, 2017. 28(1): p. 16-33.
- 4 Senkus E, Kyriakides S, Ohno S, Penault-Llorca F, Poortmans P, Rutgers E, Zackrisson S, Cardoso F, and Committee EG, *Primary breast cancer: ESMO Clinical Practice Guidelines for diagnosis, treatment and follow-up*. Ann Oncol, 2015. 26 Suppl 5: p. v8-30.
- 5 Leitlinienprogramm Onkologie. *Interdisziplinäre S3-Leitlinie für die Diagnostik, Therapie und Nachsorge des Mammakarzinoms. Kurzversion 3.0*. July 2012 (accessed 09/22/2017 at: [http://www.leitlinienprogramm-onkologie.de/fileadmin/user\\_upload/Downloads/Leitlinien/Mammakarzinom/S3-Brustkrebs-v2012-OL-Kurzversion.pdf](http://www.leitlinienprogramm-onkologie.de/fileadmin/user_upload/Downloads/Leitlinien/Mammakarzinom/S3-Brustkrebs-v2012-OL-Kurzversion.pdf)).
- 6 Leitlinienprogramm Onkologie. *Leitlinienreport zur 3-Leitlinie Früherkennung, Diagnostik, Therapie und Nachsorge des Mammakarzinoms. Konsultationsfassung 0.4.0*. June 2017 (accessed 10/15/2017 at: <http://www.leitlinienprogramm-onkologie.de/>).

fileadmin/user\_upload/Downloads/Leitlinien/Mammakarzinom\_4\_0/LL\_Mammakarzinom\_Leitlinienreport\_Konsultationsfassung.pdf).

- 7 Ferlay J, Soerjomataram I, Dikshit R, Eser S, Mathers C, Rebelo M, Parkin DM, Forman D, and Bray F, *Cancer incidence and mortality worldwide: sources, methods and major patterns in GLOBOCAN 2012*. Int J Cancer, 2015. 136(5): p. E359-86.
- 8 Malvezzi M, Bertuccio P, Levi F, La Vecchia C, and Negri E, *European cancer mortality predictions for the year 2013*. Ann Oncol, 2013. 24(3): p. 792-800.
- 9 Zentrum für Krebsregisterdaten im Robert Koch-Institut, *Bericht zum Krebsgeschehen in Deutschland 2016*. Berlin, 2016.
- 10 Rojas K and Stuckey A, *Breast Cancer Epidemiology and Risk Factors*. Clin Obstet Gynecol, 2016. 59(4): p. 651-672.
- 11 Althuis MD, Fergenbaum JH, Garcia-Closas M, Brinton LA, Madigan MP, and Sherman ME, *Etiology of hormone receptor-defined breast cancer: a systematic review of the literature*. Cancer Epidemiol Biomarkers Prev, 2004. 13(10): p. 1558-68.
- 12 Weyerstahl T and Stauber M, eds. *Gynäkologie und Geburtshilfe*. 4th ed. Duale Reihe. 2013, Thieme: Stuttgart.
- 13 Galimberti V, Monti S, and Mastropasqua MG, *DCIS and LCIS are confusing and outdated terms. They should be abandoned in favor of ductal intraepithelial neoplasia (DIN) and lobular intraepithelial neoplasia (LIN)*. Breast, 2013. 22(4): p. 431-5.
- 14 Lakhani S, Ellis I, Schnitt S, Tan P, and Vijver Mvd, eds. *WHO classification of tumours of the breast*. Vol. 4. 2012, International Agency for Research on Cancer.
- 15 Canas-Marques R and Schnitt SJ, *E-cadherin immunohistochemistry in breast pathology: uses and pitfalls*. Histopathology, 2016. 68(1): p. 57-69.
- 16 Swain SM, Baselga J, Kim SB, Ro J, Semiglazov V, Campone M, Ciruelos E, Ferrero JM, Schneeweiss A, Heeson S, Clark E, Ross G, Benyunes MC, Cortes J, and Group CS, *Pertuzumab, trastuzumab, and docetaxel in HER2-positive metastatic breast cancer*. N Engl J Med, 2015. 372(8): p. 724-34.
- 17 Howlader N, Noone AM, Krapcho M, Miller D, Bishop K, Kosary CL, Yu M, Ruhl J, Tatalovich Z, Mariotto A, Lewis DR, Chen HS, Feuer EJ, and Cronin KA. *SEER Cancer*

- Statistics Review, 1975-2014*. Based on November 2016 SEER data submission, posted to the SEER web site April 2017 (accessed 20/09/2017 at: [https://seer.cancer.gov/csr/1975\\_2014/](https://seer.cancer.gov/csr/1975_2014/)).
- 18 Grann VR, Troxel AB, Zojwalla NJ, Jacobson JS, Hershman D, and Neugut AI, *Hormone receptor status and survival in a population-based cohort of patients with breast carcinoma*. *Cancer*, 2005. 103(11): p. 2241-51.
  - 19 Manavathi B, Dey O, Gajulapalli VN, Bhatia RS, Bugide S, and Kumar R, *Derailed estrogen signaling and breast cancer: an authentic couple*. *Endocr Rev*, 2013. 34(1): p. 1-32.
  - 20 Saha Roy S and Vadlamudi RK, *Role of estrogen receptor signaling in breast cancer metastasis*. *Int J Breast Cancer*, 2012. 2012: p. 654698.
  - 21 Samavat H and Kurzer MS, *Estrogen metabolism and breast cancer*. *Cancer Lett*, 2015. 356(2 Pt A): p. 231-43.
  - 22 Burstein HJ, Lacchetti C, Anderson H, Buchholz TA, Davidson NE, Gelmon KE, Giordano SH, Hudis CA, Solky AJ, Stearns V, Winer EP, and Griggs JJ, *Adjuvant Endocrine Therapy for Women With Hormone Receptor-Positive Breast Cancer: American Society of Clinical Oncology Clinical Practice Guideline Update on Ovarian Suppression*. *J Clin Oncol*, 2016. 34(14): p. 1689-701.
  - 23 Mangelsdorf DJ, Thummel C, Beato M, Herrlich P, Schutz G, Umesono K, Blumberg B, Kastner P, Mark M, Chambon P, and Evans RM, *The nuclear receptor superfamily: the second decade*. *Cell*, 1995. 83(6): p. 835-9.
  - 24 Riggs BL and Hartmann LC, *Selective estrogen-receptor modulators -- mechanisms of action and application to clinical practice*. *N Engl J Med*, 2003. 348(7): p. 618-29.
  - 25 Howell A, Osborne CK, Morris C, and Wakeling AE, *ICI 182,780 (Faslodex): development of a novel, "pure" antiestrogen*. *Cancer*, 2000. 89(4): p. 817-25.
  - 26 Johnston SJ and Cheung KL, *Fulvestrant - a novel endocrine therapy for breast cancer*. *Curr Med Chem*, 2010. 17(10): p. 902-14.
  - 27 Cortez V, Mann M, Brann DW, and Vadlamudi RK, *Extranuclear signaling by estrogen: role in breast cancer progression and metastasis*. *Minerva Ginecol*, 2010. 62(6): p. 573-83.

- 28 Stingl J, *Estrogen and progesterone in normal mammary gland development and in cancer*. *Horm Cancer*, 2011. 2(2): p. 85-90.
- 29 Atashgaran V, Wrin J, Barry SC, Dasari P, and Ingman WV, *Dissecting the Biology of Menstrual Cycle-Associated Breast Cancer Risk*. *Front Oncol*, 2016. 6: p. 267.
- 30 Simoes BM, Alferez DG, Howell SJ, and Clarke RB, *The role of steroid hormones in breast cancer stem cells*. *Endocr Relat Cancer*, 2015. 22(6): p. T177-86.
- 31 Visvanathan K, Hurley P, Bantug E, Brown P, Col NF, Cuzick J, Davidson NE, Decensi A, Fabian C, Ford L, Garber J, Katapodi M, Kramer B, Morrow M, Parker B, Runowicz C, Vogel VG, 3rd, Wade JL, and Lippman SM, *Use of pharmacologic interventions for breast cancer risk reduction: American Society of Clinical Oncology clinical practice guideline*. *J Clin Oncol*, 2013. 31(23): p. 2942-62.
- 32 Scully OJ, Bay BH, Yip G, and Yu Y, *Breast cancer metastasis*. *Cancer Genomics Proteomics*, 2012. 9(5): p. 311-20.
- 33 Hanahan D and Weinberg RA, *Hallmarks of cancer: the next generation*. *Cell*, 2011. 144(5): p. 646-74.
- 34 Lee JM, Dedhar S, Kalluri R, and Thompson EW, *The epithelial-mesenchymal transition: new insights in signaling, development, and disease*. *J Cell Biol*, 2006. 172(7): p. 973-81.
- 35 Lim J and Thiery JP, *Epithelial-mesenchymal transitions: insights from development*. *Development*, 2012. 139(19): p. 3471-86.
- 36 Oesterreich S, Deng W, Jiang S, Cui X, Ivanova M, Schiff R, Kang K, Hadsell DL, Behrens J, and Lee AV, *Estrogen-mediated down-regulation of E-cadherin in breast cancer cells*. *Cancer Res*, 2003. 63(17): p. 5203-8.
- 37 Cardamone MD, Bardella C, Gutierrez A, Di Croce L, Rosenfeld MG, Di Renzo MF, and De Bortoli M, *ERalpha as ligand-independent activator of CDH-1 regulates determination and maintenance of epithelial morphology in breast cancer cells*. *Proc Natl Acad Sci U S A*, 2009. 106(18): p. 7420-5.
- 38 Huang Y, Fernandez SV, Goodwin S, Russo PA, Russo IH, Sutter TR, and Russo J, *Epithelial to mesenchymal transition in human breast epithelial cells transformed by 17beta-estradiol*. *Cancer Res*, 2007. 67(23): p. 11147-57.

- 39 Ye Y, Xiao Y, Wang W, Yearsley K, Gao JX, Shetuni B, and Barsky SH, *ERalpha signaling through slug regulates E-cadherin and EMT*. *Oncogene*, 2010. 29(10): p. 1451-62.
- 40 Fujita N, Jaye DL, Kajita M, Geigerman C, Moreno CS, and Wade PA, *MTA3, a Mi-2/NuRD complex subunit, regulates an invasive growth pathway in breast cancer*. *Cell*, 2003. 113(2): p. 207-19.
- 41 Voutsadakis IA, *Epithelial-Mesenchymal Transition (EMT) and Regulation of EMT Factors by Steroid Nuclear Receptors in Breast Cancer: A Review and in Silico Investigation*. *J Clin Med*, 2016. 5(1).
- 42 Rosa Mendoza ES, Moreno E, and Caguioa PB, *Predictors of early distant metastasis in women with breast cancer*. *J Cancer Res Clin Oncol*, 2013. 139(4): p. 645-52.
- 43 Younis LK, El Sakka H, and Haque I, *The Prognostic Value of E-cadherin Expression in Breast Cancer*. *Int J Health Sci (Qassim)*, 2007. 1(1): p. 43-51.
- 44 Fulga V, Rudico L, Balica AR, Cimpean AM, Saptefrati L, Margan MM, and Raica M, *Differential expression of e-cadherin in primary breast cancer and corresponding lymph node metastases*. *Anticancer Res*, 2015. 35(2): p. 759-65.
- 45 Rakha EA, Patel A, Powe DG, Benhasouna A, Green AR, Lambros MB, Reis-Filho JS, and Ellis IO, *Clinical and biological significance of E-cadherin protein expression in invasive lobular carcinoma of the breast*. *Am J Surg Pathol*, 2010. 34(10): p. 1472-9.
- 46 Querzoli P, Coradini D, Pedriali M, Boracchi P, Ambrogi F, Raimondi E, La Sorda R, Lattanzio R, Rinaldi R, Lunardi M, Frasson C, Modesti F, Ferretti S, Piantelli M, Iacobelli S, Biganzoli E, Nenci I, and Alberti S, *An immunohistochemically positive E-cadherin status is not always predictive for a good prognosis in human breast cancer*. *Br J Cancer*, 2010. 103(12): p. 1835-9.
- 47 Gould Rothberg BE and Bracken MB, *E-cadherin immunohistochemical expression as a prognostic factor in infiltrating ductal carcinoma of the breast: a systematic review and meta-analysis*. *Breast Cancer Res Treat*, 2006. 100(2): p. 139-48.
- 48 Horne HN, Oh H, Sherman ME, Palakal M, Hewitt SM, Schmidt MK, Milne RL, Hardisson D, Benitez J, Blomqvist C, Bolla MK, Brenner H, Chang-Claude J, Cora R, Couch FJ, Cuk K, Devilee P, Easton DF, Eccles DM, Eilber U, Hartikainen JM, Heikkila

- P, Holleczeck B, Hooning MJ, Jones M, Keeman R, Mannermaa A, Martens JWM, Muranen TA, Nevanlinna H, Olson JE, Orr N, Perez JIA, Pharoah PDP, Ruddy KJ, Saum KU, Schoemaker MJ, Seynaeve C, Sironen R, Smit V, Swerdlow AJ, Tengstrom M, Thomas AS, Timmermans AM, Tollenaar R, Troester MA, van Asperen CJ, van Deurzen CHM, Van Leeuwen FF, Van't Veer LJ, Garcia-Closas M, and Figueroa JD, *E-cadherin breast tumor expression, risk factors and survival: Pooled analysis of 5,933 cases from 12 studies in the Breast Cancer Association Consortium*. *Sci Rep*, 2018. 8(1): p. 6574.
- 49 Chao YL, Shepard CR, and Wells A, *Breast carcinoma cells re-express E-cadherin during mesenchymal to epithelial reverting transition*. *Mol Cancer*, 2010. 9: p. 179.
- 50 Hollestelle A, Peeters JK, Smid M, Timmermans M, Verhoog LC, Westenend PJ, Heine AA, Chan A, Sieuwerts AM, Wiemer EA, Klijn JG, van der Spek PJ, Foekens JA, Schutte M, den Bakker MA, and Martens JW, *Loss of E-cadherin is not a necessity for epithelial to mesenchymal transition in human breast cancer*. *Breast Cancer Res Treat*, 2013. 138(1): p. 47-57.
- 51 Andrews JL, Kim AC, and Hens JR, *The role and function of cadherins in the mammary gland*. *Breast Cancer Res*, 2012. 14(1): p. 203.
- 52 Baum B and Georgiou M, *Dynamics of adherens junctions in epithelial establishment, maintenance, and remodeling*. *J Cell Biol*, 2011. 192(6): p. 907-17.
- 53 Michael M and Yap AS, *The regulation and functional impact of actin assembly at cadherin cell-cell adhesions*. *Semin Cell Dev Biol*, 2013. 24(4): p. 298-307.
- 54 Nelson WJ, *Regulation of cell-cell adhesion by the cadherin-catenin complex*. *Biochem Soc Trans*, 2008. 36(Pt 2): p. 149-55.
- 55 Huveneers S and de Rooij J, *Mechanosensitive systems at the cadherin-F-actin interface*. *J Cell Sci*, 2013. 126(Pt 2): p. 403-13.
- 56 Fearon ER, *Connecting estrogen receptor function, transcriptional repression, and E-cadherin expression in breast cancer*. *Cancer Cell*, 2003. 3(4): p. 307-10.
- 57 David JM and Rajasekaran AK, *Dishonorable discharge: the oncogenic roles of cleaved E-cadherin fragments*. *Cancer Res*, 2012. 72(12): p. 2917-23.
- 58 Blanchoin L, Boujemaa-Paterski R, Sykes C, and Plastino J, *Actin dynamics, architecture, and mechanics in cell motility*. *Physiol Rev*, 2014. 94(1): p. 235-63.

- 59 Jiang WG, Sanders AJ, Katoh M, Ungefroren H, Gieseler F, Prince M, Thompson SK, Zollo M, Spano D, Dhawan P, Sliva D, Subbarayan PR, Sarkar M, Honoki K, Fujii H, Georgakilas AG, Amedei A, Niccolai E, Amin A, Ashraf SS, Ye L, Helferich WG, Yang X, Boosani CS, Guha G, Ciriolo MR, Aquilano K, Chen S, Azmi AS, Keith WN, Bilsland A, Bhakta D, Halicka D, Nowsheen S, Pantano F, and Santini D, *Tissue invasion and metastasis: Molecular, biological and clinical perspectives*. Semin Cancer Biol, 2015. 35 Suppl: p. S244-75.
- 60 Brooks SC, Locke ER, and Soule HD, *Estrogen receptor in a human cell line (MCF-7) from breast carcinoma*. J Biol Chem, 1973. 248(17): p. 6251-3.
- 61 Villalobos M, Olea N, Brotons JA, Olea-Serrano MF, Ruiz de Almodovar JM, and Pedraza V, *The E-screen assay: a comparison of different MCF7 cell stocks*. Environ Health Perspect, 1995. 103(9): p. 844-50.
- 62 Radmacher M, *Measuring the elastic properties of living cells by the atomic force microscope*. Methods Cell Biol, 2002. 68: p. 67-90.
- 63 Sneddon IN, *The relation between load and penetration in the axisymmetric boussinesq problem for a punch of arbitrary profile*. International Journal of Engineering Science, 1965. 3(1): p. 47-57.
- 64 Ferreira E and Cronje MJ, *Selection of suitable reference genes for quantitative real-time PCR in apoptosis-induced MCF-7 breast cancer cells*. Mol Biotechnol, 2012. 50(2): p. 121-8.
- 65 Welinder C and Ekblad L, *Coomassie staining as loading control in Western blot analysis*. J Proteome Res, 2011. 10(3): p. 1416-9.
- 66 Zdunski D and Ilan J, *The effect of cytosine arabinoside on the synthesis of rapidly labeled RNA during DNA replicating and non-DNA replicating periods of the cell cycle*. Cell Differ, 1980. 9(3): p. 181-91.
- 67 Hartsock A and Nelson WJ, *Adherens and tight junctions: structure, function and connections to the actin cytoskeleton*. Biochim Biophys Acta, 2008. 1778(3): p. 660-9.
- 68 Romano A, Adriaens M, Kuenen S, Delvoux B, Dunselman G, Evelo C, and Groothuis P, *Identification of novel ER-alpha target genes in breast cancer cells: gene- and cell-*

- selective co-regulator recruitment at target promoters determines the response to 17beta-estradiol and tamoxifen.* Mol Cell Endocrinol, 2010. 314(1): p. 90-100.
- 69 Sun J, Huang YR, Harrington WR, Sheng S, Katzenellenbogen JA, and Katzenellenbogen BS, *Antagonists selective for estrogen receptor alpha.* Endocrinology, 2002. 143(3): p. 941-7.
- 70 Biberger C and von Angerer E, *2-Phenylindoles with sulfur containing side chains. Estrogen receptor affinity, antiestrogenic potency, and antitumor activity.* J Steroid Biochem Mol Biol, 1996. 58(1): p. 31-43.
- 71 Compton DR, Sheng S, Carlson KE, Rebacz NA, Lee IY, Katzenellenbogen BS, and Katzenellenbogen JA, *Pyrazolo[1,5-a]pyrimidines: estrogen receptor ligands possessing estrogen receptor beta antagonist activity.* J Med Chem, 2004. 47(24): p. 5872-93.
- 72 Coue M, Brenner SL, Spector I, and Korn ED, *Inhibition of actin polymerization by latrunculin A.* FEBS Lett, 1987. 213(2): p. 316-8.
- 73 Bubb MR, Senderowicz AM, Sausville EA, Duncan KL, and Korn ED, *Jasplakinolide, a cytotoxic natural product, induces actin polymerization and competitively inhibits the binding of phalloidin to F-actin.* J Biol Chem, 1994. 269(21): p. 14869-71.
- 74 O'Connor K and Chen M, *Dynamic functions of RhoA in tumor cell migration and invasion.* Small GTPases, 2013. 4(3): p. 141-7.
- 75 Hetrick B, Han MS, Helgeson LA, and Nolen BJ, *Small molecules CK-666 and CK-869 inhibit actin-related protein 2/3 complex by blocking an activating conformational change.* Chem Biol, 2013. 20(5): p. 701-12.
- 76 MacGrath SM and Koleske AJ, *Cortactin in cell migration and cancer at a glance.* J Cell Sci, 2012. 125(Pt 7): p. 1621-6.
- 77 Ren G, Helwani FM, Verma S, McLachlan RW, Weed SA, and Yap AS, *Cortactin is a functional target of E-cadherin-activated Src family kinases in MCF7 epithelial monolayers.* J Biol Chem, 2009. 284(28): p. 18913-22.
- 78 Hanke JH, Gardner JP, Dow RL, Changelian PS, Brissette WH, Weringer EJ, Pollok BA, and Connelly PA, *Discovery of a novel, potent, and Src family-selective tyrosine kinase inhibitor. Study of Lck- and FynT-dependent T cell activation.* J Biol Chem, 1996. 271(2): p. 695-701.

- 79 Roskoski R, Jr., *Src kinase regulation by phosphorylation and dephosphorylation*. Biochem Biophys Res Commun, 2005. 331(1): p. 1-14.
- 80 Ketene AN, Roberts PC, Shea AA, Schmelz EM, and Agah M, *Actin filaments play a primary role for structural integrity and viscoelastic response in cells*. Integr Biol (Camb), 2012. 4(5): p. 540-9.
- 81 Rothman MS, Carlson NE, Xu M, Wang C, Swerdloff R, Lee P, Goh VH, Ridgway EC, and Wierman ME, *Reexamination of testosterone, dihydrotestosterone, estradiol and estrone levels across the menstrual cycle and in postmenopausal women measured by liquid chromatography-tandem mass spectrometry*. Steroids, 2011. 76(1-2): p. 177-82.
- 82 McCormack P and Sapunar F, *Pharmacokinetic profile of the fulvestrant loading dose regimen in postmenopausal women with hormone receptor-positive advanced breast cancer*. Clin Breast Cancer, 2008. 8(4): p. 347-51.
- 83 Wakeling AE, Dukes M, and Bowler J, *A potent specific pure antiestrogen with clinical potential*. Cancer Res, 1991. 51(15): p. 3867-73.
- 84 Soltysik K and Czekaj P, *Membrane estrogen receptors - is it an alternative way of estrogen action?* J Physiol Pharmacol, 2013. 64(2): p. 129-42.
- 85 Takeichi M, *Dynamic contacts: rearranging adherens junctions to drive epithelial remodelling*. Nat Rev Mol Cell Biol, 2014. 15(6): p. 397-410.
- 86 Wu SK, Gomez GA, Michael M, Verma S, Cox HL, Lefevre JG, Parton RG, Hamilton NA, Neufeld Z, and Yap AS, *Cortical F-actin stabilization generates apical-lateral patterns of junctional contractility that integrate cells into epithelia*. Nat Cell Biol, 2014. 16(2): p. 167-78.
- 87 DePasquale JA, Samsonoff WA, and Gierthy JF, *17-beta-Estradiol induced alterations of cell-matrix and intercellular adhesions in a human mammary carcinoma cell line*. J Cell Sci, 1994. 107 ( Pt 5): p. 1241-54.
- 88 Fernandez-Martin L, Marcos-Ramiro B, Bigarella CL, Graupera M, Cain RJ, Reglero-Real N, Jimenez A, Cernuda-Morollon E, Correas I, Cox S, Ridley AJ, and Millan J, *Crosstalk between reticular adherens junctions and platelet endothelial cell adhesion molecule-1 regulates endothelial barrier function*. Arterioscler Thromb Vasc Biol, 2012. 32(8): p. e90-102.

- 89 Lee NK, Fok KW, White A, Wilson NH, O'Leary CJ, Cox HL, Michael M, Yap AS, and Cooper HM, *Neogenin recruitment of the WAVE regulatory complex maintains adherens junction stability and tension*. Nat Commun, 2016. 7: p. 11082.
- 90 Giretti MS, Fu XD, De Rosa G, Sarotto I, Baldacci C, Garibaldi S, Mannella P, Biglia N, Sismondi P, Genazzani AR, and Simoncini T, *Extra-nuclear signalling of estrogen receptor to breast cancer cytoskeletal remodelling, migration and invasion*. PLoS One, 2008. 3(5): p. e2238.
- 91 Ponuwei GA, *A glimpse of the ERM proteins*. J Biomed Sci, 2016. 23: p. 35.
- 92 Zheng S, Huang J, Zhou K, Zhang C, Xiang Q, Tan Z, Wang T, and Fu X, *17beta-Estradiol enhances breast cancer cell motility and invasion via extra-nuclear activation of actin-binding protein ezrin*. PLoS One, 2011. 6(7): p. e22439.
- 93 Sanchez AM, Flamini MI, Baldacci C, Goglia L, Genazzani AR, and Simoncini T, *Estrogen receptor-alpha promotes breast cancer cell motility and invasion via focal adhesion kinase and N-WASP*. Mol Endocrinol, 2010. 24(11): p. 2114-25.
- 94 Shortrede JE, Uzair ID, Neira FJ, Flamini MI, and Sanchez AM, *Paxillin, a novel controller in the signaling of estrogen to FAK/N-WASP/Arp2/3 complex in breast cancer cells*. Mol Cell Endocrinol, 2016. 430: p. 56-67.
- 95 Yeh WL, Shioda K, Coser KR, Rivizzigno D, McSweeney KR, and Shioda T, *Fulvestrant-induced cell death and proteasomal degradation of estrogen receptor alpha protein in MCF-7 cells require the CSK c-Src tyrosine kinase*. PLoS One, 2013. 8(4): p. e60889.
- 96 Joseph JD, Darimont B, Zhou W, Arrazate A, Young A, Ingalla E, Walter K, Blake RA, Nonomiya J, Guan Z, Kategaya L, Govek SP, Lai AG, Kahraman M, Brigham D, Sensintaffar J, Lu N, Shao G, Qian J, Grillot K, Moon M, Prudente R, Bischoff E, Lee KJ, Bonnefous C, Douglas KL, Julien JD, Nagasawa JY, Aparicio A, Kaufman J, Haley B, Giltneane JM, Wertz IE, Lackner MR, Nannini MA, Sampath D, Schwarz L, Manning HC, Tantawy MN, Arteaga CL, Heyman RA, Rix PJ, Friedman L, Smith ND, Metcalfe C, and Hager JH, *The selective estrogen receptor downregulator GDC-0810 is efficacious in diverse models of ER+ breast cancer*. Elife, 2016. 5.
- 97 Huan J, Wang L, Xing L, Qin X, Feng L, Pan X, and Zhu L, *Insights into significant pathways and gene interaction networks underlying breast cancer cell line MCF-7 treated with 17beta-estradiol (E2)*. Gene, 2014. 533(1): p. 346-55.

- 98 McCormick K and Baillie GS, *Compartmentalisation of second messenger signalling pathways*. Curr Opin Genet Dev, 2014. 27: p. 20-5.
- 99 Maretzky T, Reiss K, Ludwig A, Buchholz J, Scholz F, Proksch E, de Strooper B, Hartmann D, and Saftig P, *ADAM10 mediates E-cadherin shedding and regulates epithelial cell-cell adhesion, migration, and beta-catenin translocation*. Proc Natl Acad Sci U S A, 2005. 102(26): p. 9182-7.
- 100 Schmidt TP, Goetz C, Huemer M, Schneider G, and Wessler S, *Calcium binding protects E-cadherin from cleavage by Helicobacter pylori HtrA*. Gut Pathog, 2016. 8: p. 29.
- 101 Yap AS, Gomez GA, and Parton RG, *Adherens Junctions Revisualized: Organizing Cadherins as Nanoassemblies*. Dev Cell, 2015. 35(1): p. 12-20.
- 102 Kowalczyk AP and Nanes BA, *Adherens junction turnover: regulating adhesion through cadherin endocytosis, degradation, and recycling*. Subcell Biochem, 2012. 60: p. 197-222.
- 103 de Beco S, Gueudry C, Amblard F, and Coscoy S, *Endocytosis is required for E-cadherin redistribution at mature adherens junctions*. Proc Natl Acad Sci U S A, 2009. 106(17): p. 7010-5.
- 104 De Wever O, Derycke L, Hendrix A, De Meerleer G, Godeau F, Depypere H, and Bracke M, *Soluble cadherins as cancer biomarkers*. Clin Exp Metastasis, 2007. 24(8): p. 685-97.
- 105 De Pascalis C and Etienne-Manneville S, *Single and collective cell migration: the mechanics of adhesions*. Mol Biol Cell, 2017. 28(14): p. 1833-1846.
- 106 Ladoux B, Anon E, Lambert M, Rabodzey A, Hersen P, Buguin A, Silberzan P, and Mege RM, *Strength dependence of cadherin-mediated adhesions*. Biophys J, 2010. 98(4): p. 534-42.
- 107 Hayashi K and Iwata M, *Stiffness of cancer cells measured with an AFM indentation method*. J Mech Behav Biomed Mater, 2015. 49: p. 105-11.
- 108 Li QS, Lee GY, Ong CN, and Lim CT, *AFM indentation study of breast cancer cells*. Biochem Biophys Res Commun, 2008. 374(4): p. 609-13.
- 109 Nikkhah M, Strobl JS, Schmelz EM, and Agah M, *Evaluation of the influence of growth medium composition on cell elasticity*. J Biomech, 2011. 44(4): p. 762-6.

- 110 Omidvar R, Tafazzoli-Shadpour M, Shokrgozar MA, and Rostami M, *Atomic force microscope-based single cell force spectroscopy of breast cancer cell lines: an approach for evaluating cellular invasion*. J Biomech, 2014. 47(13): p. 3373-9.
- 111 Borghi N, Sorokina M, Shcherbakova OG, Weis WI, Pruitt BL, Nelson WJ, and Dunn AR, *E-cadherin is under constitutive actomyosin-generated tension that is increased at cell-cell contacts upon externally applied stretch*. Proc Natl Acad Sci U S A, 2012. 109(31): p. 12568-73.
- 112 Lymperatou D, Giannopoulou E, Koutras AK, and Kalofonos HP, *The exposure of breast cancer cells to fulvestrant and tamoxifen modulates cell migration differently*. Biomed Res Int, 2013. 2013: p. 147514.
- 113 Vu LT, Jain G, Veres BD, and Rajagopalan P, *Cell migration on planar and three-dimensional matrices: a hydrogel-based perspective*. Tissue Eng Part B Rev, 2015. 21(1): p. 67-74.

## Eidesstattliche Versicherung

„Ich, Philip Bischoff, versichere an Eides statt durch meine eigenhändige Unterschrift, dass ich die vorgelegte Dissertation mit dem Thema ‚*Alterations at the cell membrane of breast cancer cells by estrogens and antiestrogens*‘ selbstständig und ohne nicht offengelegte Hilfe Dritter verfasst und keine anderen als die angegebenen Quellen und Hilfsmittel genutzt habe.

Alle Stellen, die wörtlich oder dem Sinne nach auf Publikationen oder Vorträgen anderer Autoren beruhen, sind als solche in korrekter Zitierung (siehe „Uniform Requirements for Manuscripts (URM)“ des ICMJE – [www.icmje.org](http://www.icmje.org)) kenntlich gemacht. Die Abschnitte zu Methodik (insbesondere praktische Arbeiten, Laborbestimmungen, statistische Aufarbeitung) und Resultaten (insbesondere Abbildungen, Graphiken und Tabellen) entsprechen den URM (s.o.) und werden von mir verantwortet.

Meine Anteile an etwaigen Publikationen zu dieser Dissertation entsprechen denen, die in der untenstehenden gemeinsamen Erklärung mit dem Betreuer angegeben sind. Sämtliche Publikationen, die aus dieser Dissertation hervorgegangen sind und bei denen ich Autor bin, entsprechen den URM (s.o.) und werden von mir verantwortet.

Die Bedeutung dieser eidesstattlichen Versicherung und die strafrechtlichen Folgen einer unwahren eidesstattlichen Versicherung (§§ 156, 161 StGB) sind mir bekannt und bewusst.“

---

Datum, Unterschrift des Doktoranden

## **Curriculum vitae**

Mein Lebenslauf wird aus datenschutzrechtlichen Gründen in der elektronischen Version meiner Arbeit nicht veröffentlicht.



## **Danksagung**

An erster Stelle möchte ich mich besonders bei meinem Doktorvater Herrn Prof. Gilbert Schönfelder bedanken, der diese Arbeit bestens betreut hat. Ohne seine wertvollen Hinweise, die zahlreichen konstruktiven Diskussionen und seine stete Unterstützung wäre die Arbeit in dieser Form nicht gelungen.

Großer Dank gilt auch dem Bundesinstitut für Risikobewertung (BfR) im Allgemeinen, an dem ich unter der Leitung von Herrn Prof. Gilbert Schönfelder als Gastwissenschaftler den Großteil meiner Laborarbeiten durchführen durfte. Ich möchte mich ferner bei den Mitarbeitern des BfR im Besonderen bedanken. Hervorheben möchte ich hierbei Dorothe Storm und Danke sagen für die kompetente Einarbeitung sowie tatkräftige Unterstützung im Labor. Des Weiteren bedanke ich mich bei Dr. Sebastian Dunst, Dr. Michael Oelgeschläger, Dr. Silvia Vogl, Marja Kornhuber, Jakob Zell und Johanna Ndikung für die inhaltliche und moralische Unterstützung sowie die immer überaus konstruktive und ebenso herzliche Zusammenarbeit.

Darüber hinaus gebührt mein Dank all denen, die als Kooperationspartner an dieser Arbeit mitgewirkt haben: Ich bedanke mich bei Dr. Thorsten Mielke und Beatrix Fauler vom Max-Planck-Institut für molekulare Genetik in Berlin für die Probenaufbereitung und Durchführung der elektronenmikroskopischen Aufnahmen. Ich bedanke mich bei Dr. Anna Taubenberger vom Biotechnologischen Zentrum der TU Dresden (BIOTEC) für die Messungen zur Zellsteifigkeit mittels Atomic Force Microscopy. Und ich bedanke mich bei Dr. Barbara Ingold-Heppner und Prof. Carsten Denkert vom Institut für Pathologie der Charité - Universitätsmedizin Berlin für die Bereitstellung von Tissue Microarrays zur Analyse von Brustkrebswebe.

Abschließend möchte ich mich bei Dominik Soll für das kritische Korrekturlesen bedanken. Nicht unerwähnt bleiben dürfen Oliver Krause und meine Eltern, die mit ihrer Unterstützung und ihrem Zuspruch ihrerseits zum Gelingen dieser Arbeit beigetragen haben.